

Report Title: **DEVELOPMENT OF A NOVEL CATALYST FOR NO DECOMPOSITION**

---

Report Type: **Final**      Reporting Period Start Date: **09/15/2003**      End Date: **06/22/2007**

---

Principal Author(s):      **Dr. Ates Akyurtlu**  
   **Dr. Jale F. Akyurtlu**

---

Report Issue Date:      **September 21, 2007**      DOE Award No.: **DE-FG26-03NT41911**

---

Submitting Organization      **Hampton University**  
   **Chemical Engineering Department**  
   **Hampton, VA 23668**

#### **DISCLAIMER**

“This report was prepared as an account of work sponsored by an agency of the United States Government. Neither the United States Government nor any agency thereof, nor any of their employees, makes any warranty, expressed or implied, or assumes any legal liability or responsibility for the accuracy, completeness, or usefulness of any information, apparatus, product, or process disclosed, or represents that its use would not infringe privately owned rights. Reference herein to any specific commercial product, process, or service by trade name, trademark, manufacturer, or otherwise does not necessarily constitute or imply its endorsement, recommendation, or favoring by the United States Government or any agency thereof. The views and opinions of authors expressed herein do not necessarily state or reflect those of the United States Government or any agency thereof.”

## ABSTRACT

Air pollution arising from the emission of nitrogen oxides as a result of combustion taking place in boilers, furnaces and engines, has increasingly been recognized as a problem. New methods to remove  $\text{NO}_x$  emissions significantly and economically must be developed. The current technology for post-combustion removal of NO is the selective catalytic reduction (SCR) of NO by ammonia or possibly by a hydrocarbon such as methane. The catalytic decomposition of NO to give  $\text{N}_2$  will be preferable to the SCR process because it will eliminate the costs and operating problems associated with the use of an external reducing species.

The most promising decomposition catalysts are transition metal (especially copper)-exchanged zeolites, perovskites, and noble metals supported on metal oxides such as alumina, silica, and ceria. The main shortcoming of the noble metal reducible oxide (NMRO) catalysts is that they are prone to deactivation by oxygen. It has been reported that catalysts containing tin oxide show oxygen adsorption behavior that may involve hydroxyl groups attached to the tin oxide. This is different than that observed with other noble metal-metal oxide combinations, which have the oxygen adsorbing on the noble metal and subsequently spilling over to the metal oxide. This observation leads one to believe that the Pt/ $\text{SnO}_2$  catalysts may have a potential as NO decomposition catalysts in the presence of oxygen. This prediction is also supported by some preliminary data obtained for NO decomposition on a Pt/ $\text{SnO}_2$  catalyst in the PI's laboratory.

The main objective of the research that is being undertaken is the evaluation of the Pt/ $\text{SnO}_2$  catalysts for the decomposition of NO in simulated power plant stack gases with particular attention to the resistance to deactivation by  $\text{O}_2$ ,  $\text{H}_2\text{O}$ , and elevated temperatures. Temperature programmed desorption (TPD) and temperature programmed reaction (TPRx) studies on Pt/ $\text{SnO}_2$  catalysts having different noble metal concentrations and pretreated under different conditions were done. It is also planned to perform NO decomposition tests in a laboratory-size packed-bed reactor to obtain long-term deactivation data.

Temperature programmed desorption and temperature controlled reaction runs were made with catalysts containing 15% Pt and 10% Pt on  $\text{SnO}_2$ . Catalysts containing 10% Pt resulted in significantly lower activities than 15% Pt catalysts. Therefore, in the remainder of the tests 15% Pt/ $\text{SnO}_2$  catalysts were used.

Isothermal reaction studies were made to elucidate the effects of temperature, oxygen, water vapor, pretreatment temperature, and space velocity on NO dissociation. It was found that the presence of oxygen and water vapor did not affect the activation energy of the NO dissociation reaction indicating the presence of the same rate controlling step for all feed compositions. Activation energy was higher for higher gas velocities suggesting the presence of mass transfer limitations at lower velocities. Presence of oxygen in the feed inhibited the NO decomposition. Having water vapor in the feed did not significantly affect the catalyst activity for catalysts pretreated at 373 K, but significantly reduced catalyst activity for catalysts pretreated at 900 K.

Long-term deactivation studies indicated that the catalyst deactivated slowly both with and without the presence of added oxygen in the feed. Deactivation started later in the presence of oxygen.

The activities of the catalysts investigated were too low below 1000 K for commercial applications. Their selectivity towards  $\text{N}_2$  was good at temperatures above 700 K. A different method for catalyst preparation is needed to improve the catalyst performance.

## TABLE OF CONTENTS

Disclaimer .....	1
Abstract .....	2
Table of Contents .....	3
List of Graphical Materials .....	4
Executive Summary .....	7
Introduction .....	9
Experimental .....	10
Results and Discussion .....	13
Conclusion .....	19
References .....	21
Appendix .....	24
Figures .....	25

## LIST OF GRAPHICAL MATERIAL

### Tables

Table 1. BET surface areas ( $\text{m}^2/\text{g}$ ) of fresh catalysts .....	11
Table 2. Summary of results for isothermal reaction runs .....	17
Table 3. Effect of water in the feed .....	18
Table 4. Effect of reactant concentrations on NO conversion .....	18

### Figures

Figure 1. Species evolved during 1-ml doses of 1.94 % NO in He on 15 % Pt/SnO <sub>2</sub> catalyst at 313 K (run 1) .....	26
Figure 2. Species evolved during 1-ml doses of 1.60 % NO in He on 15 % Pt/SnO <sub>2</sub> catalyst at 313 K (run 2) .....	27
Figure 3. Species evolved during 1-ml doses of 1.60 % NO in He on 15 % Pt/SnO <sub>2</sub> catalyst at 313 K (run 3) .....	28
Figure 4. Species evolved during 1-ml doses of 3.60 % O <sub>2</sub> in He on 15 % Pt/SnO <sub>2</sub> catalyst after treatment with NO, at 313 K .....	29
Figure 5. Species evolved during TPD after treatment of 15%Pt/SnO <sub>2</sub> catalyst with NO at 313 K .....	30
Figure 6. Species evolved during TPD after treatment of 15%Pt/SnO <sub>2</sub> catalyst with NO and O <sub>2</sub> subsequently at 313 K .....	31
Figure 7. TPRx of NO on fresh 15% Pt/SnO <sub>2</sub> catalyst .....	32
Figure 8. Second TPRx run of NO on 15% Pt/SnO <sub>2</sub> catalyst .....	33
Figure 9. Third TPRx run of NO on 15% Pt/SnO <sub>2</sub> catalyst .....	34
Figure 10. TPRx on fresh 15% Pt/SnO <sub>2</sub> catalyst. Feed O <sub>2</sub> /NO=2 .....	35
Figure 11. Second TPRx on 15% Pt/SnO <sub>2</sub> catalyst. Feed O <sub>2</sub> /NO=2 .....	36
Figure 12. TPRx on fresh 15% Pt/SnO <sub>2</sub> catalyst. Feed O <sub>2</sub> /NO=1 .....	37
Figure 13. TPRx of NO on fresh 10% Pt/SnO <sub>2</sub> catalyst .....	38
Figure 14. Second TPRx run of NO on 10% Pt/SnO <sub>2</sub> catalyst .....	39
Figure 15. Third TPRx run of NO on 10% Pt/SnO <sub>2</sub> catalyst .....	40
Figure 16. Fourth TPRx run of NO on 10% Pt/SnO <sub>2</sub> catalyst .....	41
Figure 17. TPRx of NO+O <sub>2</sub> on fresh 10% Pt/SnO <sub>2</sub> catalyst. Feed O <sub>2</sub> /NO=1 .....	42
Figure 18. Second TPRx of NO+O <sub>2</sub> on fresh 10% Pt/SnO <sub>2</sub> catalyst. Feed O <sub>2</sub> /NO=1 .....	43
Figure 19. Third TPRx of NO+O <sub>2</sub> on fresh 10% Pt/SnO <sub>2</sub> catalyst. Feed O <sub>2</sub> /NO=1 .....	44
Figure 20. TPRx of NO+O <sub>2</sub> +H <sub>2</sub> O on 15% Pt/SnO <sub>2</sub> catalyst. Feed O <sub>2</sub> /NO=0.5 .....	45
Figure 21. Arrhenius plot for TPRx of NO+O <sub>2</sub> +H <sub>2</sub> O on 15% Pt/SnO <sub>2</sub> catalyst .....	46
Figure 22. Isothermal reaction of NO+O <sub>2</sub> on 15% Pt/SnO <sub>2</sub> at 900 K, first run .....	47
Figure 23. Isothermal reaction of NO+O <sub>2</sub> on 15% Pt/SnO <sub>2</sub> at 900 K, second run .....	48
Figure 24. Isothermal reaction of NO+O <sub>2</sub> on 15% Pt/SnO <sub>2</sub> at 900 K. 60 cm <sup>3</sup> /min, pretreated at 373 K .....	49
Figure 25. Isothermal reaction of NO+O <sub>2</sub> +H <sub>2</sub> O on 15% Pt/SnO <sub>2</sub> at 900 K.	

60 cm <sup>3</sup> /min, pretreated at 373 K .....	50
Figure 26. Isothermal reaction of NO+O <sub>2</sub> on 15% Pt/SnO <sub>2</sub> at 1000 K.	
40 cm <sup>3</sup> /min, pretreated at 373 K .....	51
Figure 27. Isothermal reaction of NO+O <sub>2</sub> on 15% Pt/SnO <sub>2</sub> at 1000 K.	
40 cm <sup>3</sup> /min, pretreated at 373 K (repeat) .....	52
Figure 28. Isothermal reaction of NO+O <sub>2</sub> +H <sub>2</sub> O on 15% Pt/SnO <sub>2</sub> at 1000 K.	
40 cm <sup>3</sup> /min, pretreated at 373 K .....	53
Figure 29. Isothermal reaction of NO+O <sub>2</sub> +H <sub>2</sub> O on 15% Pt/SnO <sub>2</sub> at 900 K.	
40 cm <sup>3</sup> /min, pretreated at 373 K .....	54
Figure 30. Isothermal reaction of NO+O <sub>2</sub> on 15% Pt/SnO <sub>2</sub> at 900 K.	
40 cm <sup>3</sup> /min, pretreated at 900 K .....	55
Figure 31. Isothermal reaction of NO on 15% Pt/SnO <sub>2</sub> at 900 K.	
40 cm <sup>3</sup> /min, pretreated at 900 K .....	56
Figure 32. Isothermal reaction of NO on 15% Pt/SnO <sub>2</sub> at 1000 K.	
40 cm <sup>3</sup> /min, pretreated at 900 K .....	57
Figure 33. Isothermal reaction of NO+O <sub>2</sub> on 15% Pt/SnO <sub>2</sub> at 1000 K.	
40 cm <sup>3</sup> /min, pretreated at 900 K .....	58
Figure 34. Isothermal reaction of NO+O <sub>2</sub> on 15% Pt/SnO <sub>2</sub> at 850 K.	
40 cm <sup>3</sup> /min, pretreated at 900 K .....	59
Figure 35. Isothermal reaction of NO on 15% Pt/SnO <sub>2</sub> at 850 K.	
40 cm <sup>3</sup> /min, pretreated at 900 K .....	60
Figure 36. Isothermal reaction of NO on 15% Pt/SnO <sub>2</sub> at 950 K.	
40 cm <sup>3</sup> /min, pretreated at 900 K .....	61
Figure 37. Isothermal reaction of NO+O <sub>2</sub> on 15% Pt/SnO <sub>2</sub> at 950 K.	
40 cm <sup>3</sup> /min, pretreated at 900 K .....	62
Figure 38. Isothermal reaction of NO+O <sub>2</sub> +H <sub>2</sub> O on 15% Pt/SnO <sub>2</sub> at 900 K.	
40 cm <sup>3</sup> /min, pretreated at 373 K .....	63
Figure 39. Isothermal reaction of NO+O <sub>2</sub> on 15% Pt/SnO <sub>2</sub> at 850 K.	
60 cm <sup>3</sup> /min, pretreated at 900 K .....	64
Figure 40. Isothermal reaction of NO+O <sub>2</sub> on 15% Pt/SnO <sub>2</sub> at 900 K.	
60 cm <sup>3</sup> /min, pretreated at 900 K .....	65
Figure 41. Isothermal reaction of NO+O <sub>2</sub> on 15% Pt/SnO <sub>2</sub> at 950 K.	
60 cm <sup>3</sup> /min, pretreated at 900 K .....	66
Figure 42. Isothermal reaction of NO+O <sub>2</sub> on 15% Pt/SnO <sub>2</sub> at 1000 K.	
60 cm <sup>3</sup> /min, pretreated at 900 K .....	67
Figure 43. Isothermal reaction of NO+O <sub>2</sub> +H <sub>2</sub> O on 15% Pt/SnO <sub>2</sub> at 900 K.	
40 cm <sup>3</sup> /min, pretreated at 900 K .....	68
Figure 44. Effects of temperature, oxygen, water, and pretreatment .....	69
Figure 45. Effect of space velocity .....	70
Figure 46. NO dissociation equilibrium at 1 atm. Pure NO .....	71
Figure 47. NO dissociation equilibrium at 1 atm. 50% NO-50% O <sub>2</sub> .....	72
Figure 48. NO dissociation equilibrium at 1 atm. 40% NO-60% O <sub>2</sub> .....	73
Figure 49. NO dissociation equilibrium at 1 atm. 33% NO-67% O <sub>2</sub> .....	74
Figure 50. NO dissociation equilibrium at 1 atm. 1% NO-99% He .....	75
Figure 51. NO dissociation equilibrium at 1 atm. 1% NO-98% He-1% Air .....	76
Figure 52. NO dissociation equilibrium at 1 atm. 1% O <sub>2</sub> -97% He-1% Air .....	77

Figure 53. Deactivation of 15% Pt/SnO <sub>2</sub> catalyst during isothermal reaction at 900 K. NO feed. Species concentration .....	78
Figure 54. Deactivation of 15% Pt/SnO <sub>2</sub> catalyst during isothermal reaction at 900 K. NO feed. NO conversion .....	79
Figure 55. Deactivation of 15% Pt/SnO <sub>2</sub> catalyst during isothermal reaction at 900 K. O <sub>2</sub> /NO=1.5. Species concentration .....	80
Figure 56. Deactivation of 15% Pt/SnO <sub>2</sub> catalyst during isothermal reaction at 900 K. O <sub>2</sub> /NO=1.5. NO conversion .....	81
Figure 57. TPRx of NO+O <sub>2</sub> with no catalyst. O <sub>2</sub> /NO=1 .....	82

## EXECUTIVE SUMMARY

Air pollution arising from the emission of nitrogen oxides as a result of combustion taking place in boilers, furnaces and engines, has increasingly been recognized as a problem. New methods to remove  $\text{NO}_x$  emissions significantly and economically must be developed. The current technology for post-combustion removal of NO is the selective catalytic reduction (SCR) of NO by ammonia or possibly by a hydrocarbon such as methane. The catalytic decomposition of NO to give  $\text{N}_2$  will be preferable to the SCR process because it will eliminate the costs and operating problems associated with the use of an external reducing species.

The most promising decomposition catalysts are transition metal (especially copper)-exchanged zeolites, perovskites, and noble metals supported on metal oxides such as alumina, silica, and ceria. The main shortcoming of the noble metal reducible oxide (NMRO) catalysts is that they are prone to deactivation by oxygen. It has been reported that catalysts containing tin oxide show oxygen adsorption behavior that may involve hydroxyl groups attached to the tin oxide. This is different than that observed with other noble metal-metal oxide combinations, which have the oxygen adsorbing on the noble metal and subsequently spilling over to the metal oxide. This observation leads one to believe that the Pt/ $\text{SnO}_2$  catalysts may have a potential as NO decomposition catalysts in the presence of oxygen.

The main objective of this research is the evaluation of the Pt/ $\text{SnO}_2$  catalysts for the decomposition of NO in simulated power plant stack gases with particular attention to the resistance to deactivation by  $\text{O}_2$ ,  $\text{H}_2\text{O}$ , and elevated temperatures. Temperature programmed desorption (TPD) and temperature programmed reaction (TPRx) studies were done on Pt/ $\text{SnO}_2$  catalysts having different noble metal concentrations and pretreated under different conditions. It is also planned to perform NO decomposition tests in a laboratory-size packed-bed reactor to obtain long-term deactivation data.

To understand the reaction process and establish a performance window for the catalysts, temperature programmed desorption and temperature programmed reaction runs on the 15% Pt and 10% Pt catalysts were performed using  $\text{NO}+\text{He}$  and  $\text{NO}+\text{O}_2+\text{He}$  reactant gas mixtures.

The catalyst was active for NO decomposition only above 600 K and at these temperatures no appreciable  $\text{N}_2\text{O}$  was observed. For feeds containing additional oxygen, the NO decomposition activity was less when fresh and the catalyst lost most of its activity in the subsequent runs. This may be due to the oxidation of Pt, coverage of active Pt sites with oxygen, and the loss of OH groups from the  $\text{SnO}_2$  surface. Catalysts containing 10% Pt were significantly less active than those containing 15% Pt. Therefore the remaining runs were done using 15% Pt catalysts.

Temperature programmed reaction of  $\text{NO} + \text{O}_2 + \text{H}_2\text{O}$  on 15 % Pt/ $\text{SnO}_2$  catalyst was also done. The reaction of NO and  $\text{O}_2$  in the presence of water vapor appears to show two different reaction schemes, one below and the other above 750 K. Activation energy below 750 K was estimated to be 204 kJ/mol and that at higher temperatures was estimated as 43kJ/mol.

In addition, reactions of dry and wet mixtures of NO and  $\text{O}_2$  were carried out for over 3 hours. No apparent deactivation was observed.

Reactions of NO and an equimolar amount of  $\text{O}_2$  with and without 4%  $\text{H}_2\text{O}$  were done at 1000 K. Since OH groups are thought to be very active in the  $\text{O}_2$ -involving processes on the catalyst surface an additional set of runs were done with catalyst samples pre-treated at 900 K to drive off most of the OH groups.

Runs were made at varying temperatures between 800 K and 1000 K to establish the variation of NO conversion with temperature. To identify the effect of space velocity, two different gas flow rates, 40 cm<sup>3</sup>/min and 60 cm<sup>3</sup>/min, were used while keeping the amount of catalyst constant at 150 mg. The conclusions were that the presence of oxygen and water vapor did not affect the activation energy of the NO dissociation reaction indicating the presence of the same rate controlling step for all feed compositions. Activation energy was higher for higher gas velocities suggesting the presence of mass transfer limitations at lower velocities. Presence of oxygen in the feed inhibited the NO decomposition. Having water vapor in the feed did not significantly affect the catalyst activity for catalysts pretreated at 373 K, but significantly reduced catalyst activity for catalysts pretreated at 900 K.

The BET surface areas of the catalysts were also measured and found to be around 80 m<sup>2</sup>/g.

Long-term deactivation studies indicated that the catalyst deactivated slowly both with and without the presence of added oxygen in the feed, Deactivation started later in the presence of oxygen.

## INTRODUCTION

Air pollution arising from the emission of nitrogen oxides as a result of combustion taking place in boilers, furnaces and engines, has increasingly been recognized as a problem. New methods to remove NO<sub>x</sub> emissions significantly and economically must be developed. The current technology for post-combustion removal of NO is the selective catalytic reduction (SCR) of NO by ammonia or possibly by a hydrocarbon such as methane. The catalytic decomposition of NO to give N<sub>2</sub> will be preferable to the SCR process because it will eliminate the costs and operating problems associated with the use of an external reducing species. In the utility boiler system, there are two locations convenient for inserting an NO removal reactor: The first one is after the economizer at a temperature of 625-725 K; and the second one is after the air preheater at a temperature of 375-425 K. Therefore, the potential NO decomposition catalyst is preferred to have acceptable activity and selectivity at least in one of these temperature ranges if changes in the boiler design.

The most promising decomposition catalysts are transition metal (especially copper)-exchanged zeolites, perovskites, and noble metals supported on metal oxides such as alumina, silica, and ceria<sup>(1, 2, 3, 4, 5, 6, 7, 8, 9, 10, 11, 12)</sup>. The main shortcoming of the noble metal reducible oxide (NMRO) catalysts is that they are prone to deactivation by oxygen<sup>(13)</sup>. The NMRO catalysts that are of interest are based on either platinum or gold as noble metal. Platinum is generally associated with SnO<sub>2</sub> as the reducible oxide for operation below 373 K and with ceria or titania for higher temperature service such as automobile exhaust applications. Pt/SnO<sub>2</sub>-based catalysts were extensively studied for CO<sub>2</sub> laser applications by NASA/LARC researchers and investigators in associated universities<sup>(14, 15, 16, 17, 18, 19, 20)</sup>. These studies have led to the optimization of the Pt/SnO<sub>2</sub>-based catalysts with 15-20 % Pt. It has been reported that catalysts containing tin oxide show oxygen adsorption behavior that may involve hydroxyl groups attached to the tin oxide<sup>(21)</sup>. This is different from that observed with other noble metal-metal oxide combinations, which have the oxygen adsorbing on the noble metal and subsequently spilling over to the metal oxide. This observation leads one to believe that the Pt/SnO<sub>2</sub> catalysts may have a potential as NO decomposition catalysts in the presence of oxygen. In a previous research work performed at Hampton University, the effect of water on the activity of Pt/SnO<sub>2</sub> catalysts was investigated. Some observations made during that research also suggested that these catalysts may have a potential for the catalytic decomposition of NO and not be seriously affected by the presence of large quantities of oxygen<sup>(22)</sup>.

The main objective of the proposed research is the evaluation of the Pt/SnO<sub>2</sub> catalysts for the decomposition of NO in simulated power plant stack gases with particular attention to the resistance to deactivation by O<sub>2</sub>, H<sub>2</sub>O, and elevated temperatures. Therefore, it is proposed to perform temperature programmed desorption (TPD) and temperature programmed reaction (TPRx) studies on Pt/SnO<sub>2</sub> catalysts having different noble metal concentrations and pretreated under different conditions. Long-term NO decomposition tests were performed to obtain deactivation data.

## EXPERIMENTAL

To evaluate the performance of Pt/SnO<sub>2</sub> catalysts for the decomposition of nitric oxide (NO), Temperature-Programmed Desorption (TPD), Temperature Programmed Reaction (TPRx) experiments were performed using the Micromeritics Pulse Chemisorb 2705 with TPD/TPR option. A mass spectrometer-gas chromatograph system (SATURN 2000MS/3800GC) from Varian is used for the identification of desorbed species and reaction products. A Supelco 45/60 Carboxen capillary column was used in the gas chromatogram. The column oven was kept at 35 °C until the NO peak was obtained (4 min) and then heated to 115 °C at 30 °C/min. A limitation of this column was that if it stayed idle for some time, the first few chromatograms after this idle period showed significantly larger O<sub>2</sub>, N<sub>2</sub>, and water peaks. These measurements needed to be discarded. This shortcoming was especially important for the long-term testing, because, after an overnight operation, several measurements had to be made until a stable reading was obtained.

Gases and certified gas mixtures were obtained from the local Air Products (later National Welders) supplier and were used without further treatment. Since NO+O<sub>2</sub> mixtures were unstable, the gas mixture needed to be prepared from separate bottles. The new feed system was constructed using two existing gas flow controllers. Data at the 60 cm<sup>3</sup>/min flow rate were taken using this system. At the end of these runs the gas flow controllers were accidentally contaminated and became inoperable. To minimize the delay a new feed system was prepared using surplus rotameters and manual valves. Obtaining reliable data with this system required practice and modification of procedures. After confirming that the results were reliable, the rest of the experiments were done using this setup. Water was introduced by bubbling the gases through a water bottle held at 295 K. This corresponds to about 4 % water vapor in the gas mixture.

Initially the bench scale laboratory setup was planned to be used for long-term deactivation studies because the feed system on this setup was automatic and could operate without supervision. To test the operation of the setup, runs were made to investigate the effects of NO and O<sub>2</sub> concentrations on NO conversion. NO measurements were done using the Thermoenvironmental 42H chemiluminescence NO<sub>x</sub> analyzer. After evaluating these preliminary results, it was decided that more consistent data would be obtained if the feed system were connected to the Micromeritics equipment and the gases analyzed using the GC/MS apparatus. Another advantage of this modification was the ability to use a smaller amount of catalyst and feed gases for the tests.

The GC/MS measurements were calibrated to give species concentrations in ppm, using analyzed gas mixtures obtained from Scot Specialty Gases.

### a. Catalyst

The Pt/ SnO<sub>2</sub> catalysts were prepared by the co-precipitation method used in the preparation of the original NASA CO oxidation catalysts. Catalysts containing 15 % Pt and 10% Pt were studied. Fifteen per cent platinum was found to be optimum during the CO oxidation studies. In this study it was planned to test catalysts containing smaller amounts of platinum. Since the conversions obtained using 10 % platinum were significantly lower than those obtained with the 15% Pt catalyst, catalysts containing less than 10 % Pt were not studied.

The BET surface areas of the 15 % Pt and 10 % Pt catalysts were measured using the Micromeritics Pulse Chemisorb apparatus. The results are reported in Table 1 below.

Table 1. BET surface areas ( $\text{m}^2/\text{g}$ ) of fresh catalysts

Catalyst	Surface Area, $\text{m}^2/\text{g}$	
	1 <sup>st</sup> Measurement	2 <sup>nd</sup> Measurement
15%Pt/SnO <sub>2</sub>	75.1	82.9
10%Pt/SnO <sub>2</sub>	77.1	82.9

This table shows that the amount of platinum on the catalyst does not change the surface area.

### b. Temperature-Programmed Desorption Experiments

Temperature-Programmed Desorption (TPD) Experiments were used to evaluate the NO and O<sub>2</sub> chemisorption capacities of the catalysts and to identify the surface species and desorption species.

Absorption runs were made before the TPD experiments. Repeated 1-ml samples of the adsorbate were injected onto a 150-mg (nominal) catalyst sample using a calibrated loop and the exiting gases were analyzed using the GC/MS system.

A typical TPD run is described below:

1. Pretreat all the samples in He (40 ml/min) at 313 K for 2 hours. This thermal treatment will prevent any appreciable oxygen uptake.
2. Carry out NO (NO+O<sub>2</sub> or O<sub>2</sub>) adsorption at 313 K by flowing a NO/He mixture (or a similar mixture containing other adsorbents) containing 1.94 % NO in He, 3.6 % O<sub>2</sub> in He. Measure the species in the exit gas stream at the time corresponding to the maximum in the desorption curve.  
Flow rate: 40 ml/min  
Temperature range: 308 K – 1000 K  
Temperature ramp: 3 K/min
3. Flush the sample with a stream of dry helium at 313 K to eliminate gaseous NO and weakly adsorbed NO (or any other adsorbent).
4. When no NO (or any other adsorbent) is observed, heat the sample to 1000 K in flowing He stream. Record the desorbed species.
5. Repeat this procedure for two more cycles. Cool the sample to 323 K.

### c. Temperature-Programmed Reaction Experiments

To obtain information on the catalyst activity and selectivity for NO decomposition to nitrogen and oxygen, a series of temperature programmed reaction (TPRx) experiments were run.

A typical TPRx run is described below:

1. Pretreat all the samples in He (40 ml/min) at 313 K for 2 hours. This thermal treatment will prevent any appreciable oxygen uptake.

2. Replace the carrier gas by NO+He or NO+O<sub>2</sub>+He reactant gas mixture and heat the catalyst to 800 K at a rate of 3K/min. Measure the amount of species in the exit gas stream.  
Flow rate: 40 ml/min  
Temperature range: 308 K – 800 K
3. Cool to 308 K under He and flush the sample with a stream of dry helium at 308 K for 2 hours.
4. Repeat this procedure for more cycles as needed.

#### **d. Isothermal Reaction Experiments**

To establish the effects of temperature, pretreatment, presence of oxygen and water vapor in the feed, and space velocity on NO conversion, isothermal runs were made at varying temperatures between 800 K and 1000 K. This temperature range was used because the TPD and TPRx results indicated that no appreciable NO decomposition occurred below 700 K. To identify the effect of space velocity, two different gas flow rates, 40 cm<sup>3</sup>/min and 60 cm<sup>3</sup>/min, were used while keeping the amount of catalyst constant at 150 mg (nominal).

After the test chamber was filled with the catalyst, it was heated to the reaction temperature under helium. In the mean time, the feed gas mixture was sent through the bypass and analyzed periodically until stable concentrations were measured. Then the feed was switched to the test cell and the reaction products were analyzed periodically until an apparent steady state was reached. For some runs, the feed composition after the TPRx runs were also measured.

#### **c. NO Equilibrium Studies**

For this purpose CHEMKIN Release 4.0.2 was used. The mixtures used were pure NO, 50 % NO – 50 % O<sub>2</sub>, 60 % O<sub>2</sub> – 40 % NO, 67 % O<sub>2</sub> – 33 % NO, 98 % He – 1 % Air – 1% NO, 97 % He – 1 % Air – 1 % O<sub>2</sub> – 1 % NO, and 99% He – 1 % NO. The mixtures with He simulate the experimental conditions. Product species considered were O, O<sub>2</sub>, N<sub>2</sub>, NO, NO<sub>2</sub>, N<sub>2</sub>O, N<sub>2</sub>O<sub>3</sub>, N<sub>2</sub>O<sub>4</sub>, and N. It would have been very informative if we could add tin oxides and tin nitrates to this list, but CHEMKIN library does not contain them. Our literature search did not provide the required data to include these solid components in our computations.

#### **d. Long Term Deactivation Runs**

Long term deactivation runs were done using the feed section of the bench scale laboratory setup to prepare the feed gas mixture for the Micromeritics TPRx setup. The test cell was heated to 900 K under helium while the feed gas was switched to bypass to make sure that a correct, steady feed composition was obtained. Then the feed was switched to the test cell and the test was started. It took several measurements until a steady exit composition was obtained. At least 3 samples were analyzed per data point and the mean was reported as the gas composition and used in the calculation of the NO conversion.

## RESULTS AND DISCUSSION

### a. Temperature-Programmed Desorption Experiments

#### i. Reproducibility of species measurements during adsorption

Figures 1 through 3 show the analysis of the exit gas during injections of 1-ml pulses of 1.94% NO in He on the 15% Pt/SnO<sub>2</sub> catalyst for 3 replicate runs. All three figures show equal concentrations of N<sub>2</sub> and O<sub>2</sub> indicating some NO decomposition. This observation is confirmed by the decrease in the NO concentration compared to the NO in feed. Some of this decrease is believed to be due to the retention of NO on the catalyst surface as nitrogen containing surface species such as nitrates and/or nitrites.

The repeatability of the results was deemed to be satisfactory considering the many sources of random error in the measurements.

#### ii. Species observed during NO injections

When the catalyst sample is subjected to NO pulses it is expected that some NO be retained on the catalyst and form surface nitrite and nitrate species while some may dissociate or react to form other gaseous species. Figures 1-3 show that after four 1-ml pulses of 1.94% NO in He, the retention of NO on the 150-g catalyst sample reached steady state for the subsequent pulses. The mean NO content of the pulse gas is also shown on the figures. Comparison indicates that a portion of NO is either dissociated into N<sub>2</sub> and O<sub>2</sub> with both the N<sub>2</sub> and O<sub>2</sub> amounts in the exit gas reaching a steady state or continues to chemisorb at steady state. The N<sub>2</sub>/O<sub>2</sub> ratios in the steady state region were very close to 1 indicating at least some dissociation of NO. Considering the decrease in the NO concentration, it is likely that some NO was retained on the surface as solid nitrogen compounds. Very little N<sub>2</sub>O formation was observed, NO<sub>2</sub> was not detected.

#### iii. Species observed during subsequent O<sub>2</sub> injections

Figure 4 shows the species observed in the exit gas during 1-ml pulses of 3.6% O<sub>2</sub> in He on the 15% Pt/SnO<sub>2</sub> catalyst treated with NO. No NO and N<sub>2</sub>O were observed indicating that the chemisorbed nitrogen species were stable at 313 K. The N<sub>2</sub> and O<sub>2</sub> amounts did not vary with the number of injections.

#### iv. TPD after NO chemisorption

Figure 5 presents the species desorbed during the controlled heating of the 15% Pt/SnO<sub>2</sub> catalyst treated with NO only. A large N<sub>2</sub>O peak at 473 K and a large NO peak at 513 K were observed. A similar increase in nitrogen was observed during N<sub>2</sub>O desorption with no change in the oxygen amount. On the other hand, nitrogen sharply decreases with NO desorption. A slight dip in the amount of oxygen was observed during NO desorption. The N<sub>2</sub>/O<sub>2</sub> ratio remains close to one, but exhibits two peaks, one corresponding to the maximum in the N<sub>2</sub>O curve (480 K) and the other to the end of the NO peak (590 K).

#### v. TPD after subsequent NO and O<sub>2</sub> chemisorptions

Figure 6 shows the species evolved during 3 K/s heating of the 15% Pt/SnO<sub>2</sub> catalyst treated with subsequent pulses of NO and O<sub>2</sub>. The N<sub>2</sub>O and NO peaks occur at the same temperatures as in the case of only NO chemisorption (Figure 5), but in this case, the N<sub>2</sub>O peak is larger. The N<sub>2</sub> and O<sub>2</sub> amounts sharply increase at the start of the N<sub>2</sub>O peak (at about 350 K), then at about 380 K, rate of increase of N<sub>2</sub> slows down and becomes constant for the rest of the run while the O<sub>2</sub> starts decreasing at the same temperature. The amount of oxygen becomes a minimum at N<sub>2</sub>O peak temperature (490 K) and then slowly increases. The N<sub>2</sub>/O<sub>2</sub> ratio also peaks at 490 K and eventually reaches about one at around 600 K.

#### **vi. TPD after subsequent NO and O<sub>2</sub> chemisorptions**

Figure 6 shows the species evolved during 3 K/s heating of the 15% Pt/SnO<sub>2</sub> catalyst treated with subsequent pulses of NO and O<sub>2</sub>. The N<sub>2</sub>O and NO peaks occur at the same temperatures as in the case of only NO chemisorption (Figure 5), but in this case, the N<sub>2</sub>O peak is larger. The N<sub>2</sub> and O<sub>2</sub> amounts sharply increase at the start of the N<sub>2</sub>O peak (at about 350 K), then at about 380 K, rate of increase of N<sub>2</sub> slows down and becomes constant for the rest of the run while the O<sub>2</sub> starts decreasing at the same temperature. The amount of oxygen becomes a minimum at N<sub>2</sub>O peak temperature (490 K) and then slowly increases. The N<sub>2</sub>/O<sub>2</sub> ratio also peaks at 490 K and eventually reaches about one at around 600 K.

### **b. Temperature Programmed Reaction Studies**

#### **i. Temperature Programmed Reaction of NO on 15%Pt/SnO<sub>2</sub> Catalyst**

From Figures 7 - 9 it can be seen that oxygen adsorbs on the catalyst up to 520 K. There is no NO decomposition below 750 K, but some N<sub>2</sub>O formation is observed above 370 K, which peaks at 520 K. There also seems to be a smaller N<sub>2</sub>O peak around 620 K, but no N<sub>2</sub>O is present above 750 K. At 520 K, nitrogen to oxygen ratio peaks and NO concentration shows a local minimum at the same temperature, indicating some NO decomposition around 520 K. The N<sub>2</sub>/O<sub>2</sub> ratio decreases to about 1 beyond 750 K.

Two different NO decomposition mechanisms are expected to take place on the catalyst. One occurring on the Pt surface and the other involving intermediate surface nitrogen species formation on the oxide and their subsequent decomposition giving N<sub>2</sub> and O<sub>2</sub>. The O<sub>2</sub> formed during NO decomposition is expected to preferentially adsorb on the Pt surface. Both the oxygen adsorption and the formation of the surface nitrogen species can explain the decrease of oxygen concentration up to about 520 K. Again, both the O<sub>2</sub> desorption and O<sub>2</sub> formation as the result of the decomposition of surface nitrate/nitrite species can explain the increase in O<sub>2</sub> concentration above 520 K.

After 750 K, NO concentration starts decreasing rapidly. The changes in the gaseous NO concentration can also be explained by the two NO decomposition processes mentioned above. The desorption of O<sub>2</sub> at high temperatures may free up Pt sites for the NO reactions, and higher temperatures may increase the rate of decomposition of the nitrate/nitrite surface species.

The peak in the N<sub>2</sub>O formation corresponds to the minimum in the gaseous O<sub>2</sub> concentration and the maximum in the gaseous NO concentration indicating the contribution of N<sub>2</sub>O formation to the decrease in the gaseous O<sub>2</sub> concentration.

The results of the second and third runs with the same catalyst sample show very similar behavior, except that there is no NO concentration minimum at 520 K and the N<sub>2</sub>/O<sub>2</sub> ratio peak at that temperature is smaller.

### **ii. Temperature Programmed Reaction of NO+O<sub>2</sub> on 15%Pt/SnO<sub>2</sub> Catalyst**

Figures 10 and 11 show the TPRx of a gas mixture containing O<sub>2</sub> and NO in He with the nominal O<sub>2</sub>/N<sub>2</sub>=2. Clearly, the presence of oxygen inhibits the decomposition of NO. The small amount of decomposition activity starts around 425 K on fresh catalyst. During the second run the NO decomposition activity does not start until 575 K, but appears to be faster than on fresh catalyst. On the other hand, slightly more N<sub>2</sub>O formation was observed during the second TPRx run. The N<sub>2</sub>O concentration has a small peak around 530 K, which corresponds to a minimum in the oxygen concentration. The species concentrations appear to follow the same trends explained for the runs without added oxygen in the feed.

When the feed O<sub>2</sub>/NO ratio was cut by one-half, the N<sub>2</sub>O production on the fresh catalyst was significantly reduced (Figure 12). The reduction in the feed oxygen content also appeared to improve the NO decomposition activity. Figure 12 indicates a significant increase in NO retention at lower temperatures on the fresh catalyst. The gaseous NO concentration continuously increases up to about 575 K then starts decreasing slowly at higher temperatures. During the run, gaseous NO concentration remained below the feed concentration.

### **iii. Temperature Programmed Reaction of NO on 10%Pt/SnO<sub>2</sub> Catalyst**

The reactions taking place on fresh 10% Pt/SnO<sub>2</sub> catalyst were similar to those observed on the 15% Pt/SnO<sub>2</sub> catalyst above 500 K except that the amount of N<sub>2</sub>O formed was larger on the 10% Pt catalyst (Figure 13). The NO conversion on both fresh catalysts were about 20% at 773 K. At 400 K, there is a NO concentration minimum corresponding to an oxygen concentration maximum. These peaks were not observed during the second and third runs with the same catalyst, but reappeared during the fourth run (Figure 16).

Second run on the 10% Pt catalyst (Figure 14) was very similar to that on the 15% Pt catalyst giving about 16% conversion at 773 K. The amount of N<sub>2</sub>O formed was also similar. Conversion of NO on the 10% Pt catalyst during the third run (Figure 15) at 773 K was slightly lower (about 14.5%) compared to that on the 15% Pt catalyst (about 18.5%). Therefore, a fourth run on the 10% Pt catalyst was done (Figure 16), which produced again 14.5% NO conversion. Therefore, it was concluded that the slight drop in conversion after the second run was not an indication of continuous deactivation of the 10% Pt catalyst. The N<sub>2</sub>O production on the 10% Pt catalyst for the second through fourth runs was very small.

These observations can also be explained by the two NO reduction mechanisms suggested above. It is known that under reducing atmospheres SnO<sub>2</sub> is completely deactivated at temperatures above 600 K and the activity cannot be restored by an oxidation treatment. For the current tests it can be postulated that if the decomposition of NO, and the formation of N<sub>2</sub>O, on SnO<sub>2</sub> involve lattice oxygen, thus effectively reducing SnO<sub>2</sub>, then the NO decomposition activity of SnO<sub>2</sub> will gradually decrease until the SnO<sub>2</sub> is deactivated. After that time the only NO decomposition activity will be on the Pt sites. If we accept that the N<sub>2</sub>O formation occurs only on SnO<sub>2</sub>, then this will explain the decrease of N<sub>2</sub>O formation after the first run. It will also explain the initial decrease in NO

dissociation activity, which levels off at a higher value on the 15% Pt catalyst.

#### **iv. Temperature Programmed Reaction of NO+O<sub>2</sub> on 10%Pt/SnO<sub>2</sub> Catalyst**

Figures 17-19 for the 10% Pt catalyst show very little activity at temperatures below 800 K and a slightly higher rate of N<sub>2</sub>O formation. These observations are consistent with the explanation given above in terms of two NO dissociation mechanisms, and deactivation of SnO<sub>2</sub> by reduction if the surface nitrite/nitrate formation occurs at the Pt-SnO<sub>2</sub> interface and requires the adsorption of NO on the Pt sites. Presence of a large amount of oxygen is expected to saturate the Pt sites and leave little room for NO adsorption. Although SnO<sub>2</sub> may not be reduced as fast under the O<sub>2</sub>-containing reactant gas, the formation of nitrite and nitrate surface species is greatly retarded resulting in very little NO decomposition activity.

#### **v. Temperature Programmed Reaction of NO + O<sub>2</sub> + H<sub>2</sub>O**

The feed contained equimolar amounts of NO and O<sub>2</sub>, and was saturated with water at 295 K. Figure 20 shows that NO decomposition starts at around 700 K with a high selectivity to N<sub>2</sub> and O<sub>2</sub>. There appears to be two rate controlling processes, one below 750 K and the other above 750 K. Arrhenius plot given in Figure 21 confirms this. The apparent activation energy obtained for temperatures less than 750 K is 204 kJ/mol and that for higher temperatures is 43 kJ/mol. Although 43 kJ/mol might be too high to indicate total mass transfer control, presence of some external mass transfer limitations is possible.

Water content of the feed gas appears to enhance the decomposition activity slightly but also decreases N<sub>2</sub> selectivity as indicated by a slight increase in the N<sub>2</sub>O formation. Figures 5 and 6 indicate that at 900 K, NO conversion is higher and presence of H<sub>2</sub>O again affects the NO conversion favorably. At this higher temperature the effect of water on N<sub>2</sub>O formation is not very significant. This observation contradicts the prediction that the presence of OH ions on the tin oxide will hinder the desorption of surface oxygen and thus adversely affect the catalyst activity. The observed enhancement activity may be due to the attraction of surface oxygen to these hydroxyl groups preventing the coverage of the Pt sites by the adsorbed oxygen.

### **c. Isothermal Reaction Experiments**

The results of the isothermal reaction experiments are shown in figures 22 through 43. The results of all the runs are summarized in Table 2. If the only reaction occurring is the decomposition of NO according to the equation  $\text{NO} \rightarrow \frac{1}{2} \text{N}_2 + \frac{1}{2} \text{O}_2$ , there will be no change in the total number of moles and the ratio of the change in NO concentration to N<sub>2</sub> concentration will be 2 and the ratio of the change in N<sub>2</sub> concentration to the change in O<sub>2</sub> concentration will be 1. Therefore, to identify the presence of complex reaction processes, the changes in the concentrations are also reported in Table 2.

Table 2 indicates that  $\Sigma\Delta$  is generally not close to zero but this discrepancy is likely to be the result of experimental errors and not due to the presence of different reaction mechanisms as suggested in an earlier report based on a few preliminary data. For most runs  $\Delta\text{O}_2/\Delta\text{N}_2$  is between 0.87 and 1.61, which is sufficiently close to one as expected. The few exceptions are for relatively small changes and appear to be the result of the inaccuracies in the measurements. No further conclusions could be drawn at this point.

Two different pre-treatment methods were used. One at 373 K under flowing He for 2 hours mainly to drive off the air and other physically adsorbed gases, the other at 900 K under flowing He for 2 hours to drive off most of the OH groups attached to the tin oxide that contribute to the non-specific adsorption of emission effluent species that might mitigate the catalytic activity. Figure 44 indicates that pretreatment at 900 K results in a higher activity for dry runs, but this effect is reversed for feeds containing water vapor as seen in Table 2. This result was anticipated because the presence of water will replenish the surface hydroxyl groups.

Figure 44 also shows that the presence of equimolar amount of O<sub>2</sub> drastically inhibits the dissociation of NO. In the presence of oxygen, the NO conversion is reduced from 30 % to 13% at 1000 K. The Arrhenius plots shown in Figure 1 indicate that the presence of oxygen and the pretreatment temperature do not significantly affect the activation energy, indicating the presence of the same rate controlling reaction step in all cases.

Figure 45 shows the Arrhenius plots for the NO dissociation in the presence of equimolar amount of oxygen at two different space velocities. It can be seen that the apparent activation energy at the lower space velocity is lower, suggesting the presence of mass transfer limitations at lower space velocities.

**Table 2.** Summary of results for isothermal reaction runs.  $\Delta$ s indicate the difference between the feed and product concentrations in ppm.  $\Sigma\Delta$  indicates the sum of concentration changes for NO, N<sub>2</sub>, and O<sub>2</sub>.

Reactants	Pre-treatment	Flow rate ccpm	Temp. K	$\Delta$ NO	$\Delta$ O <sub>2</sub> /N <sub>2</sub>	$\Sigma\Delta$	Conv. NO
NO+O <sub>2</sub>	He 373 K 2 h	40	1000	-103	1.41	37	9.0
NO+O <sub>2</sub>	He 373 K 2 h	40	1000	-109	1.15	93	9.3
NO+O <sub>2</sub> +H <sub>2</sub> O	He 373 K 2 h	40	1000	-100	1.58	99	8.9
NO+O <sub>2</sub> +H <sub>2</sub> O	He 373 K 2 h	40	900	-114	1.05	636	9.0
NO+O <sub>2</sub> +H <sub>2</sub> O	He 373 K 2 h	40	900	-128	3.44	130	8.1
NO+O <sub>2</sub> +H <sub>2</sub> O	He 373 K 2 h	40	800	-103	0.907	-21	6.4
NO+O <sub>2</sub>	He 373 K 2 h	40	800	-94	1.56	242	5.6
NO+O <sub>2</sub>	He 900 K 2 h	40	1000	-148	1.19	373	12.7
NO+O <sub>2</sub>	He 900 K 2 h	40	950	-141	1.61	171	11.6
NO+O <sub>2</sub>	He 900 K 2 h	40	900	-93	1.06	388	8.0
NO+O <sub>2</sub>	He 900 K 2 h	40	850	-124	1.19	205	9.2
NO	He 900 K 2 h	40	1000	-401	1.30	255	29.7
NO	He 900 K 2 h	40	950	-417	0.968	79	26.3
NO	He 900 K 2 h	40	900	-284	1.24	288	21.5
NO	He 900 K 2 h	40	850	-239	1.34	147	16.3
NO+O <sub>2</sub> +H <sub>2</sub> O	He 900 K 2 h	40	900	-54	2.35	23	4.7
NO+O <sub>2</sub>	He 900 K 2 h	60	850	-43	1	-43	3.5
NO+O <sub>2</sub>	He 900 K 2 h	60	900	-78	1	-38	6.3
NO+O <sub>2</sub>	He 900 K 2 h	60	950	-79	2.91	-36	6.4
NO+O <sub>2</sub>	He 900 K 2 h	60	1000	-110	1.48	-56	9.0

NO+O <sub>2</sub>	He 373 K 2 h	60	900	-75	1.42	85	8.0
NO+O <sub>2</sub>	He 373 K 2 h	60	900	-64	1.09	74	7.3
NO+O <sub>2</sub>	He 373 K 2 h	60	900	-67	1.21	86	6.7
NO+O <sub>2</sub> +H <sub>2</sub> O	He 373 K 2 h	60	900	-65	0.870	79	6.4

Table 3 shows that the presence of water vapor in the feed causes a small decrease in NO conversion for samples pretreated at 373 K, but inhibits catalyst activity significantly for catalysts pretreated at 900 K.

**Table 3.** Effect of water in the feed. Since the 8 % conversion obtained for the reaction of NO + O<sub>2</sub> on catalyst pretreated at 900 K was an outlier, the conversion obtained at 900 K through the regression of the data was also included in the table in brackets.

Reactants	Pre-treatment	Flow rate ccpm	Temp. K	ΔNO	ΔO <sub>2</sub> /N <sub>2</sub>	ΣΔ	Conv. NO
NO+O <sub>2</sub>	He 373 K 2 h	40	1000	-109	1.15	93	9.3
NO+O <sub>2</sub> +H <sub>2</sub> O	He 373 K 2 h	40	1000	-100	1.58	99	8.9
NO+O <sub>2</sub>	He 900 K 2 h	40	900	-93	1.06	388	8.0[9.7]
NO+O <sub>2</sub> +H <sub>2</sub> O	He 900 K 2 h	40	900	-54	2.35	23	4.7
NO+O <sub>2</sub>	He 373 K 2 h	60	900	-67	1.21	86	6.7
NO+O <sub>2</sub> +H <sub>2</sub> O	He 373 K 2 h	60	900	-65	0.870	79	6.4

#### d. Bench scale reactor tests

The results of the runs using 2g 15% Pt/SnO<sub>2</sub> catalyst in the bench scale packed bed reactor system are summarized in Table 4. The results show that, within the concentration ranges used, the NO conversion did not depend significantly on the reactant concentrations.

**Table 4.** Effect of reactant concentrations on NO conversion on the 15% Pt/SnO<sub>2</sub> catalyst at 900 K.

NO conc. ppm	O <sub>2</sub> Conc. ppm	Conversion
630	0	9.9
520	0	10
410	0	10
280	0	9.0
600	900	7.1
750	1500	7.2

### e. NO Dissociation Equilibrium Calculations

The results of chemical equilibrium computations are presented in figures 46 through 52. Figures 46 through 50 indicate that the only effect of excess oxygen is the slight suppression of  $N_2O$  formation. At all temperatures investigated (300 K to 1000 K), equilibrium favors oxygen and nitrogen formation. The equilibrium amounts of  $NO_2$ ,  $NO$  and  $N_2O$  increase with temperature,  $N_2O$  being favored at low temperatures and  $NO$  at high temperatures, the crossover taking place around 750 K. No other nitrogen species exist in the equilibrium mixture below 1000 K.

Figures 51 through 52 show that the addition of inert to  $NO$  suppresses the amount of  $NO_2$  compared to  $NO$  and the crossover takes place at around 600 K. Addition of air to the mixture does not seem to have an effect on the equilibrium composition, but excess oxygen in addition to air favors the formation of  $NO_2$  compared to  $NO$  and increases the crossover temperature.

### f. Long-Term Deactivation Studies

Long-term deactivation results without and with oxygen are given in figures 53 through 56. Both species concentrations and  $NO$  conversions are presented. For each data point presented in figures 54 and 56, mean of the last 3 or 4 measurements were used. The results indicate that the catalysts deactivate slowly. The deactivation of the 15% Pt catalyst during reaction without added oxygen slows down after 24 hours. On the other hand, during the reaction with added oxygen, the catalyst starts deactivating after about 24 hours. Under both conditions, catalysts retained a significant portion of their activity after 50 hours of operation.

### g. Non-catalytic NO Decomposition

To see if there was any non-catalytic decomposition, a TPRx run without the catalyst was made. Figure 57 shows that without the catalyst there is no appreciable  $NO$  decomposition up to 1000K.

## CONCLUSIONS

### a. Temperature Programmed Desorption Studies

- During pulse chemisorption, about half of  $NO$  is either dissociated into  $N_2$  and  $O_2$  or retained on the catalyst at a steady rate. Based on the  $N_2/O_2$  ratio of about 1 and the extent of  $NO$  retention on the catalyst surface, both processes were deemed possible.
- During TPD, the  $N_2$ ,  $N_2O$ , and  $NO$  peaks were separated by about 25 K. There were two  $O_2$  minima, one corresponding to the  $N_2O$  peak and the other to the termination of  $NO$  peak.
- No  $NO_2$  was observed.
- The observed  $NO$  peak could be due to the presence of free surface nitrite or nitrate species, but the presence of  $N_2O_4$  and  $N_2O_3$  is more likely.
- The 25 K separation between the  $N_2$  and  $N_2O$  peaks suggests that these two species are produced, at least partially, by different surface reaction schemes.
- During the TPD after successive adsorptions of  $NO$  and  $O_2$ , the  $N_2O$  and  $NO$  peaks and the single  $O_2$  minima were all observed around 490 K suggesting that in the presence of excess  $O_2$ , both  $N_2O$  and  $NO$  were produced by parallel surface reactions.
- Presence of excess oxygen increased the production of  $N_2O$ .

## **b. Temperature Programmed Reaction Studies**

- There was no NO decomposition below 520 K. Some N<sub>2</sub>O formed above 370 K, which peaked at 520 K, but no N<sub>2</sub>O was present above 750 K. NO desorption started at 520 K and increased with temperature.
- The N<sub>2</sub>O formation on the used catalysts was significantly smaller than that on the fresh catalyst.
- The presence of oxygen inhibits the decomposition of NO and promotes the formation of N<sub>2</sub>O. On catalysts with 15% Pt, some decomposition activity starts around 425 K on fresh catalyst. During the second run, there was no NO decomposition activity up to about 550 K, but significantly less N<sub>2</sub>O formation was observed.
- On fresh catalysts with 10% Pt, there was very little decomposition activity, but at lower temperatures, N<sub>2</sub>O was formed. During the second run, NO dissociation activity increased and N<sub>2</sub>O formation decreased.

## **c. Isothermal Reaction Studies**

- The NO conversion was much lower when O<sub>2</sub> was present in the stream, explicitly illustrating the inhibitory effect of O<sub>2</sub>. Our results show that the presence of equimolar amount of O<sub>2</sub> drastically reduces the conversion from 30 % to 13% for reaction at 1000 K.
- Water in the feed has no significant effect on NO conversion for the catalyst pretreated at 373 K, under the reaction conditions in this study. This is taken as an indication that as long as hydroxyl groups are present on the catalyst, additional water does not significantly influence the reaction process.
- NO conversion was enhanced by pretreating catalysts at 900K for 2h in He (13 % compared to 9 % obtained on the catalyst treated at low temperature). This may be due to the fact that high temperature treatment helps drive off most of the OH groups attached to the tin oxide that contribute to the non-specific adsorption of the effluent species that might mitigate the catalytic activity. Contrary to our prediction, it appears that the OH groups on tin oxide inhibit the NO dissociation. The activity of catalyst increased with reaction temperature. One contributing factor is that the thermal desorption of oxygen from the Pt surface is facilitated at high temperatures, regenerating the active sites of the catalyst.
- The activation energies obtained for the dissociation of NO with and without the presence of O<sub>2</sub> in the feed are about the same (30 kJ/mol) indicating the same rate-controlling step. The relatively low activation energies suggest the presence of mass transfer effects. This was confirmed by the results of the runs at a higher volumetric feed flow rate, which showed a higher activation energy (45 kJ/mol).

## **d. NO Dissociation Equilibrium**

The equilibrium computations showed that the only effect of excess oxygen is the slight suppression of N<sub>2</sub>O formation. At all temperatures investigated (300 K to 1000 K), equilibrium favored oxygen and nitrogen formation. The equilibrium amounts of NO<sub>2</sub>, NO and N<sub>2</sub>O increased with temperature, N<sub>2</sub>O being favored at low temperatures and NO at high temperatures, the crossover taking place around 750 K. No other nitrogen species exist in the equilibrium mixture below 1000 K.

## **e. Long-Term Deactivation Studies**

Without added oxygen in the feed, the deactivation of the catalyst begins immediately and levels off after 24 hour of operation, while with oxygen, the activity is significantly lower, but the deactivation does not start before about 24 hours of reaction. One explanation may be that the presence of oxygen in the gas phase can prevent the loss of lattice oxygen to form surface nitrogen species, thus inhibiting the deactivation of the tin oxide.

## **f. General Conclusions**

The results indicate that although the 15% Pt/SnO<sub>2</sub> catalyst shows promise as a NO decomposition catalyst, as used, does not have sufficient activity at low temperatures to be used as a commercial catalyst. In the utility boiler system, there are two locations convenient for inserting a NO removal reactor: The first one is after the economizer at a temperature of 625 K-725 K; and the second one is after the air preheater at a temperature of 375-425 K. Therefore, the potential NO decomposition catalyst needs to have acceptable activity and selectivity at least in one of these temperature ranges not to require substantial boiler design changes. The selectivity of the catalyst to N<sub>2</sub> and O<sub>2</sub> is good at the temperatures at which the catalyst is active.

One way to improve the catalyst is to use a different method to make it. One way would be to use a sol-gel method to disperse nano-sized Pt or Au particles in a nano-structured SnO<sub>2</sub> support. The dispersion in the support will prevent agglomeration of the active particles and slow the deactivation process. Nano-sized metal particles will be significantly more active and the nano-structured support will provide a much larger surface area. The enhancement of activity may lead to catalysts with lower amounts of active metal.

If the activity of the catalyst could be enhanced to decrease the NO decomposition temperature, attention must be paid to its selectivity, because our results indicate that there may be more N<sub>2</sub>O formation at lower temperatures. The proposed method of catalyst preparation will allow tailoring catalyst properties to increase the selectivity.

To be able to understand the reaction mechanism, reaction equilibrium calculations need to be done including the solid surface nitrogen species. In-situ measurements are need to identify the intermediate species.

## **REFERENCES**

1. Iwamoto, M., Furukawa, H., Mine, Y., Uemura, F., Mikuriya, S., and Kagawa, S., *J. Chem. Soc. Chem. Commun.*, 1272 (1986).
2. Moretti, G., Dossi, C., Fusi, A., Recchia, S., and Psaro, R., *Appl. Catal. B* 20, 67-73 (1999).
3. Tofan, C., Klvana, D., and Kirchnerova, J., *Appl. Catal. A* 223, 275-286 (2002).
4. Tofan, C., Klvana, D., and Kirchnerova, J., *Appl. Catal. A* 226, 225-240 (2002).
5. Tofan, C., Klvana, D., and Kirchnerova, J., *Appl. Catal. B* 36, 311-323 (2002).
6. Pirone, R., Ciambelli, P., Moretti, G., and Russo, G., *Appl. Catal. B*, 197 (1996).

7. Chang, Y. and McCarty J. G., *J. Catal.*, **165**, 1 (1997).
8. Vanice, M. A., Walters, A. B., and Zhang, X., **159**, 119 (1996).
9. Xie, S., Rosynek, M. P., and Lunsford J. H., *J. Catal.*, **188**, 24 (1999).
10. Loof, P., Kasemo, B., Andersson, S., and Frestad A., *J. Catal.*, **130**, 181 (1991).
11. Ogata, A., Obuchi, A., Mizuno, K., Ohi, A., and Ohuchi, H., *J. Catal.*, **144**, 452 (1993).
12. Kudo, A., Steinberg, M., Bard, A. J., Campion, A., Fox, M. A., Mallouk, T. E., Webber, S. E., and White, J. M., *J. Catal.*, **125**, 565 (1990).
13. Herz, R. K., in "Low Temperature CO-Oxidation Catalysts for Long-Life CO<sub>2</sub> Lasers", *NASA Conf. Publ. 3076*, D. R. Schryer and G. B. Hoflund, Eds., pp. 21-40, National Information Service, Springfield, VA, 1990.
14. Schryer, D. R., Upchurch, B. T., Hess, R. V., Wood, G. M., Sydney, B. D., Miller, I. M., Brown, K. G., Van Norman, J. D., Schryer, J., Brown, D. R., Hoflund, G. B., and Herz, R. K., in "Low Temperature CO-Oxidation Catalysts for Long-Life CO<sub>2</sub> Lasers", *NASA Conf. Publ. 3076*, D. R. Schryer and G. B. Hoflund, Eds., pp. 41-53, National Information Service, Springfield, VA, 1990.
15. Upchurch, B. T., Kielin, E. J., and Miller, I. M., in "Low Temperature CO-Oxidation Catalysts for Long-Life CO<sub>2</sub> Lasers", *NASA Conf. Publ. 3076*, D. R. Schryer and G. B. Hoflund, Eds., pp. 69-90, National Information Service, Springfield, VA, 1990.
16. Van Norman, J. D., Brown, K. G., Schryer, J., Schryer, D. R., Upchurch, B. T., Sydney, B. D., in "Low Temperature CO-Oxidation Catalysts for Long-Life CO<sub>2</sub> Lasers", *NASA Conf. Publ. 3076*, D. R. Schryer and G. B. Hoflund, Eds., pp. 181-191, National Information Service, Springfield, VA, 1990.
17. Upchurch, B. T., Wood, G. M., Schryer, D. R., Hess, R. V., Miller, I. M., Kielin, E. J., in "Low Temperature CO-Oxidation Catalysts for Long-Life CO<sub>2</sub> Lasers", *NASA Conf. Publ. 3076*, D. R. Schryer and G. B. Hoflund, Eds., pp. 41-53, National Information Service, Springfield, VA, 1990.
18. Gardner, S. D., Hoflund, G. B., Schryer, D. R., Upchurch, B. T., in "Low Temperature CO-Oxidation Catalysts for Long-Life CO<sub>2</sub> Lasers", *NASA Conf. Publ. 3076*, D. R. Schryer and G. B. Hoflund, Eds., pp. 217-229, National Information Service, Springfield, VA, 1990.
19. Keiser, J. T. and Upchurch, B. T., in "Low Temperature CO-Oxidation Catalysts for Long-Life CO<sub>2</sub> Lasers", *NASA Conf. Publ. 3076*, D. R. Schryer and G. B. Hoflund, Eds., pp. 313-320, National Information Service, Springfield, VA, 1990.
20. Brown, K. G., Ohorodnik, S. K., Van Norman, J. D., Schryer, J., Upchurch, B. T., Schryer, D. R., in "Low Temperature CO-Oxidation Catalysts for Long-Life CO<sub>2</sub> Lasers", *NASA Conf. Publ. 3076*, D. R. Schryer and G. B. Hoflund, Eds., pp. 41-53, National Information Service, Springfield, VA, 1990.
21. Schryer, D. R., Upchurch, B. T., "Low Temperature Oxidation Catalysts: A Mechanistic Overview", unpublished private communication.

22. Akyurtlu, J. F., Akyurtlu, A., and Schryer, D., “Development of Catalysts for Low-Temperature CO Oxidation and NO Decomposition”, presented at Session 373 of the 2002 AIChE Annual Meeting, Indianapolis, Indiana.

## **APPENDIX**

### **a. Presentations**

Akyurtlu, Ates, Akyurtlu, Jale F., Bridges, Wesley, and Jillyan Harlan, “Development of a Novel Catalyst for NO Decomposition” presented at the AIChE 2004 Annual Meeting at Austin, TX, Nov.7-12, 2004.

Xu, Qing, Akyurtlu, Jale F., and Akyurtlu Ates: “Decomposition Of Nitric Oxide By Platinum Supported On Tin Oxide”, Paper 280d presented at the 2006 AIChE Annual Meeting, San Francisco, CA, Nov. 14, 2006.

A paper, entitled “Development of a Novel Catalyst for NO Decomposition” was presented by Ates Akyurtlu at the DOE 2005 University Coal Research/Historically Black Colleges and Universities and Other Minority Institutions Contractors Review Conference.

### **b. Student Participants**

Shaia Anderson, Shanitra Sanders, Jilyan Harlan, Victor Robers, Valerie Brown, and Wesley Bridges.

Post-doctoral associate: Qing Xu

## **FIGURES**

Figure 1. Species evolved during injections of 1-ml doses of 1.94% NO in He on 15% Pt/SnO<sub>2</sub> catalyst at 313 K. (Run 1)

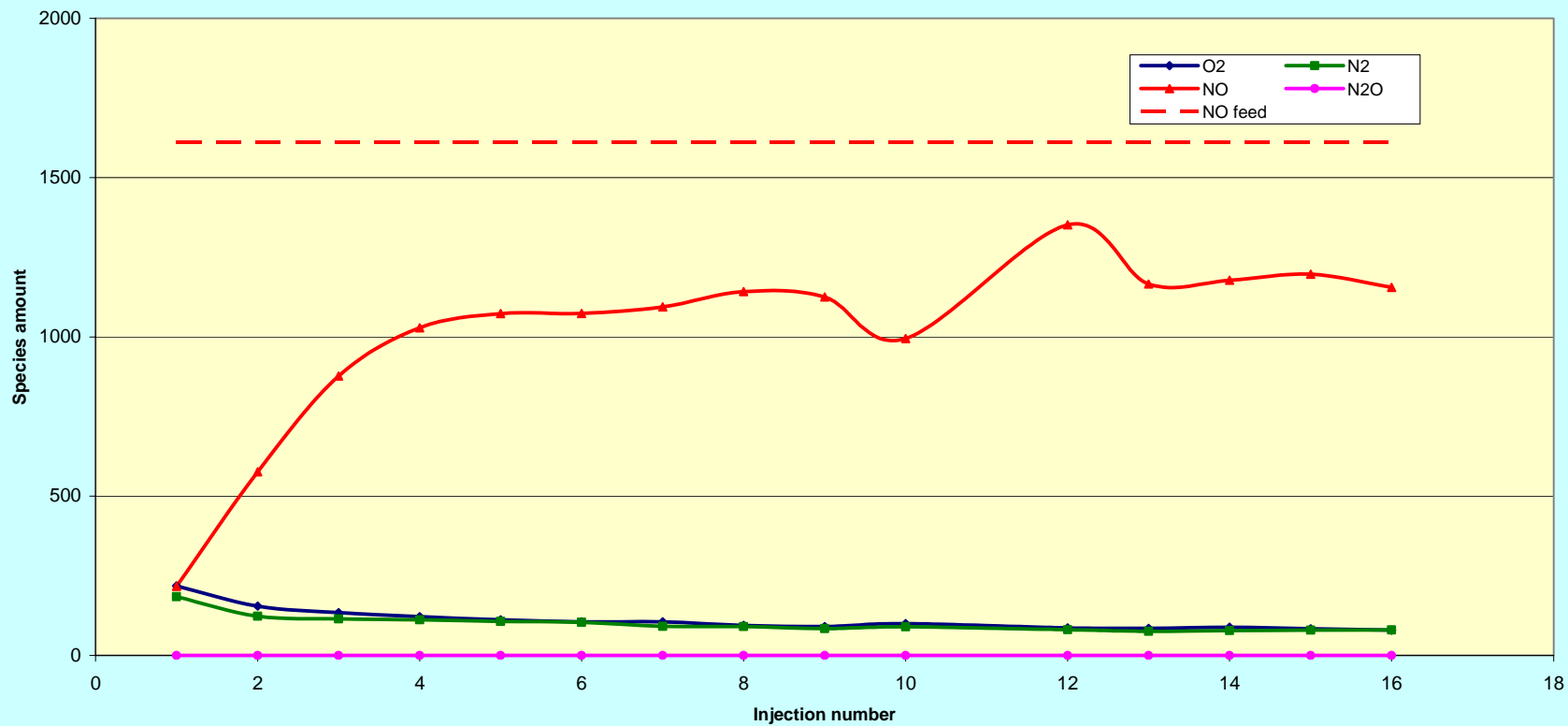


Figure 2. Species evolved during injections of 1-ml doses of 1.6% NO in He on 15% Pt/SnO<sub>2</sub> catalyst at 40°C. (Run 2)

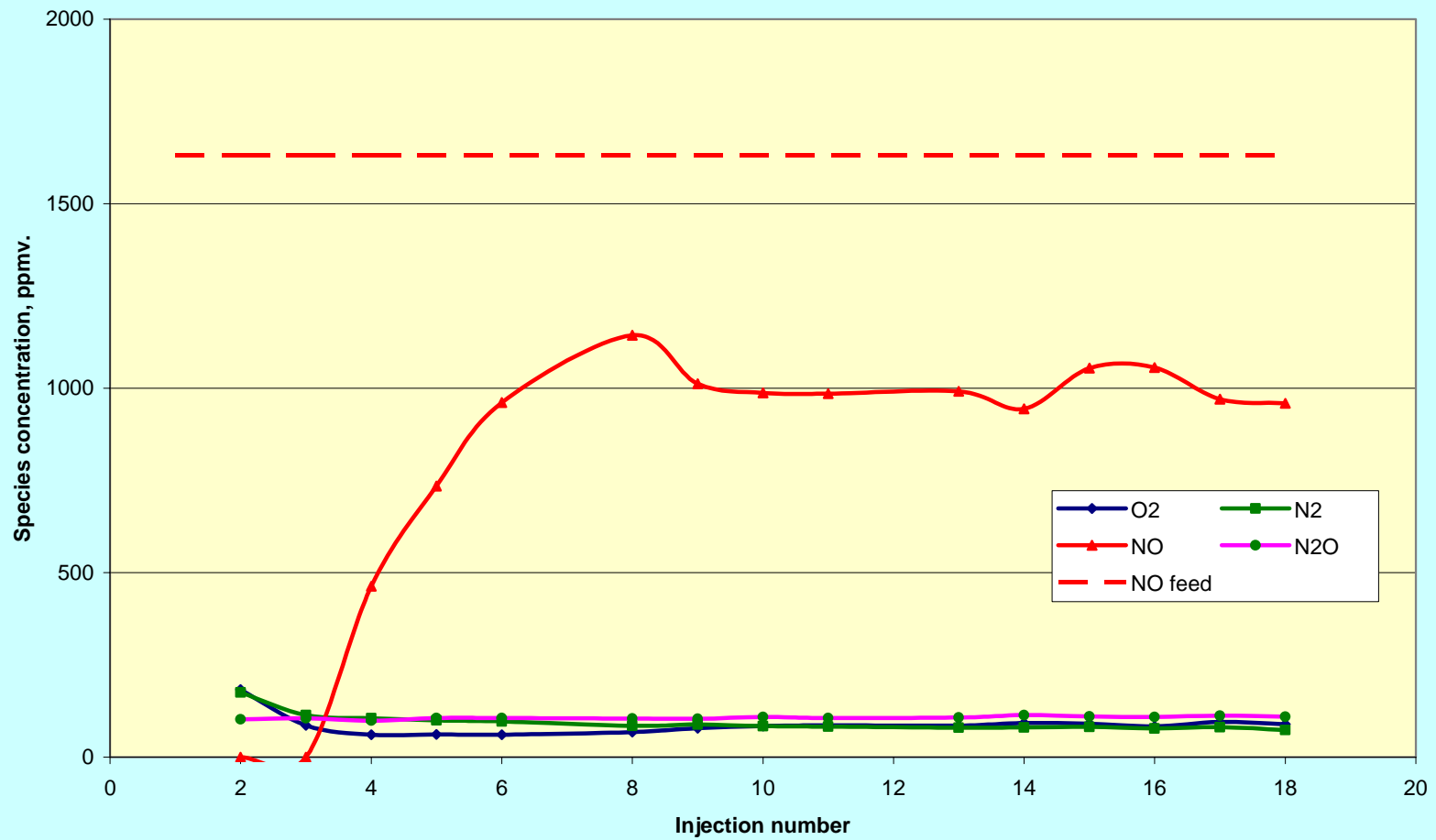


Figure 3. Species evolved during injection of 1-ml doses of 1.6%NO in He on 15% Pt/SnO<sub>2</sub> catalyst at 40°C. (Run 3)

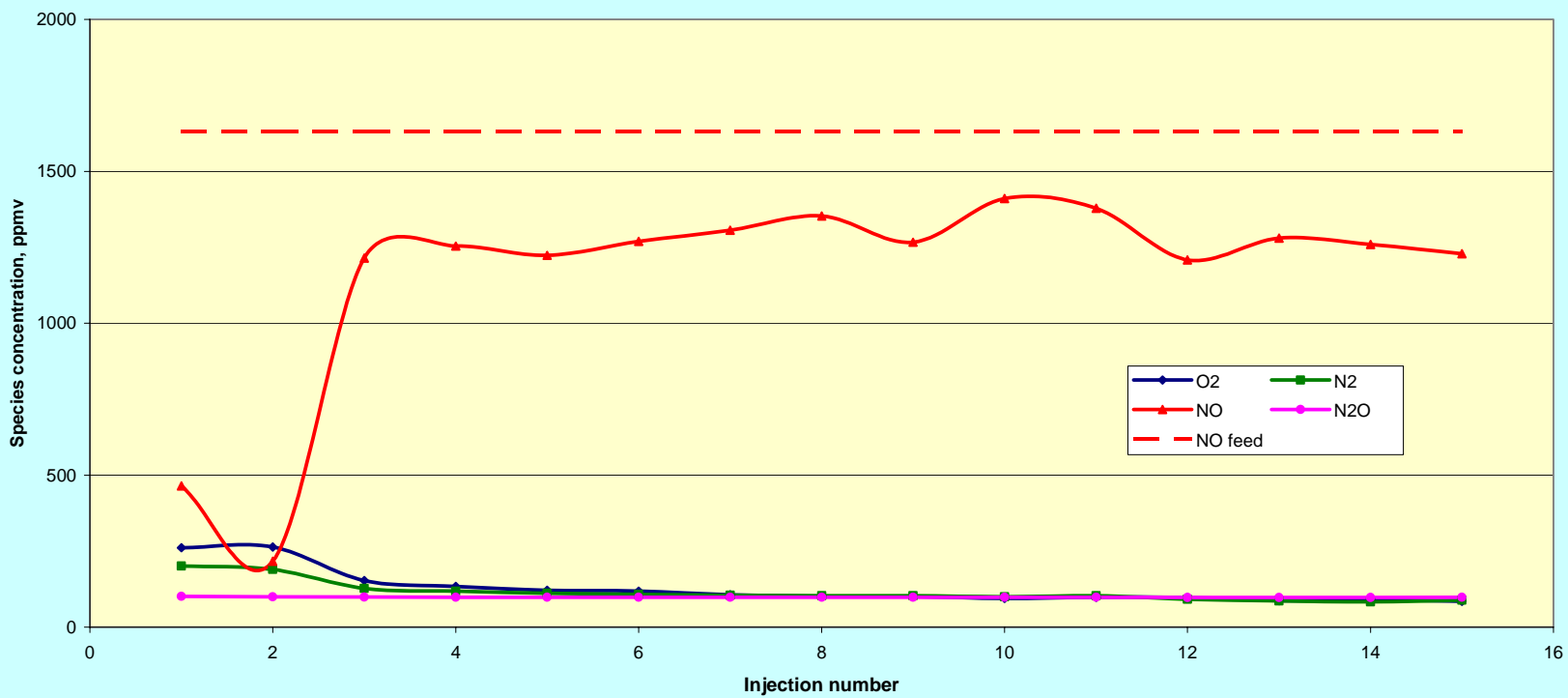


Figure 4. Species evolved during injection of 1-ml doses of 3.6% O<sub>2</sub> in He on 15% Pt/SnO<sub>2</sub> catalyst after treatment with NO, at 313 K.

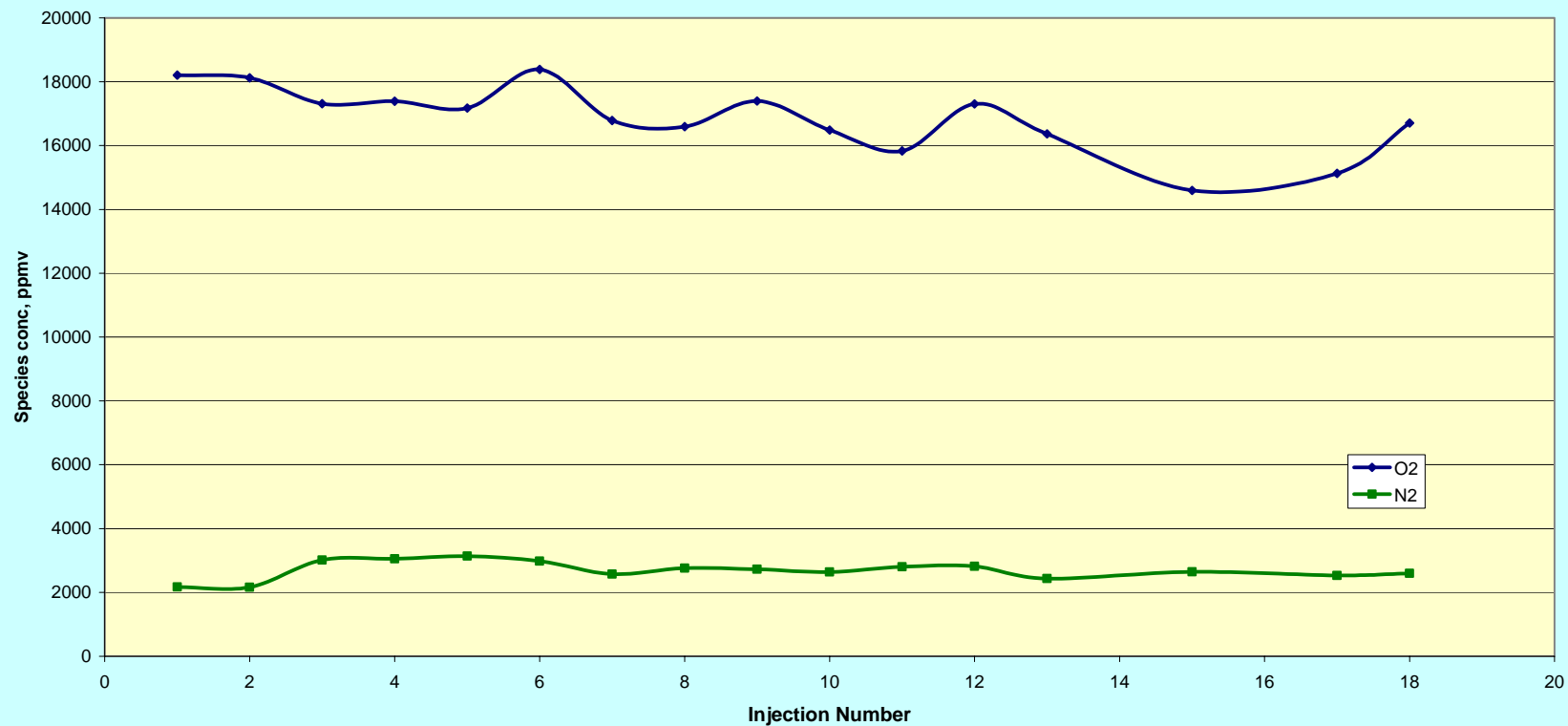


Figure 5. Species evolved during TPD after treatment of 15% Pt/SnO<sub>2</sub> catalyst with NO at 313 K.

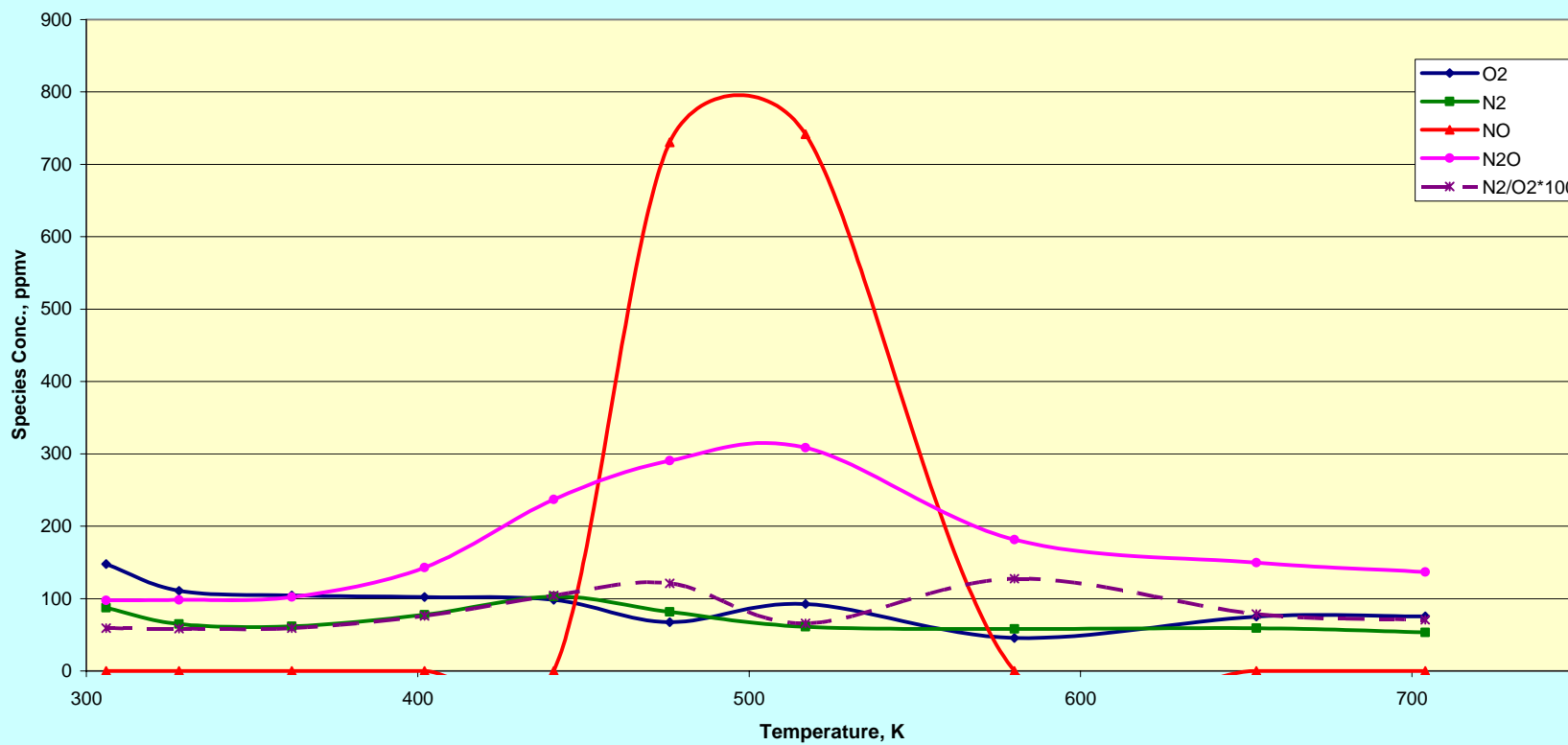


Figure 6. Species evolved during TPD after the treatment of 15% Pt/SnO<sub>2</sub> catalyst with NO and O<sub>2</sub> subsequently at 313K.

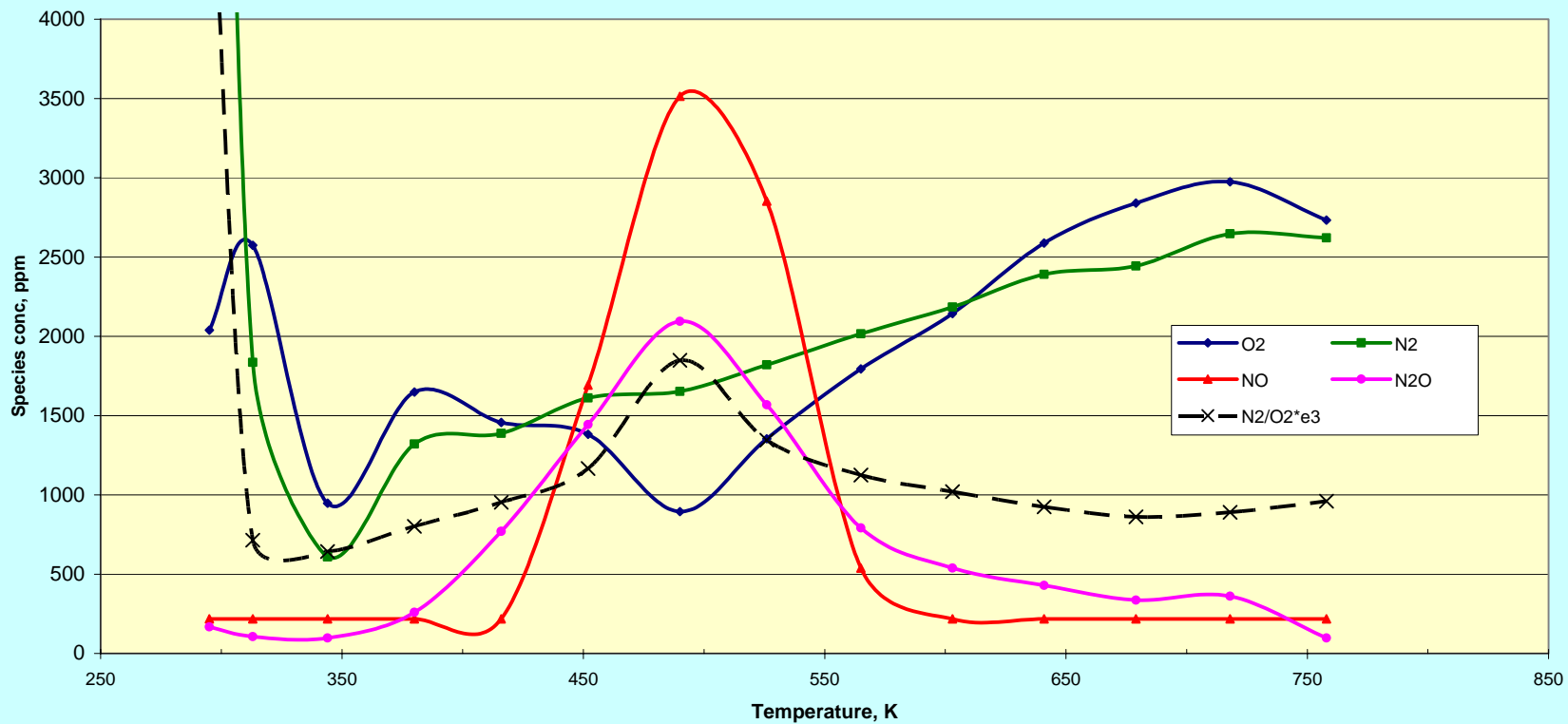


Figure 7. TPRx of NO on Fresh15% Pt/SnO2 Catalyst

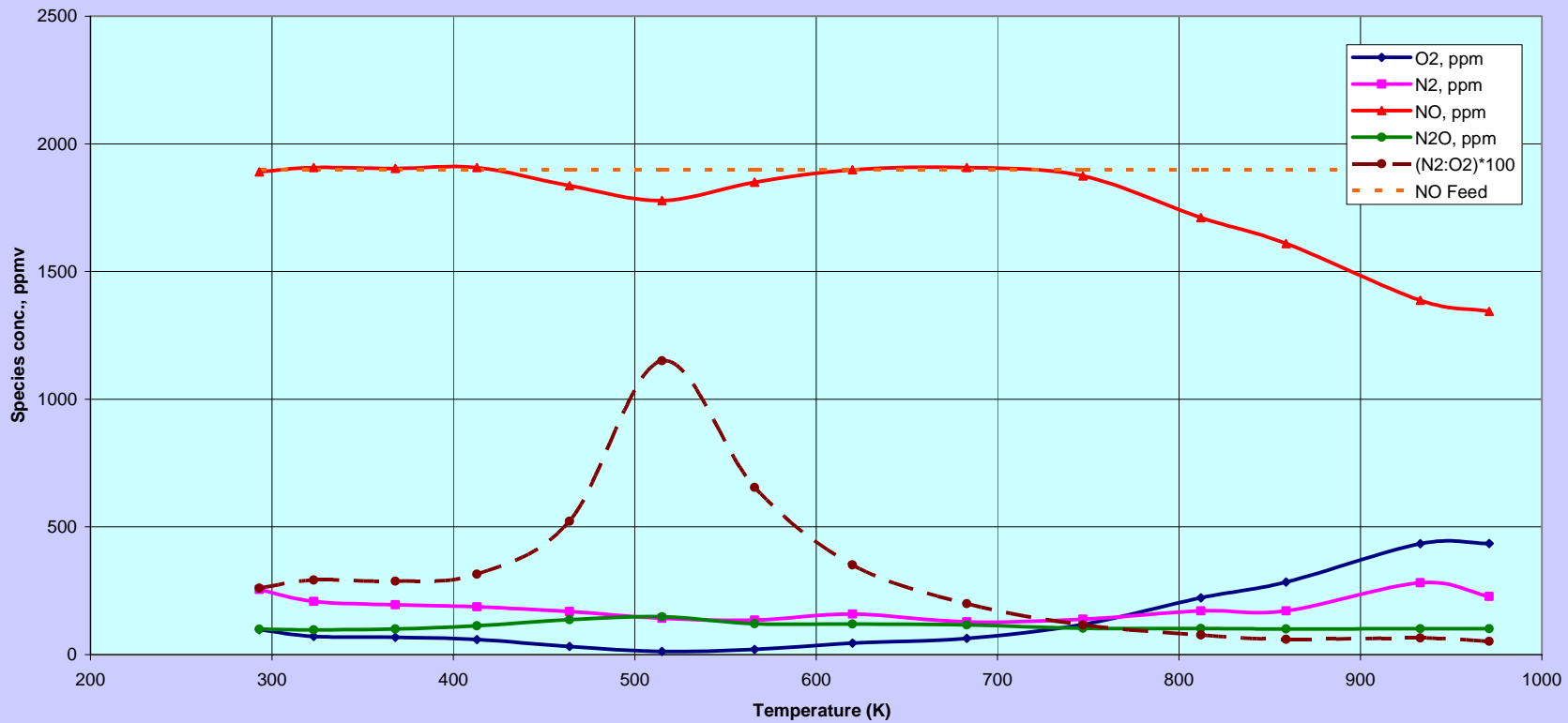


Figure 8. Second TPRx run of NO on 15% Pt/SnO<sub>2</sub> Catalyst.

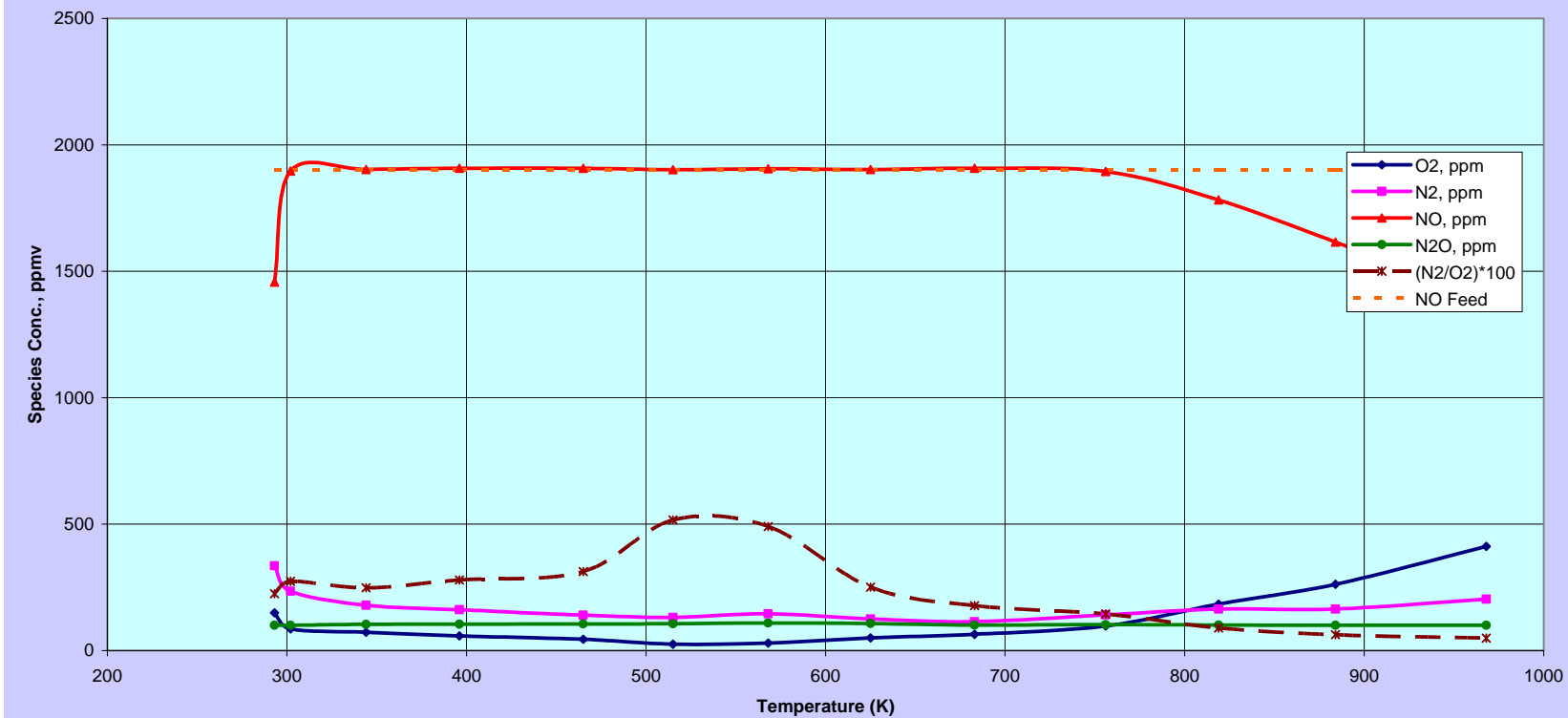


Figure 9. Third TPRx run of NO on 15% Pt/SnO2 Catalyst.

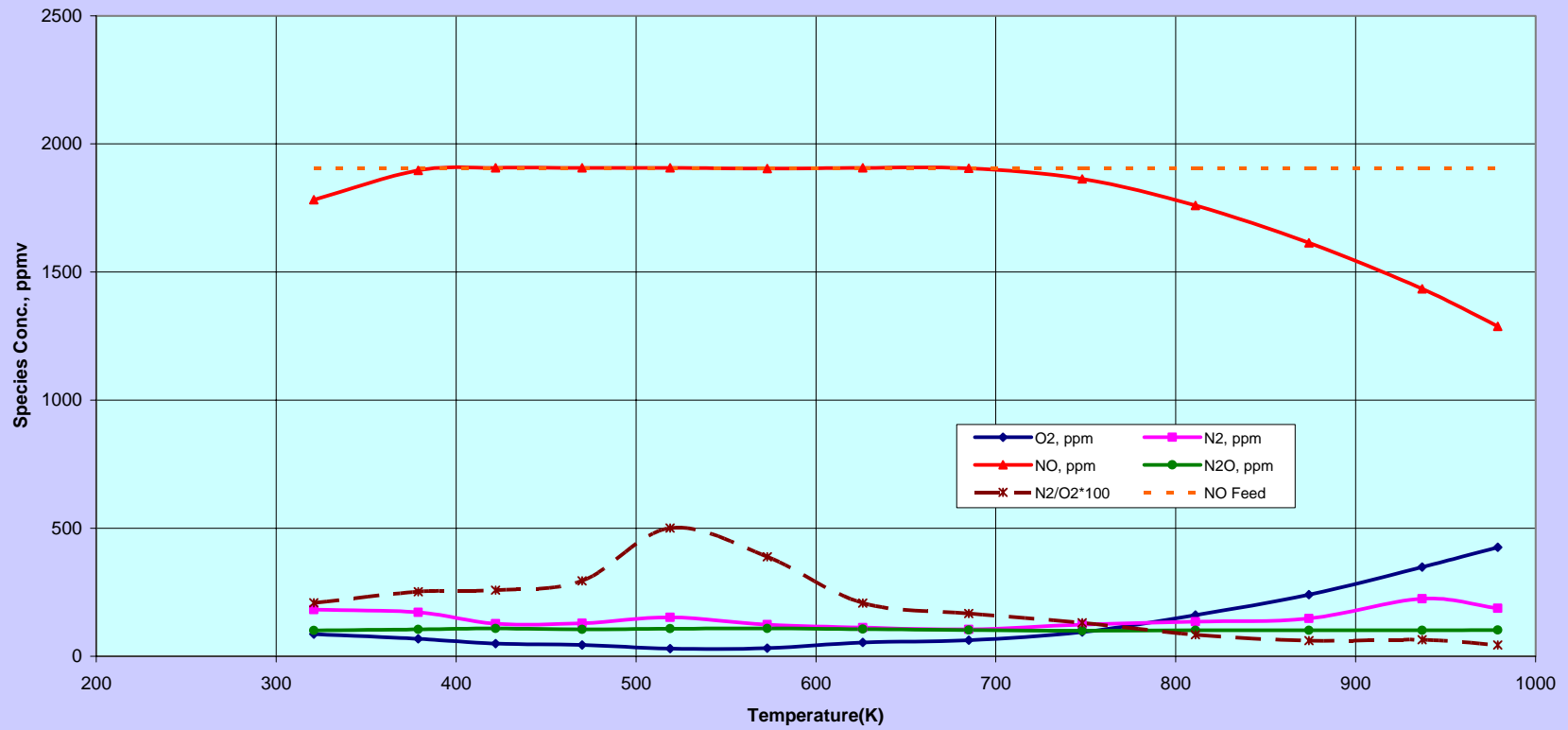


Figure 10. TPReaction on fresh NASA 15% Pt/SnO<sub>2</sub> Catalyst. Feed O<sub>2</sub>/NO=2

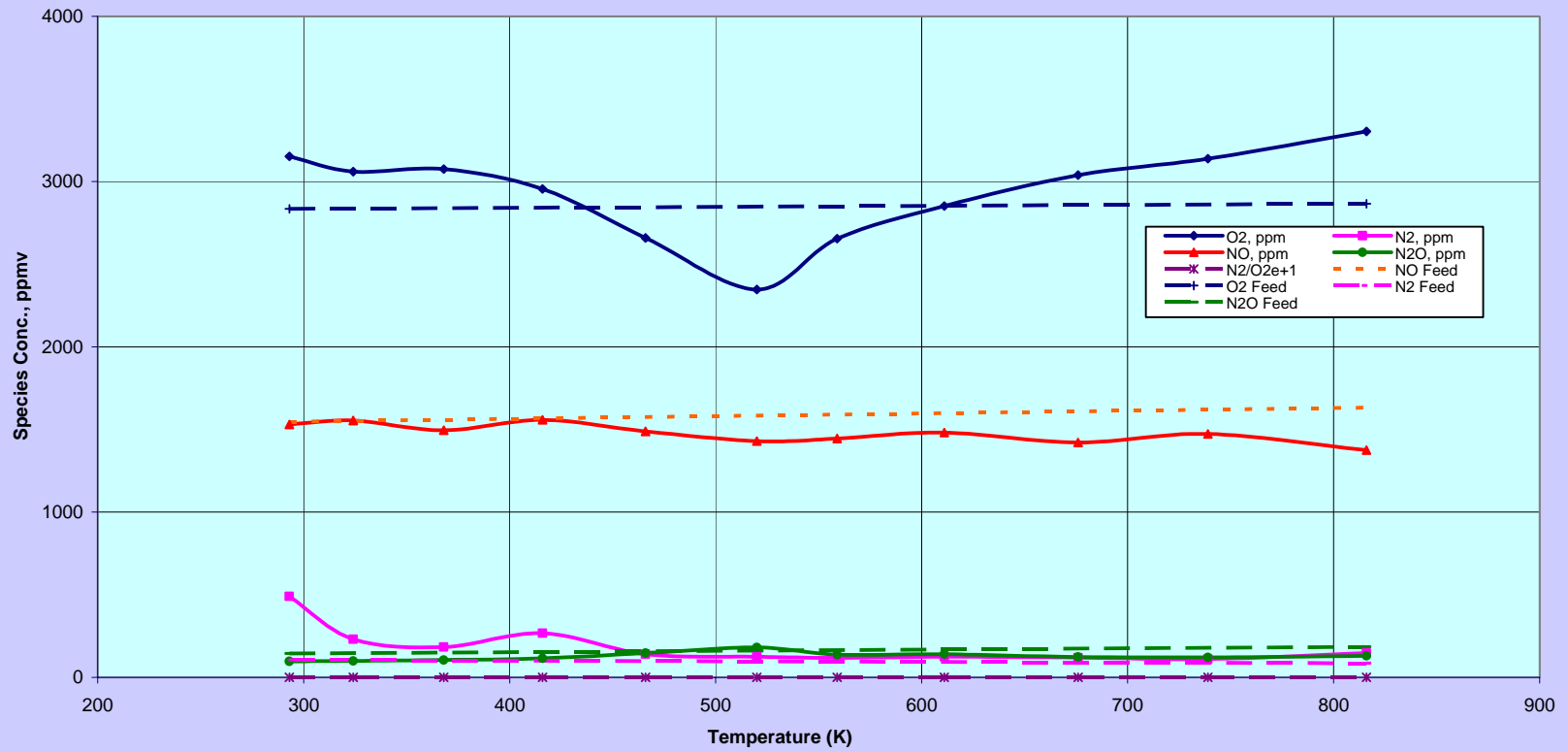


Figure 11. Second TPReaction Run on NASA 15% Pt/SnO<sub>2</sub> Catalyst. Feed O<sub>2</sub>/NO=2

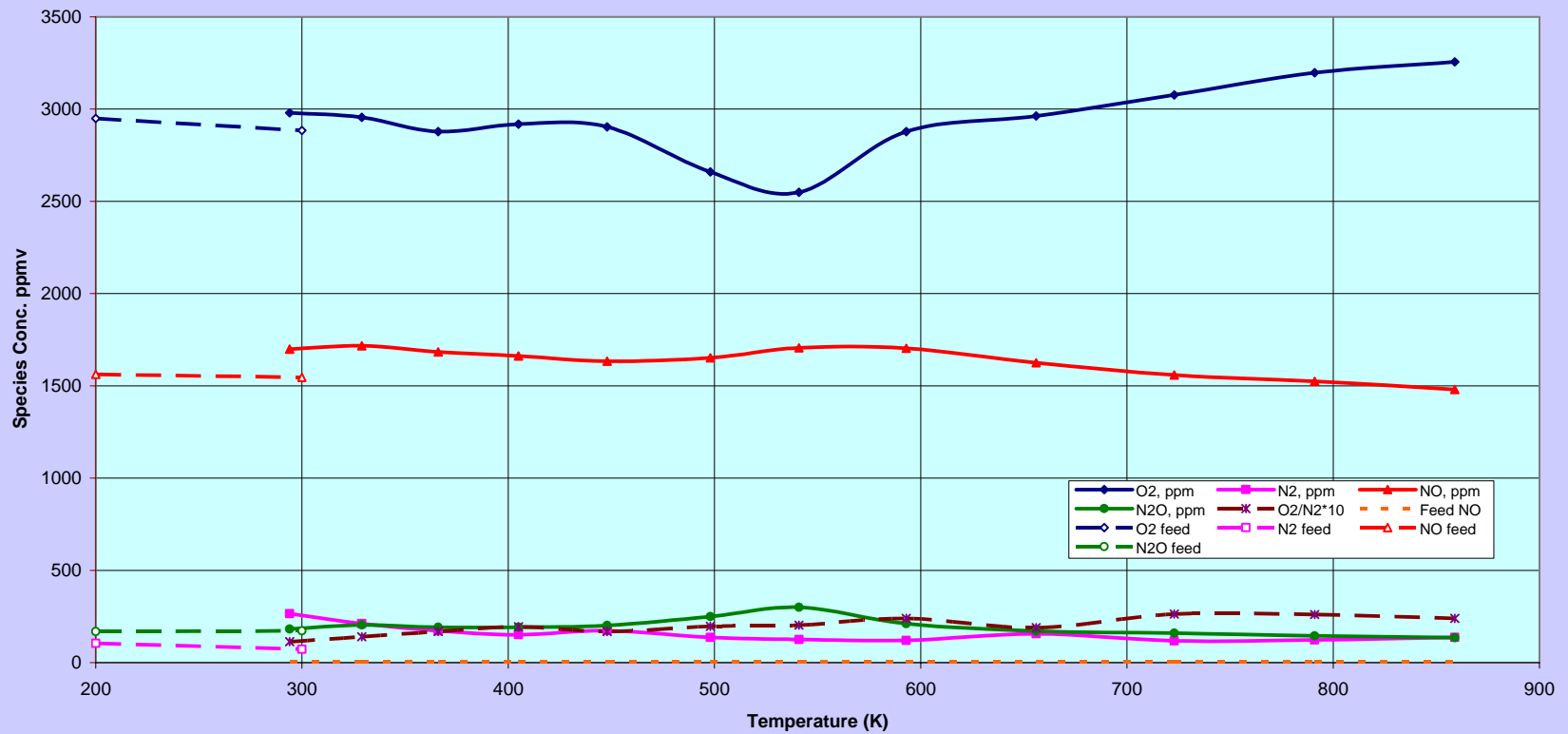


Figure 12. TPRx on Fresh NASA 15% Pt/SnO<sub>2</sub> Catalyst. Feed O<sub>2</sub>/NO= 1

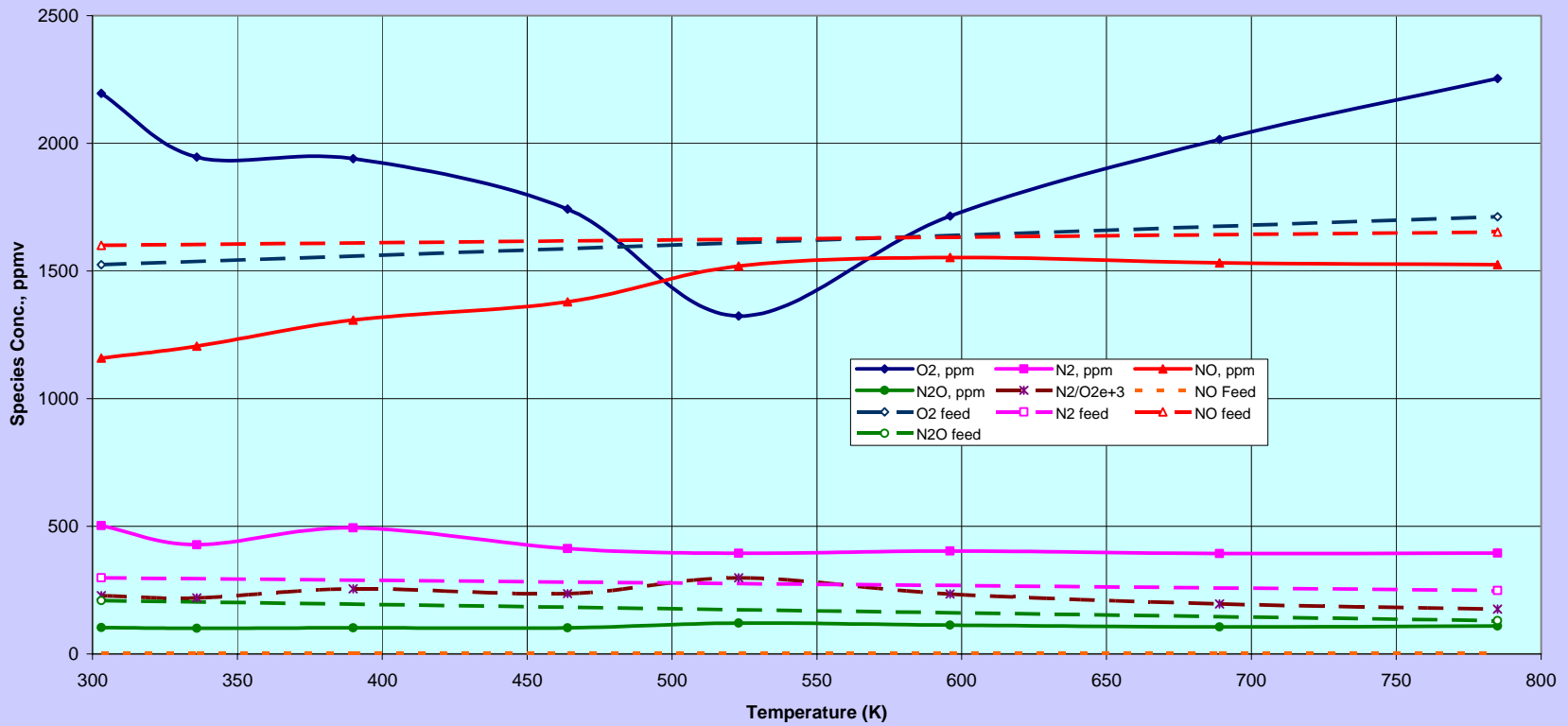


Figure 13. TPRx of NO on Fresh 10% Pt/SnO<sub>2</sub> Catalyst. Feed Gas NO in He

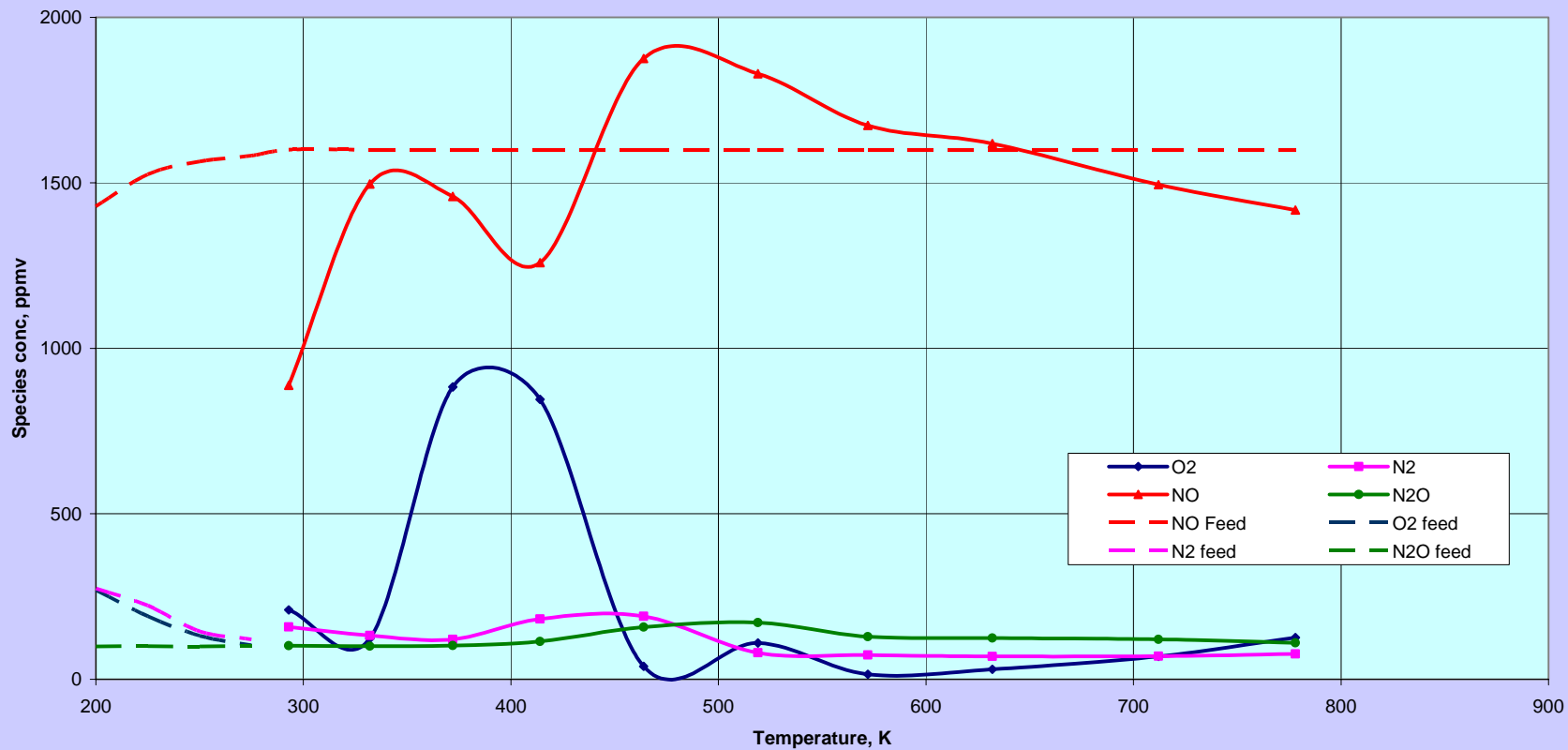


Figure 14. Second TPRx of NO on 10% Pt/SnO<sub>2</sub> Catalyst. Feed Gas NO in He

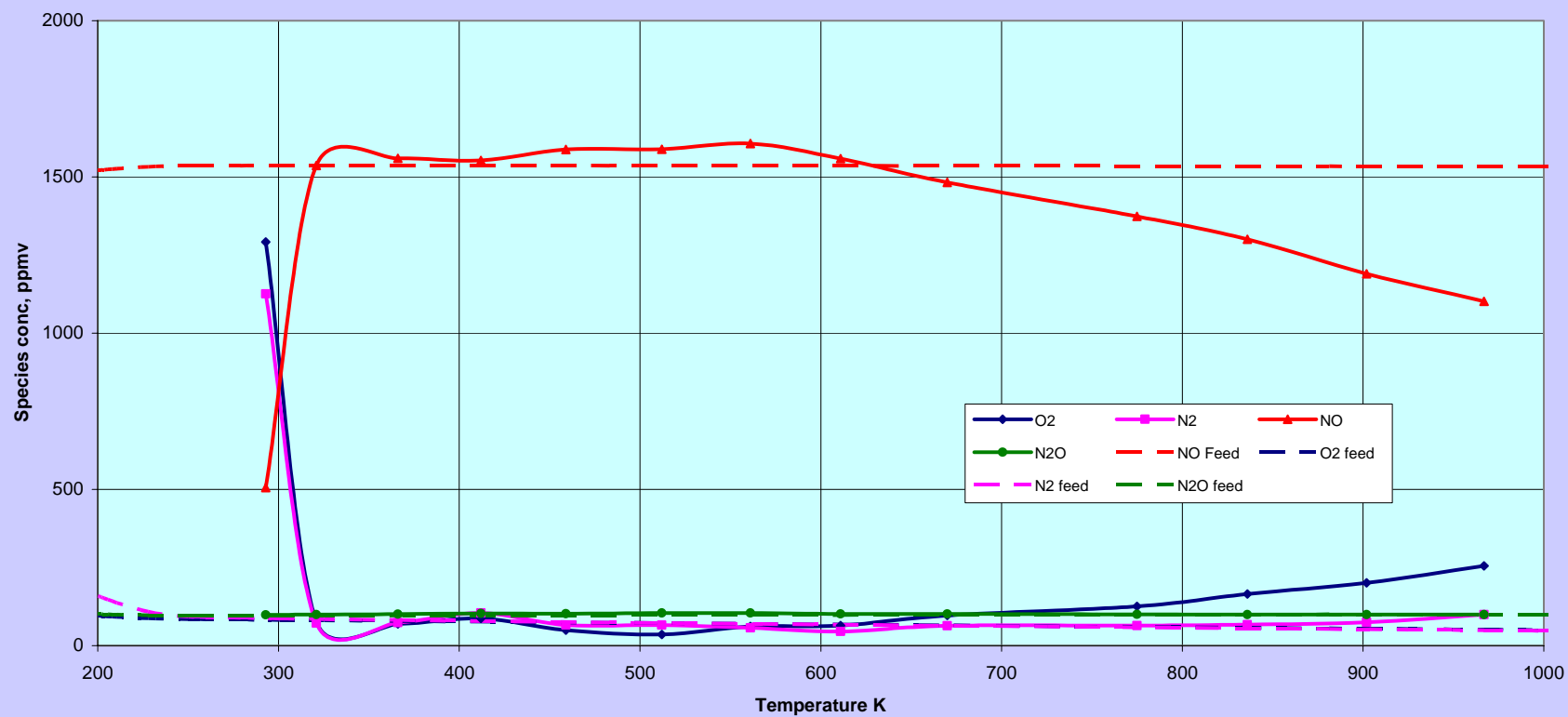


Figure 15. Third TPRx of NO on 10% Pt/SnO<sub>2</sub> Catalyst. Feed Gas NO in He

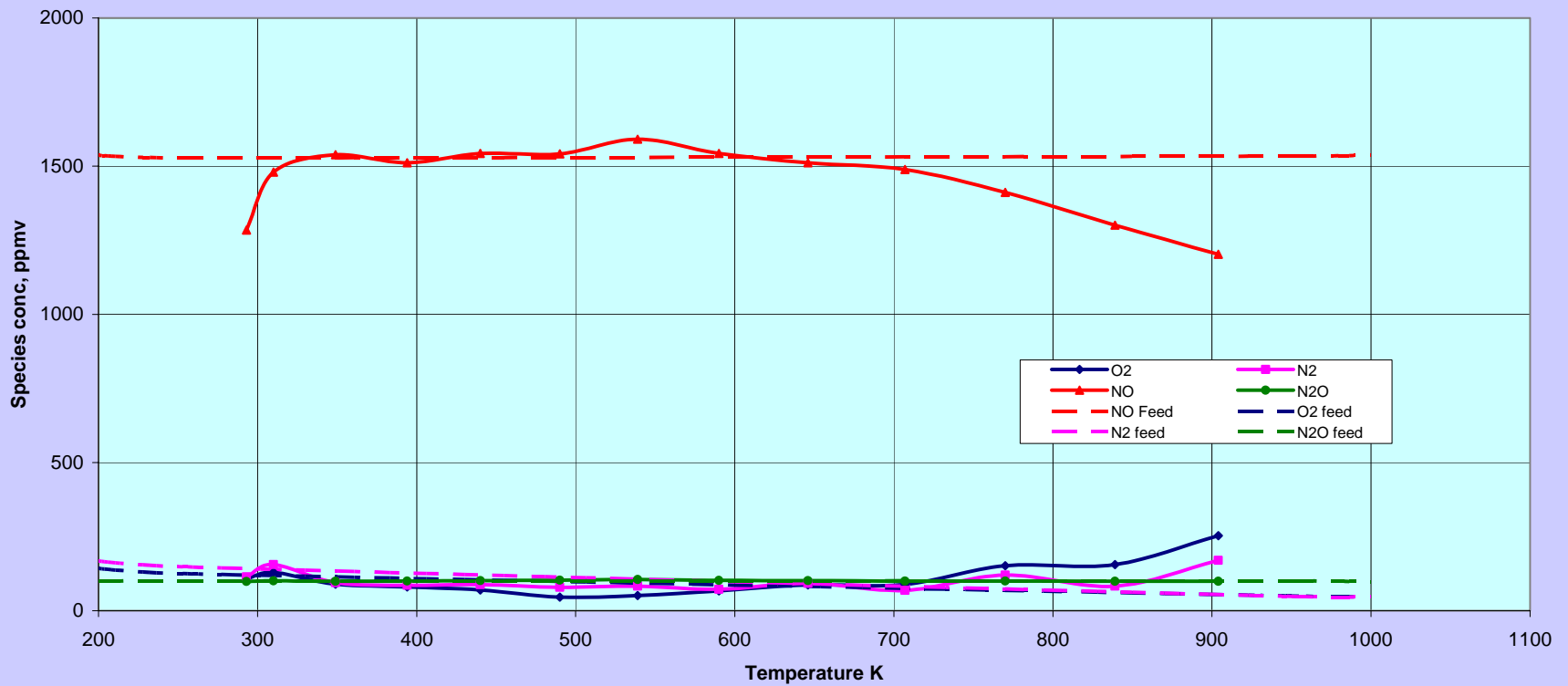


Figure 16. Fourth TPReaction of NO on 10% Pt/SnO<sub>2</sub> Catalyst. Feed Gas NO in He

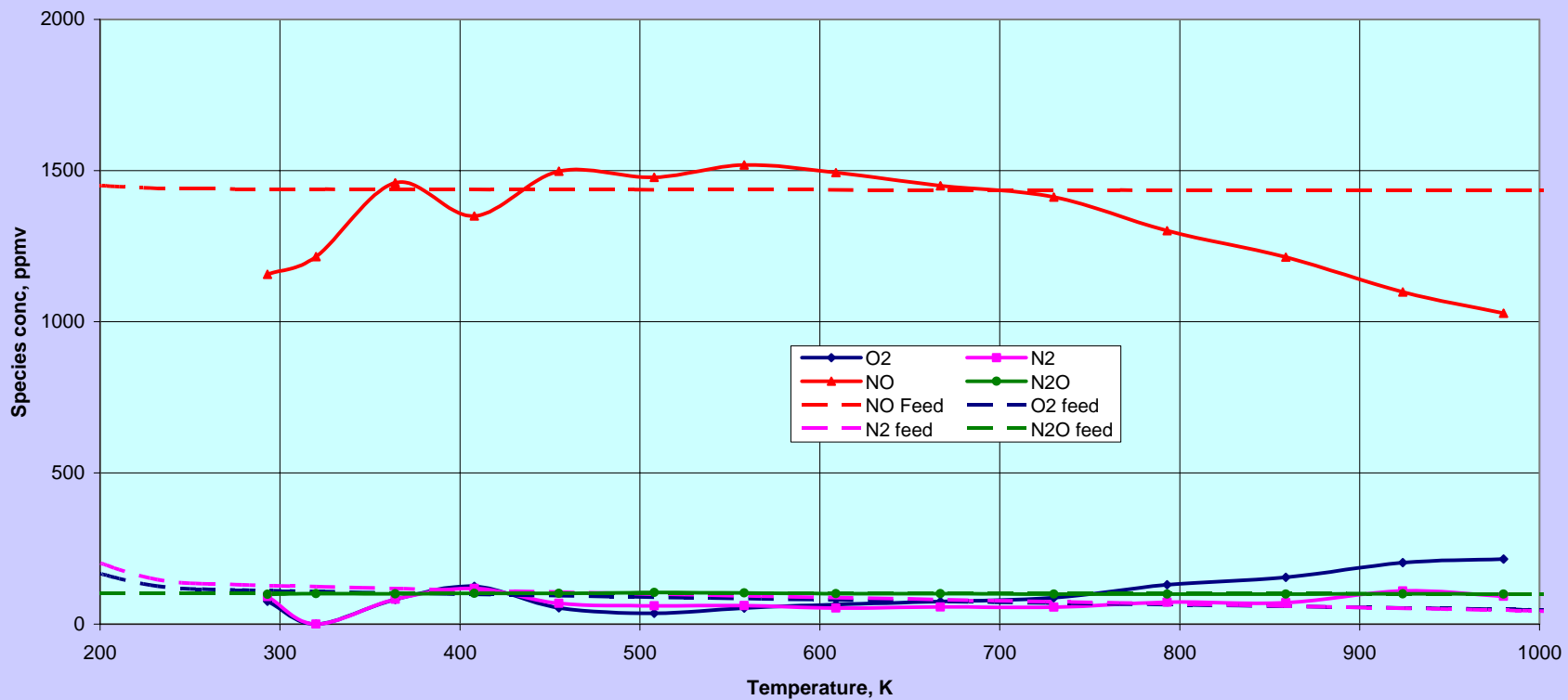


Figure 17. TPRx of NO+O<sub>2</sub> on Fresh10% Pt/SnO<sub>2</sub> Catalyst. Feed O<sub>2</sub>/NO= 1

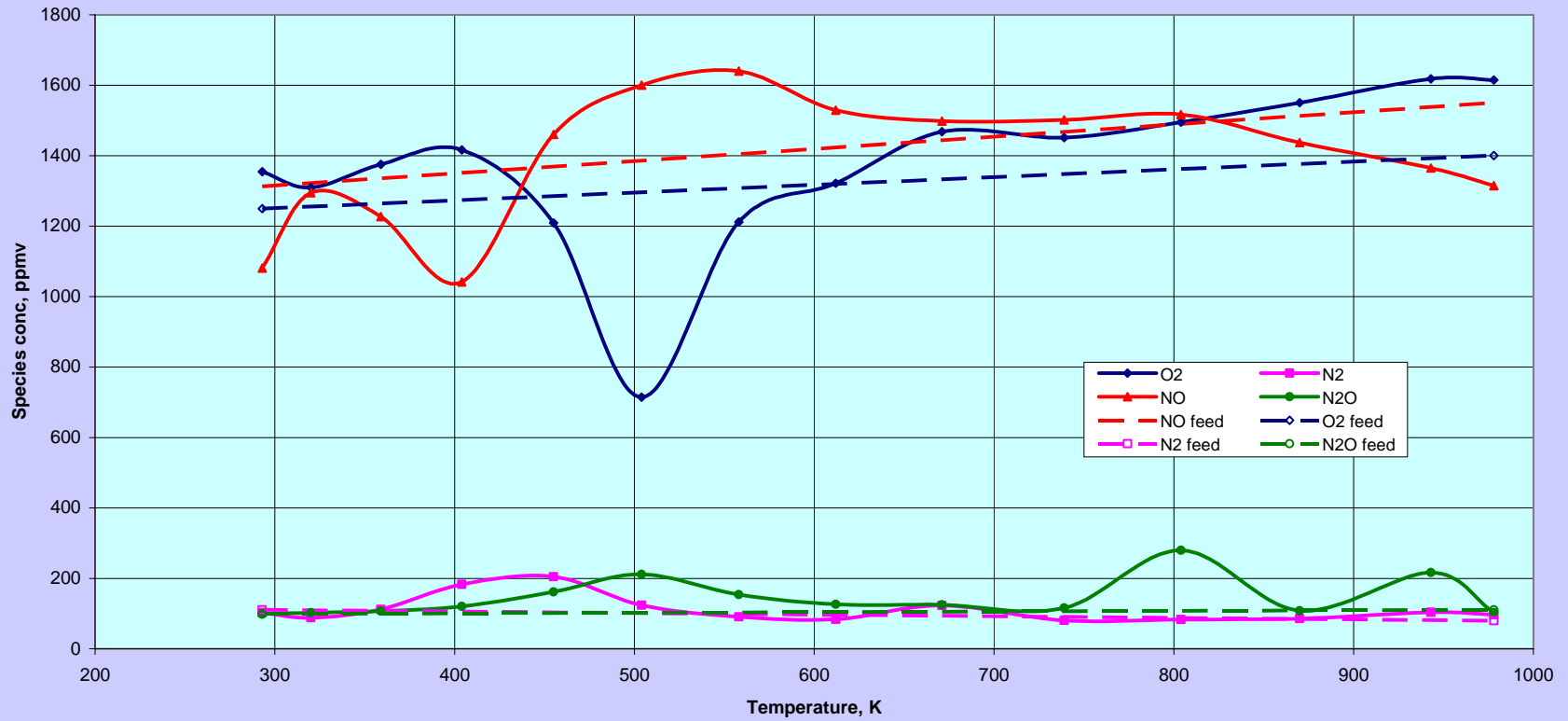


Figure 18. Second TPRx of NO+O<sub>2</sub> on 10% Pt/SnO<sub>2</sub> Catalyst. Feed O<sub>2</sub>/NO= 1

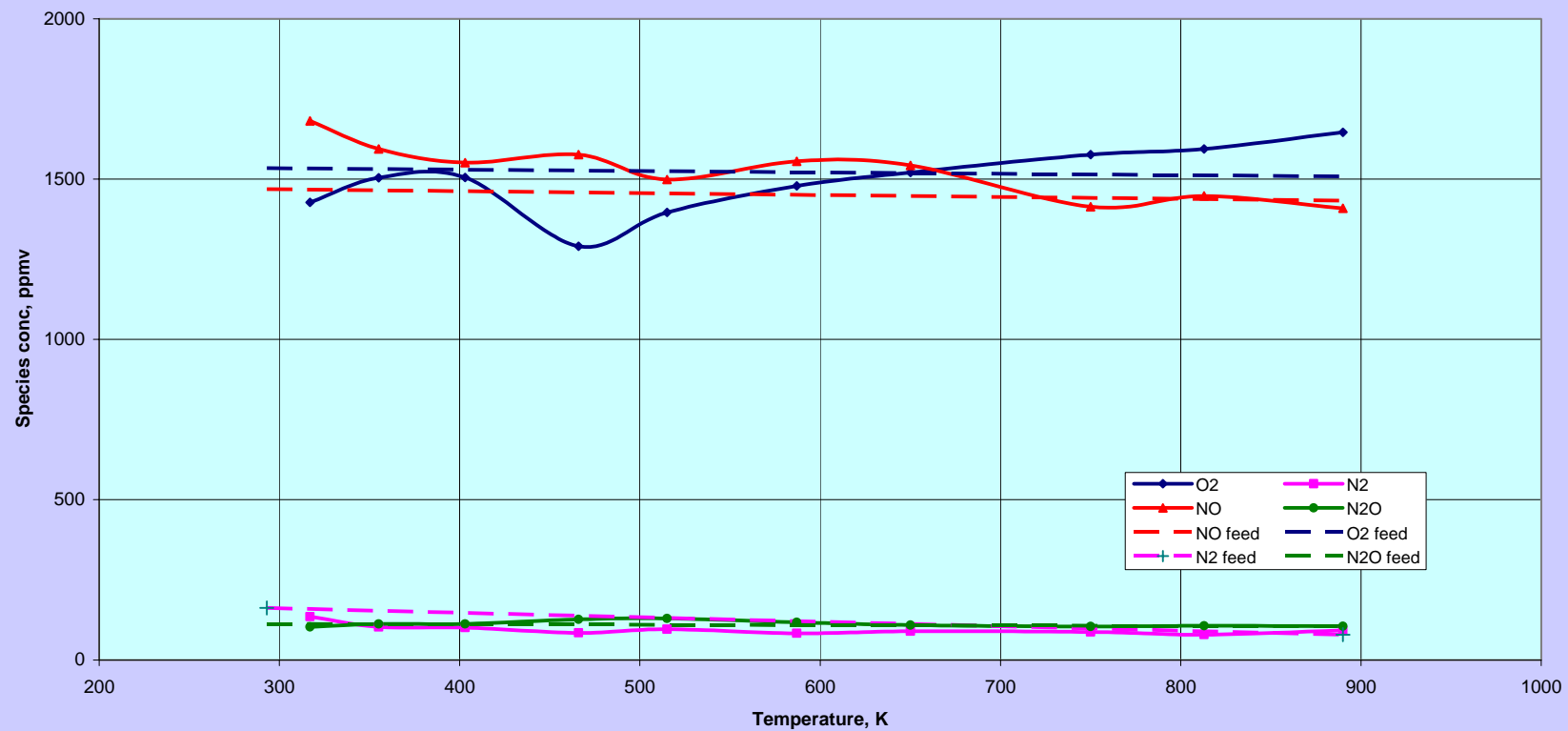


Figure 19. Third TPRx of NO+O<sub>2</sub> on 10% Pt/SnO<sub>2</sub> Catalyst. Feed O<sub>2</sub>/NO= 1

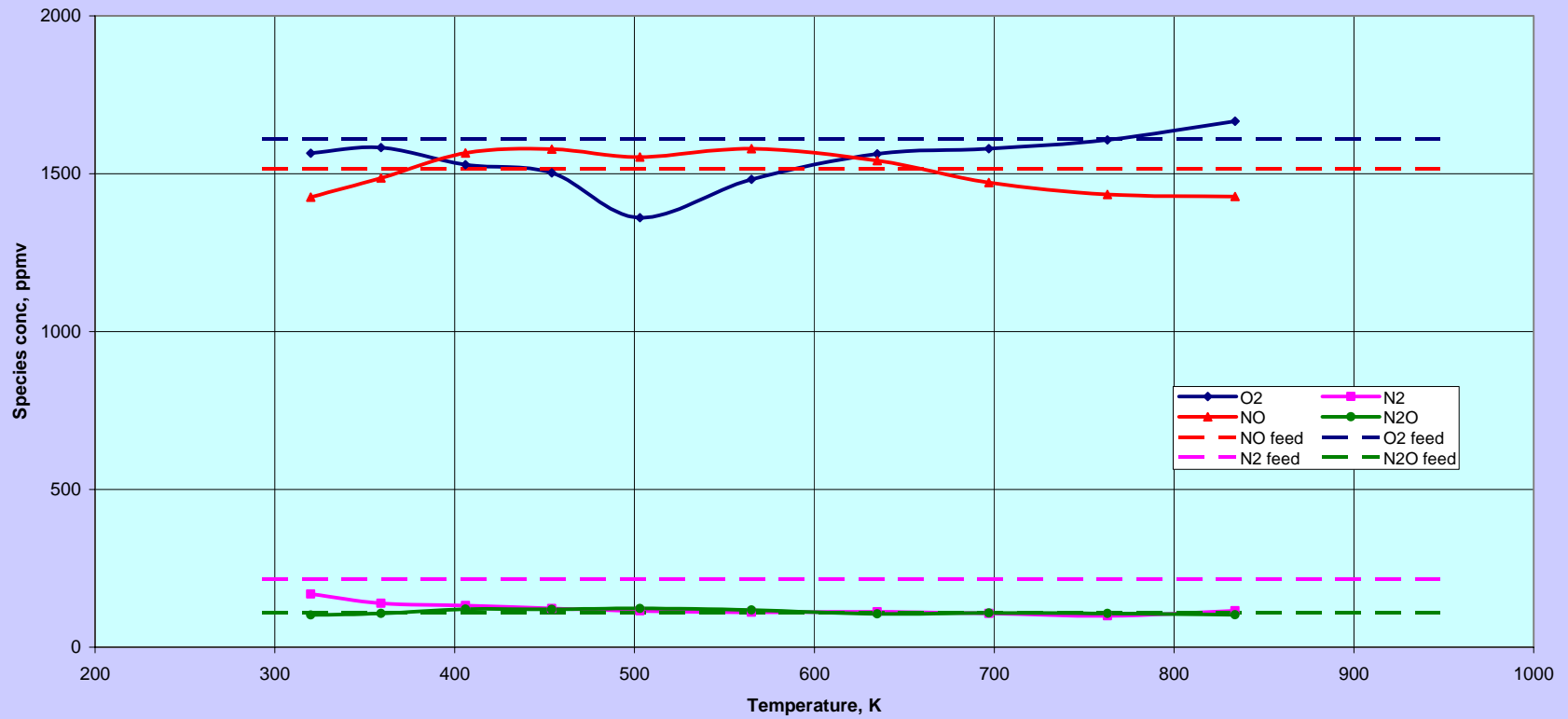


Figure 20. TPRx of NO+O<sub>2</sub>+H<sub>2</sub>O on 15%Pt/SnO<sub>2</sub> Catalyst. O<sub>2</sub>/NO=0.5

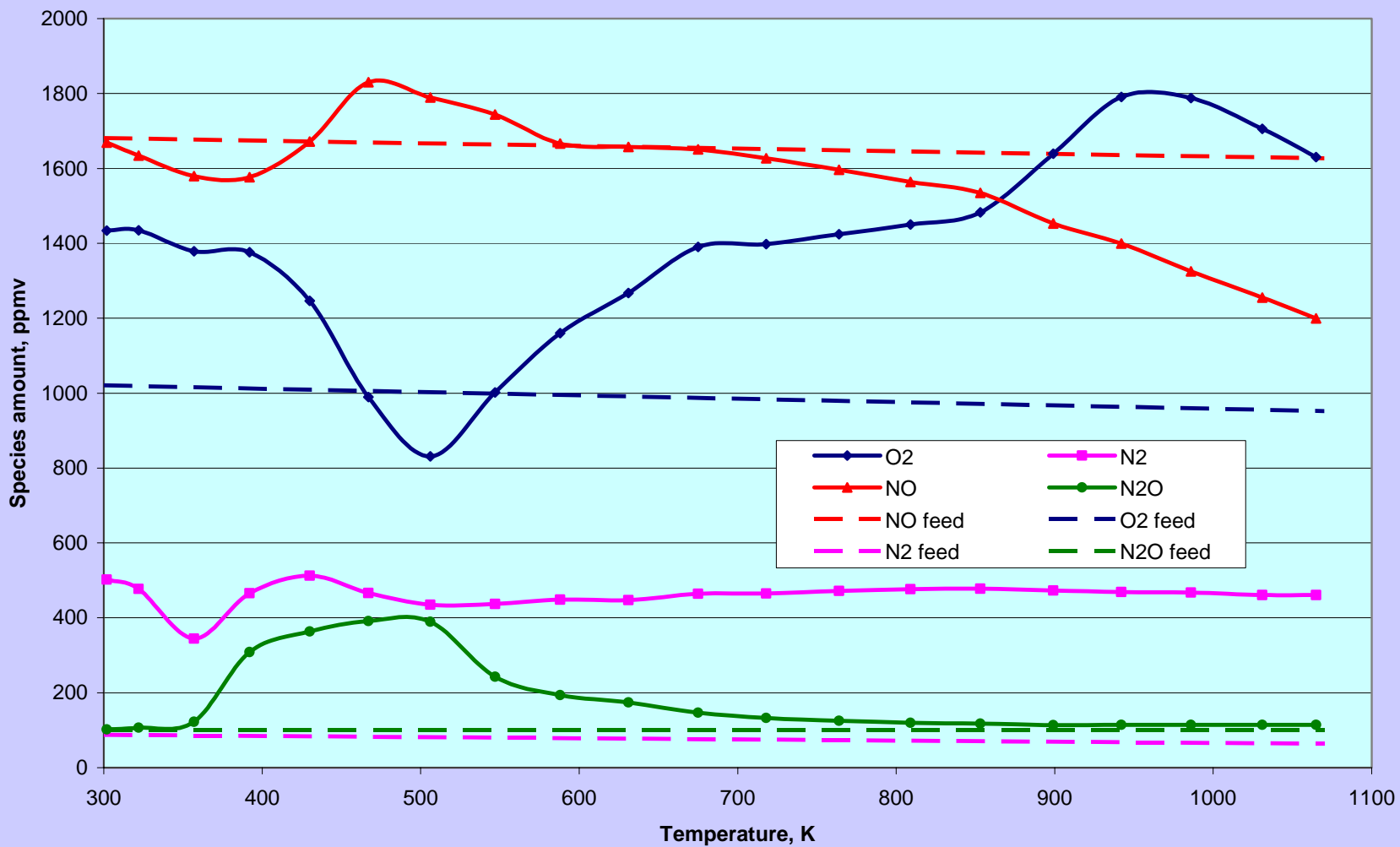


Figure 21. Arrhenius plot for TPRx of NO+O<sub>2</sub>+H<sub>2</sub>O on 15%Pt/SnO<sub>2</sub> catalyst

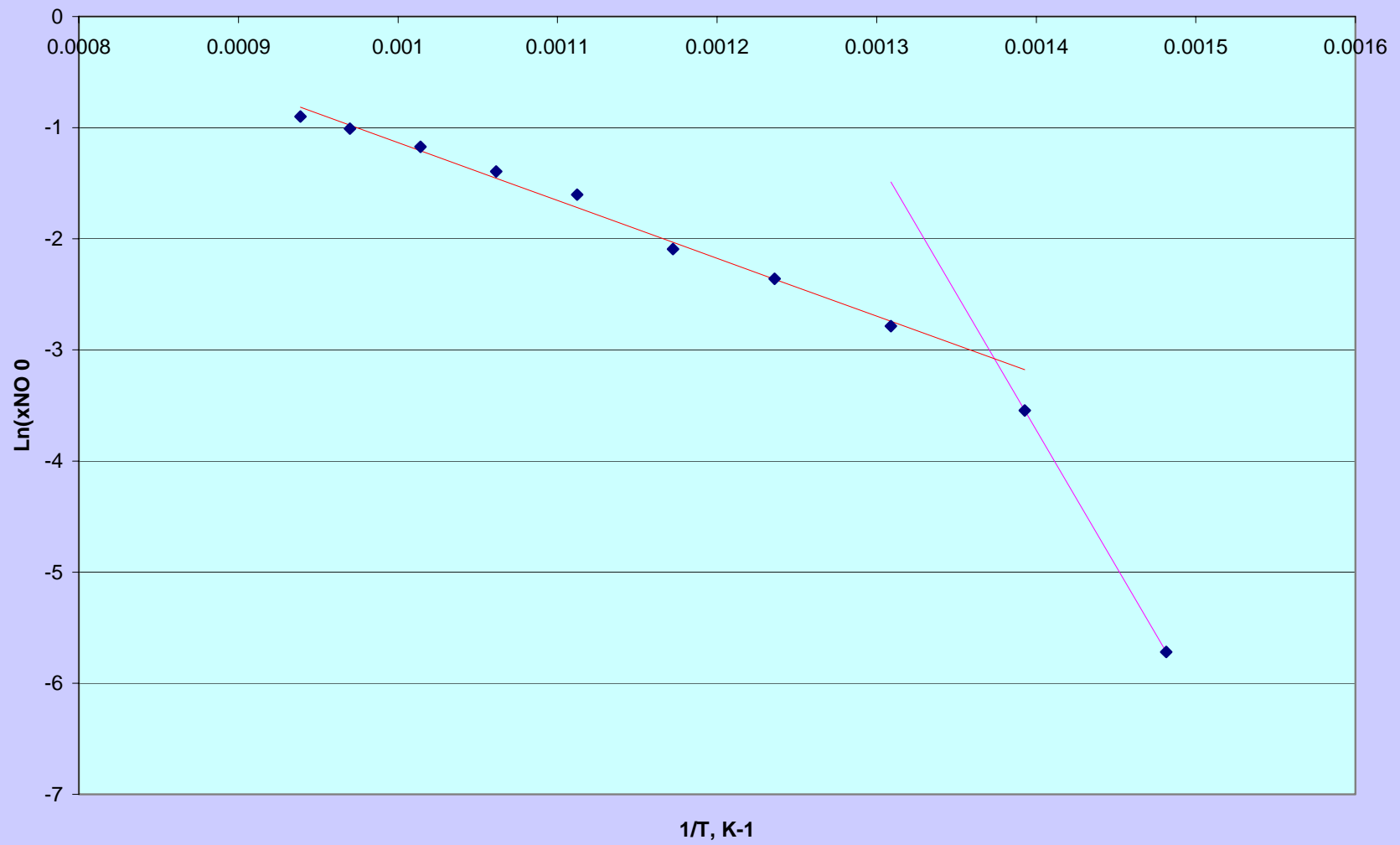


Figure 22. Isothermal Reaction of NO+O2 on 15%Pt%SnO2 at 900K, 1st run

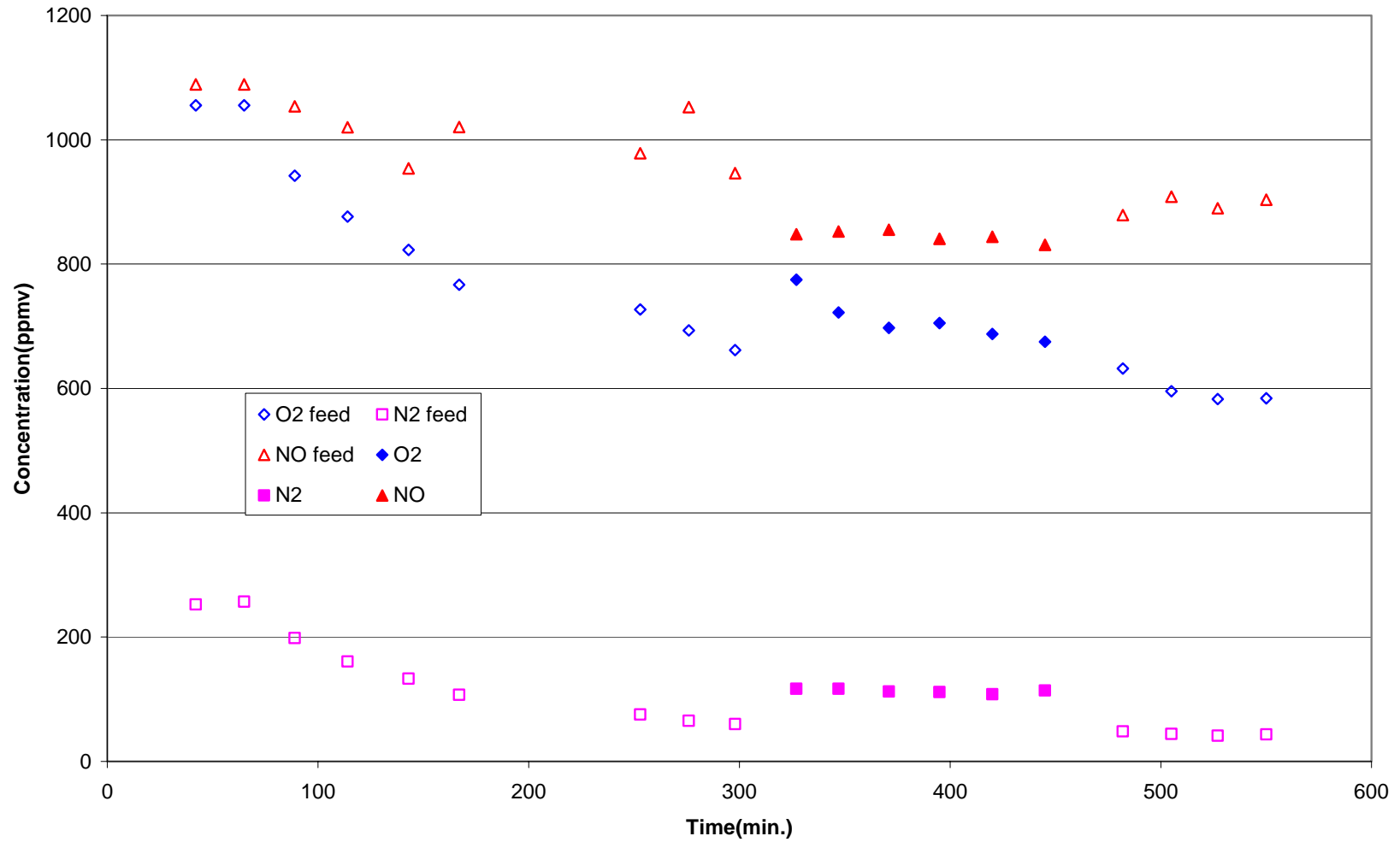


Figure 23. Isothermal Reaction of NO+O2 on 15%Pt%SnO2 at 900K, 2nd run

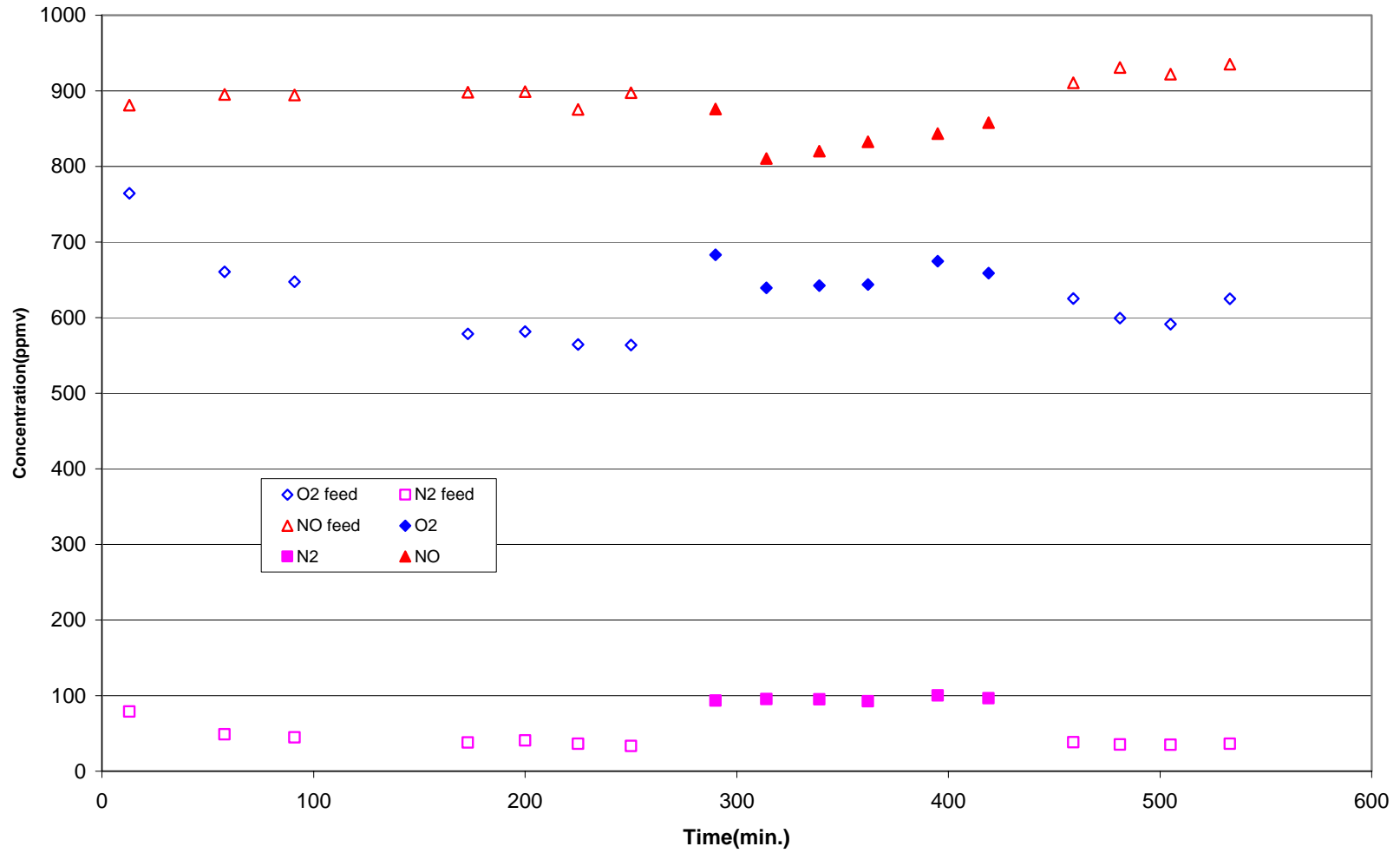


Figure 24. Isothermal Reaction of NO+O<sub>2</sub> on 15%Pt%SnO<sub>2</sub> at 900K, 3rd run  
60sccm,dry. Pretreated at 373 K

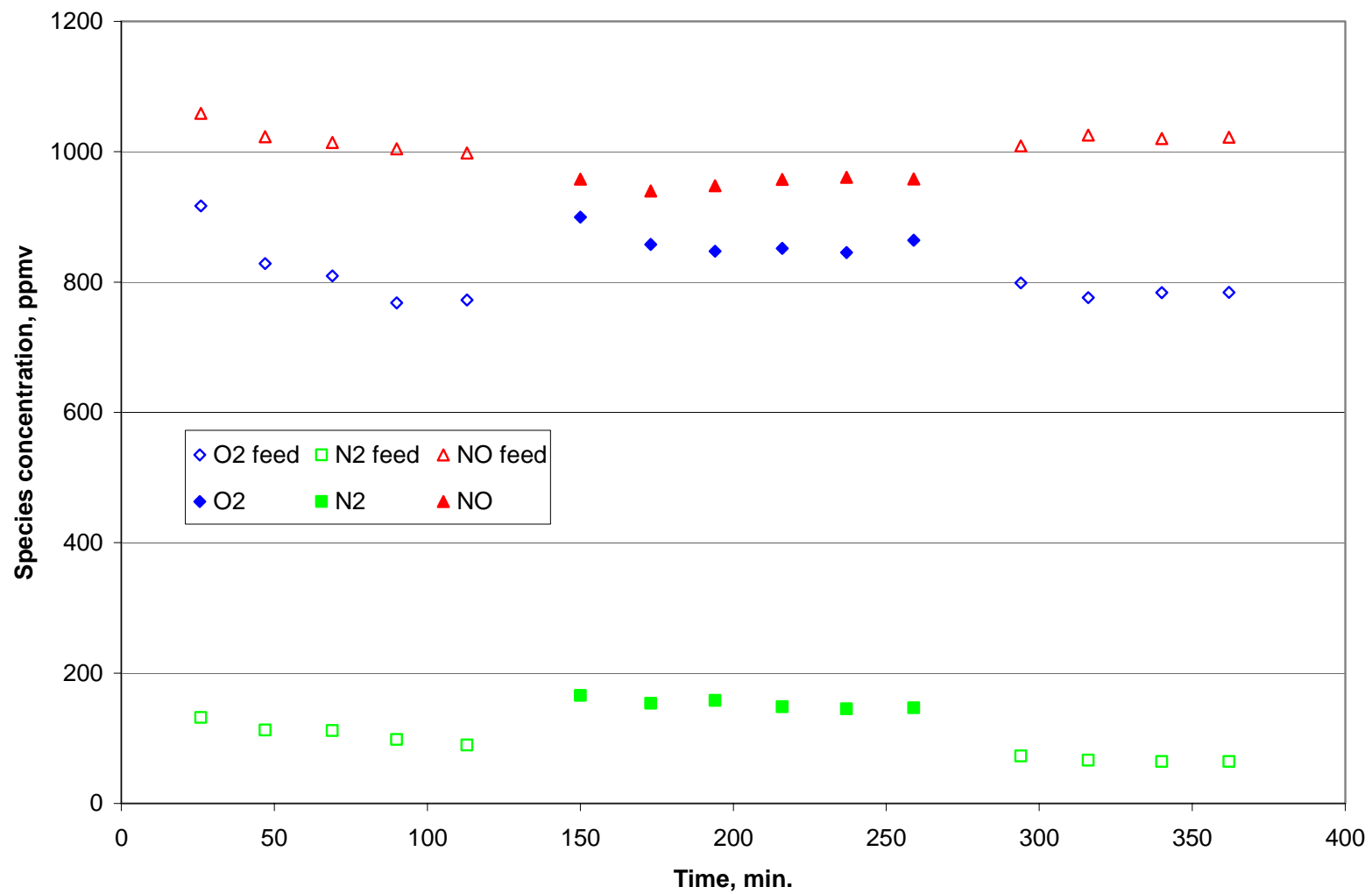


Figure 25. Isothermal Reaction of NO+O<sub>2</sub> on 15%Pt%SnO<sub>2</sub> at 900K,60sccm,with water 4th run  
Pretreated at 373 K

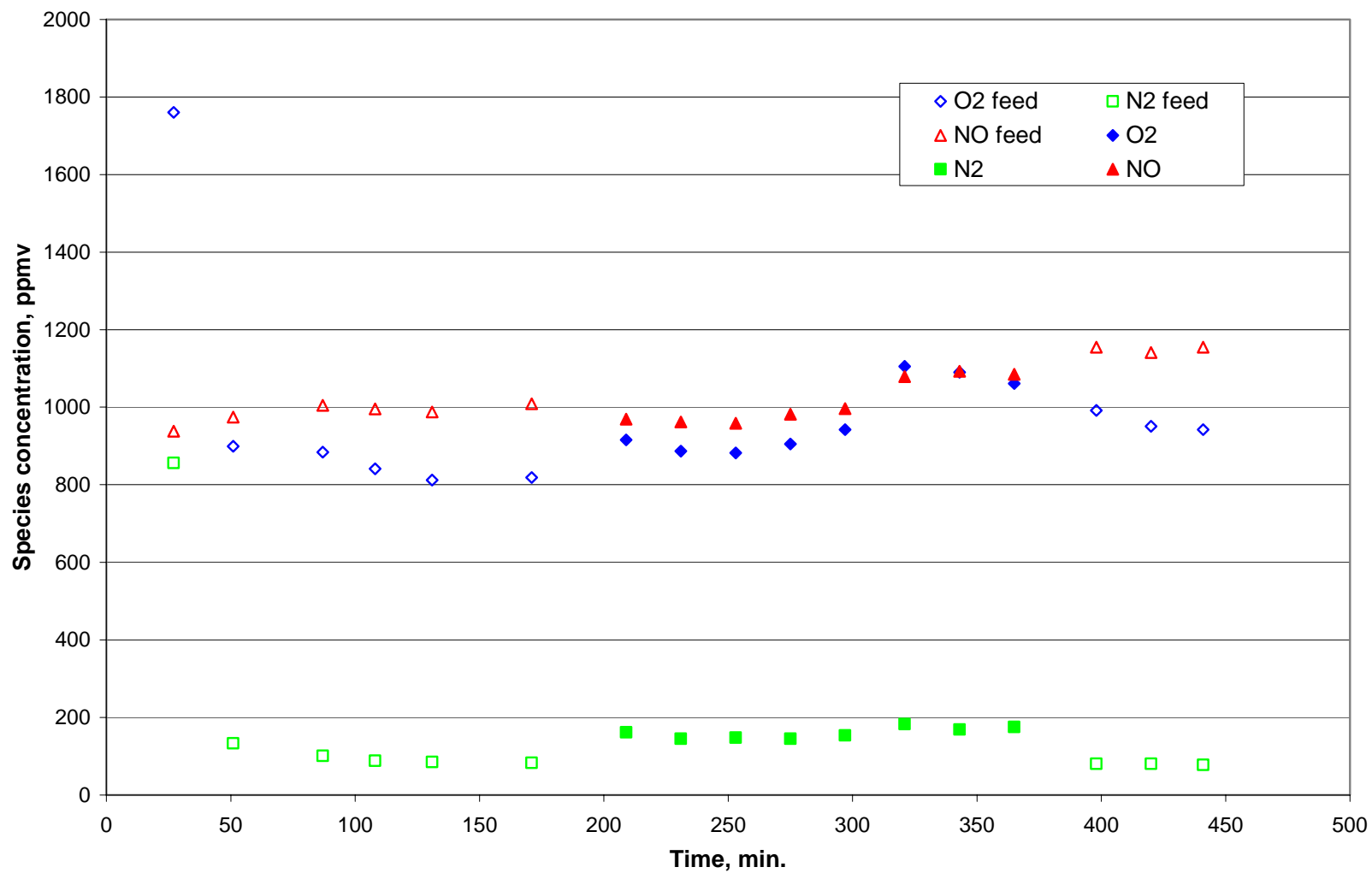
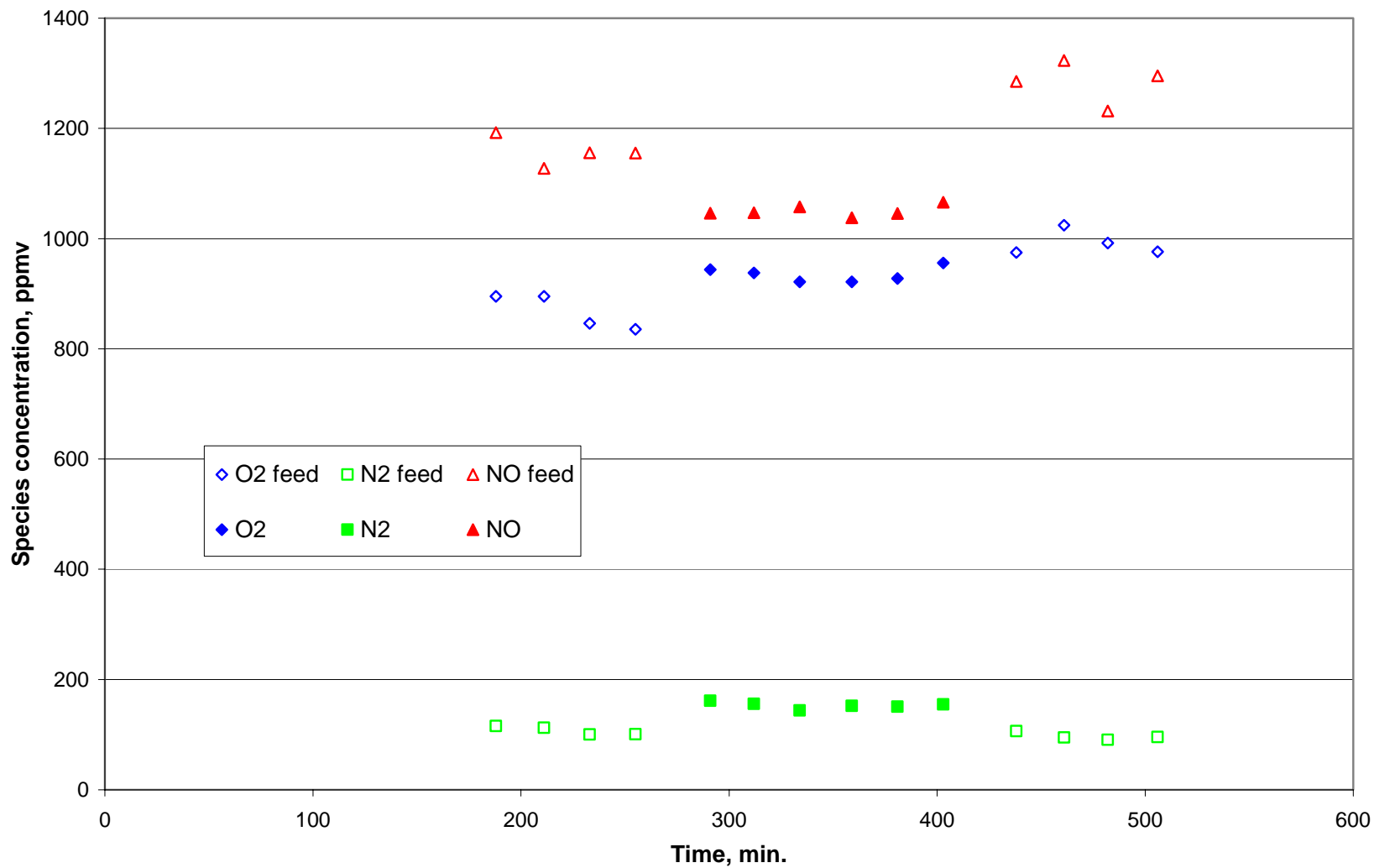


Figure 26. Isothermal Reaction of NO+O<sub>2</sub> on 15% Pt%SnO<sub>2</sub> at 1000K,40sccm,dry  
Pretreated at 373 K



**Figure 27. Isothermal Reaction of NO+O<sub>2</sub> on 15% Pt%SnO<sub>2</sub> at 1000K-repeat of 5th run  
1000K,40sccm,dry. Pretreated at 373 K**

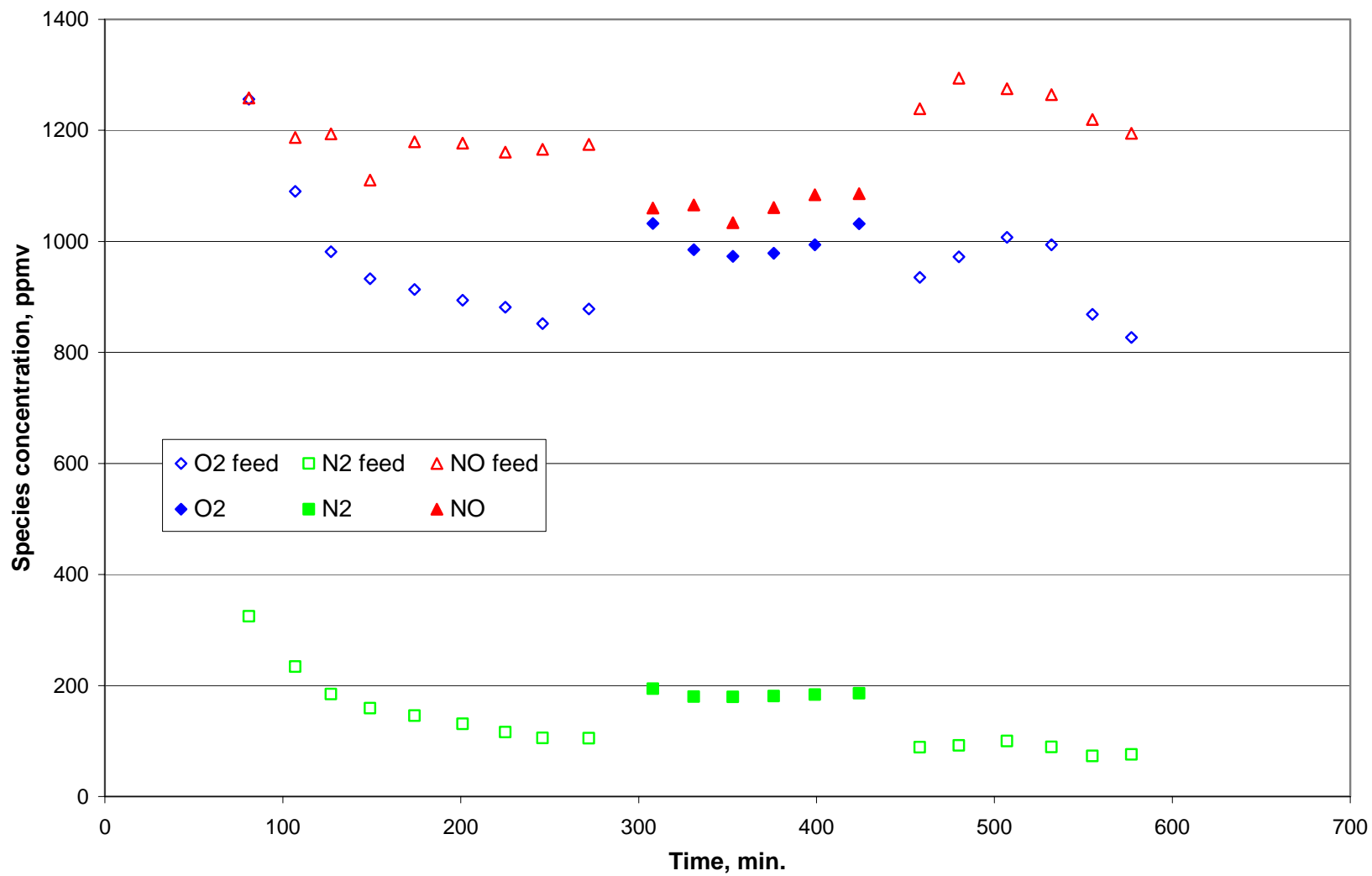


Figure 28. Isothermal Reaction of NO+O2 on 15% Pt%SnO2 at 1000K,40sccm,with water Pretreated at 373 K

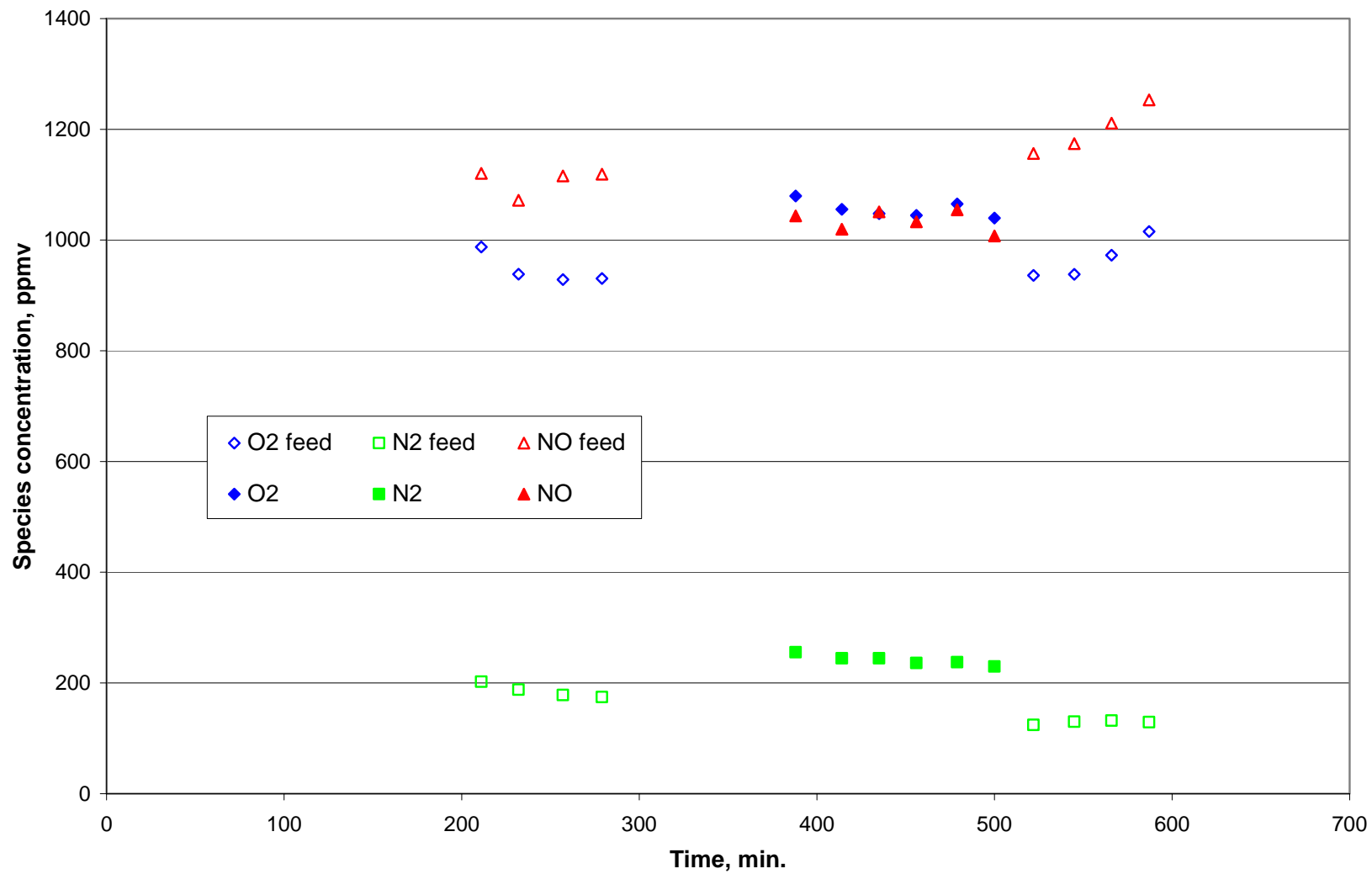


Figure 29. Isothermal Reaction of NO+O2 on 15% Pt%SnO2 at 900K ,40sccm, with water Pretreated at 373 K

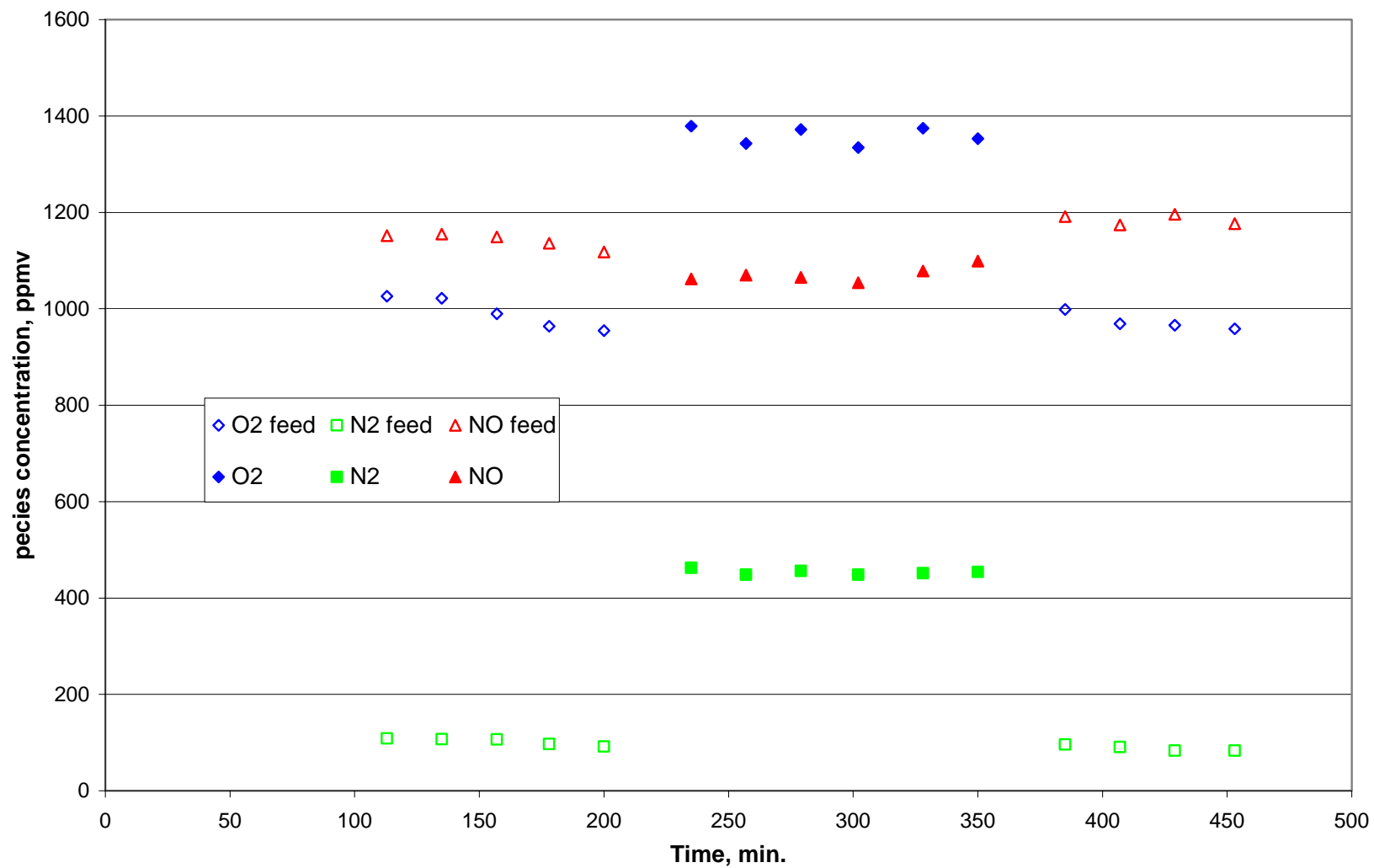


Figure 30. Isothermal Reaction of NO+O<sub>2</sub> on 15% Pt%SnO<sub>2</sub> at 900K,40sccm, with catalyst pretreated at 900K

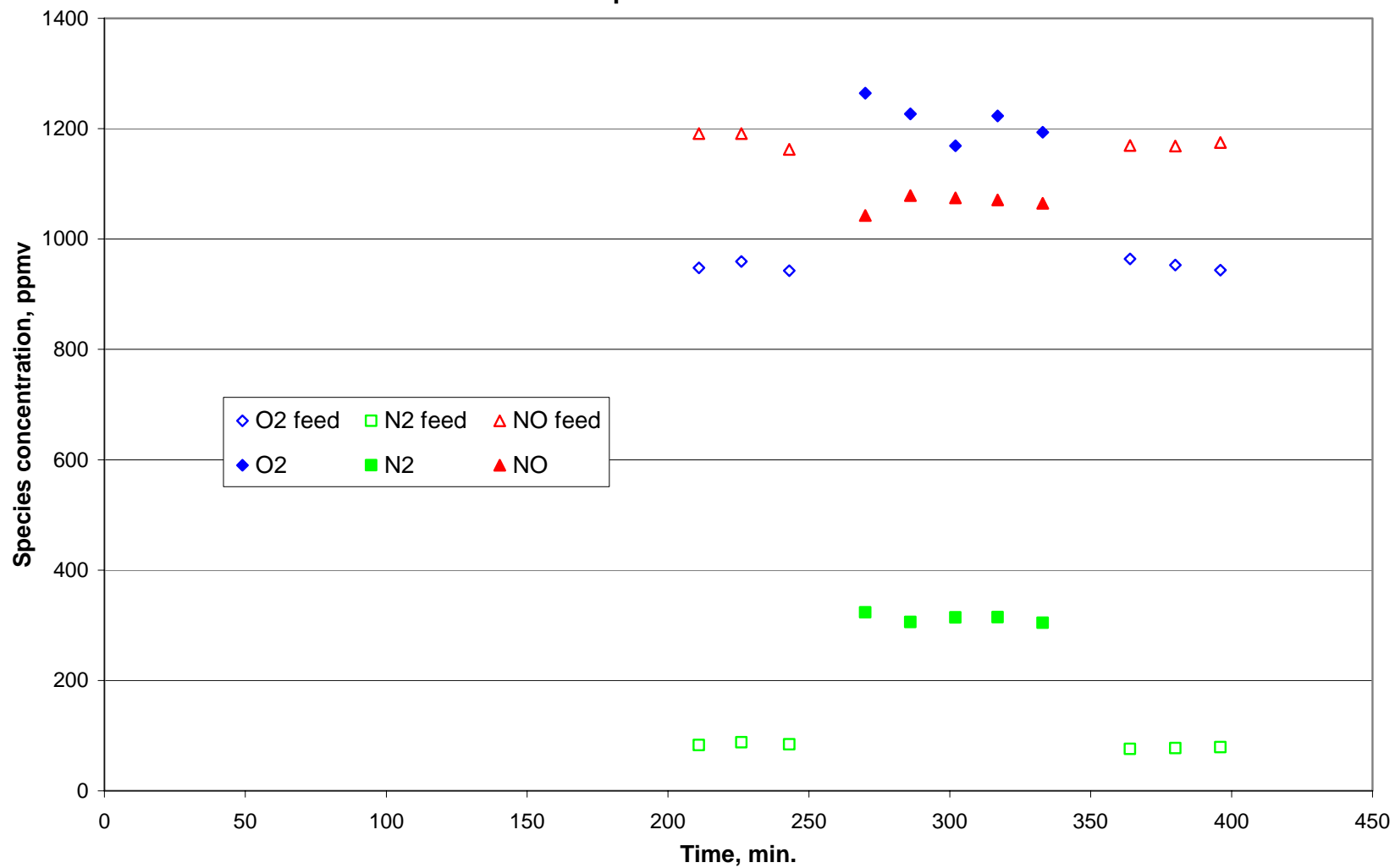


Figure 31. Isothermal Reaction of NO on 15% Pt%SnO2 at 900K,40sccm, with catalyst pretreated at 900K

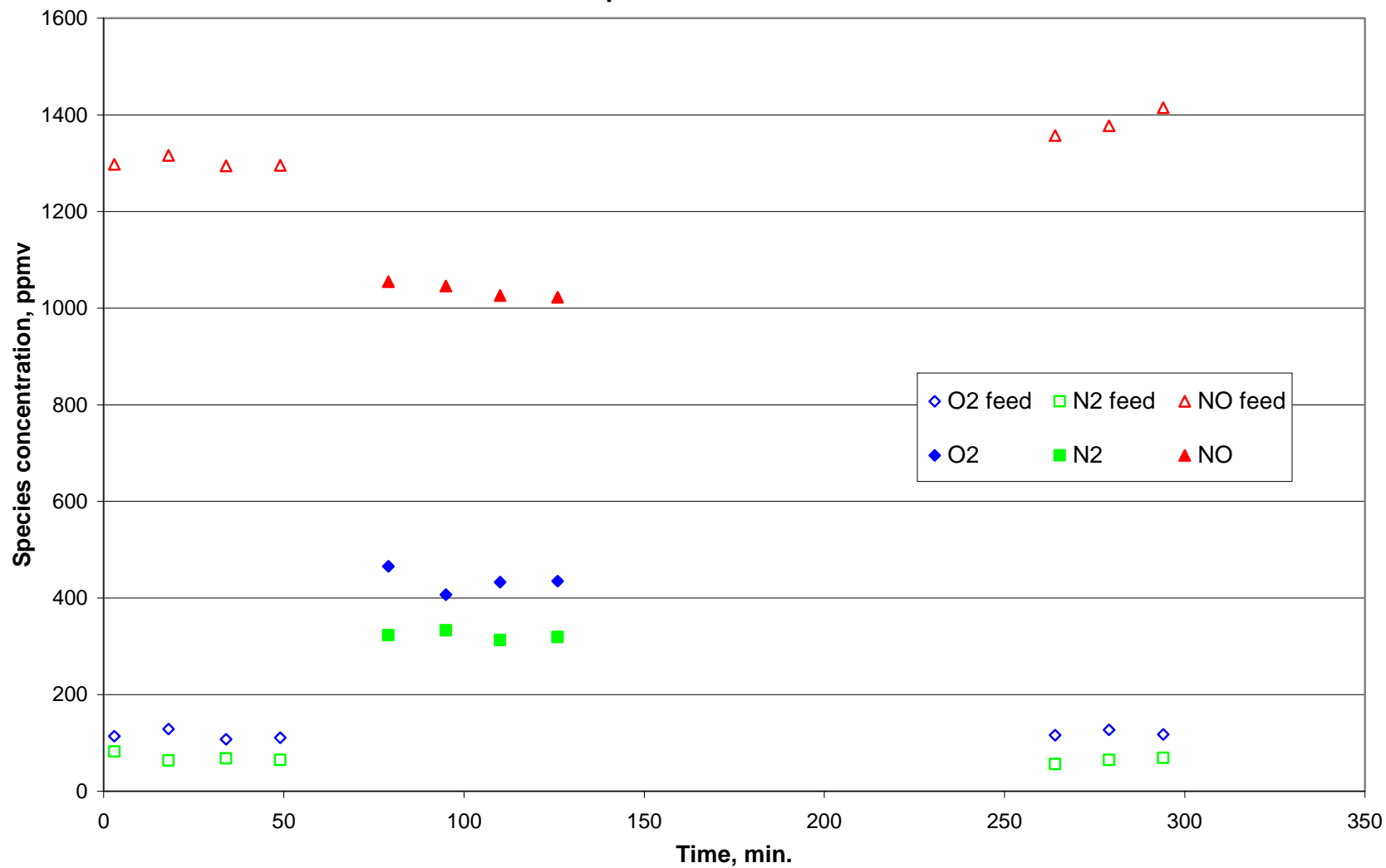


Figure 32. Isothermal Reaction of NO on 15% Pt%SnO<sub>2</sub> at 1000K,40sccm, with catalyst pretreated at 900K

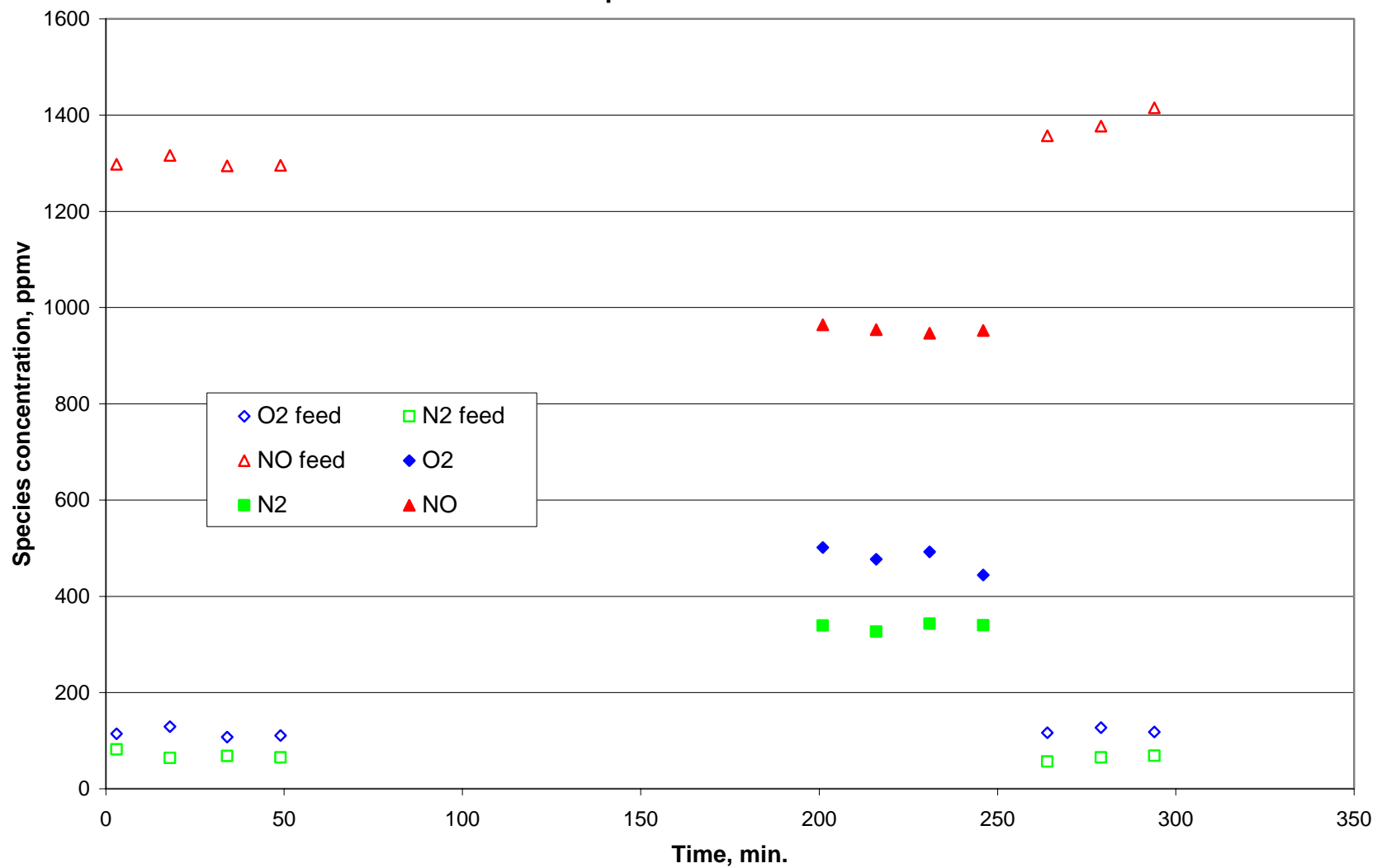


Figure 33. Isothermal Reaction of NO+O<sub>2</sub> on 15% Pt%SnO<sub>2</sub> at 1000K,40sccm, with catalyst pretreated at 900K

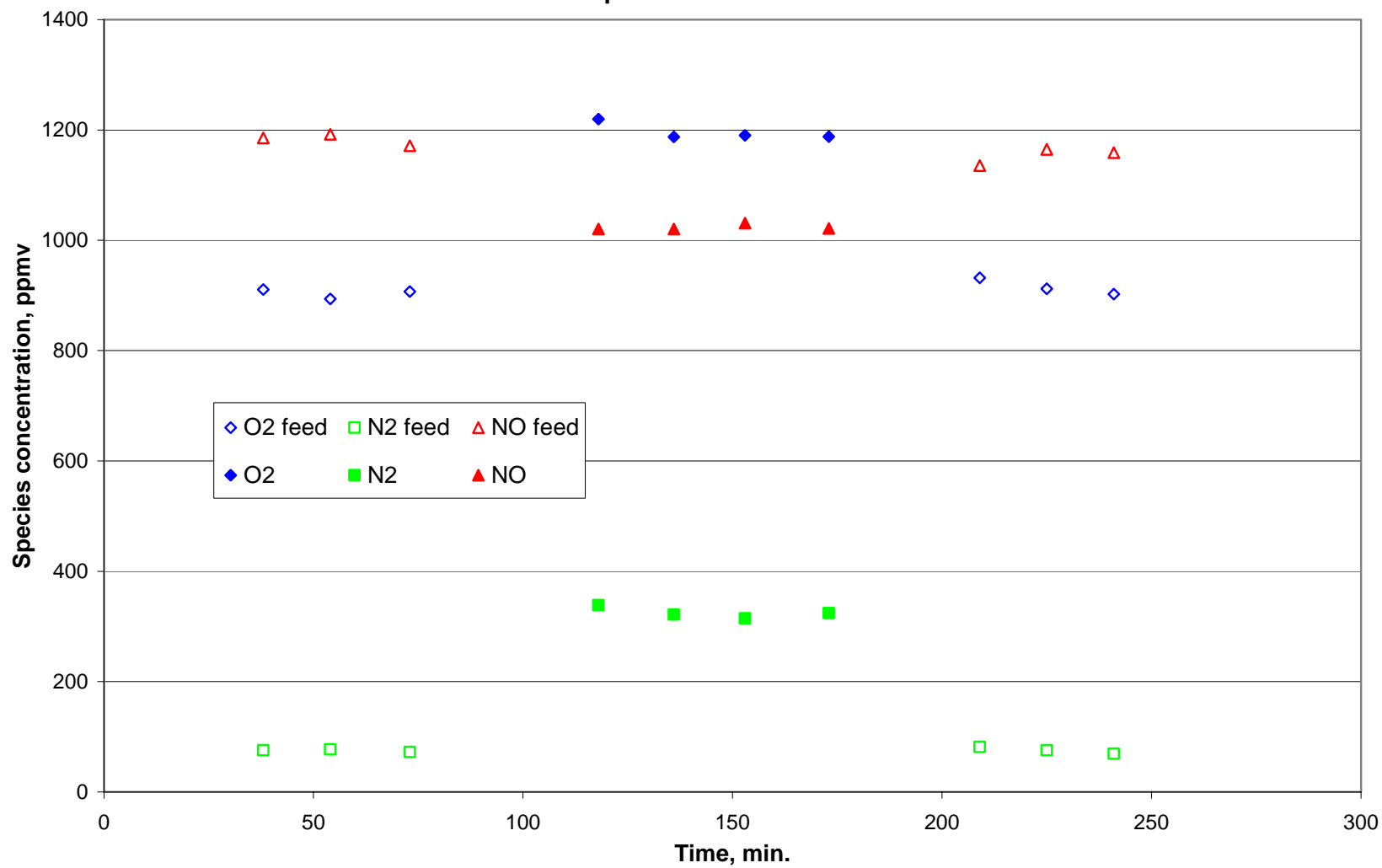


Figure 34. Isothermal Reaction of NO+O<sub>2</sub> on 15% Pt%SnO<sub>2</sub> at 850K,40sccm, with catalyst pretreated at 900K

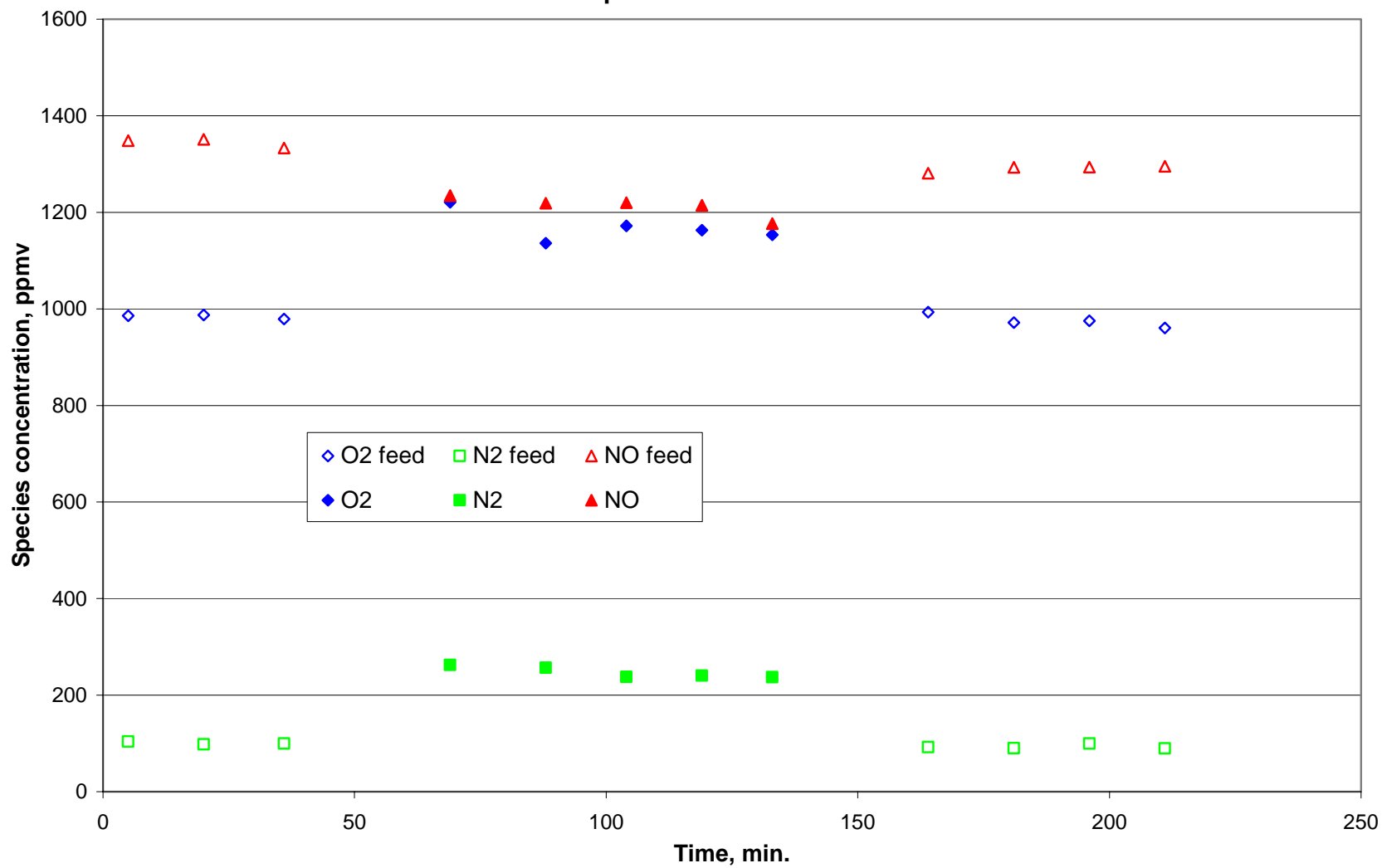


Figure 35. Isothermal Reaction of NO on 15% Pt%SnO<sub>2</sub> at 850K,40sccm, with catalyst pretreated at 900K

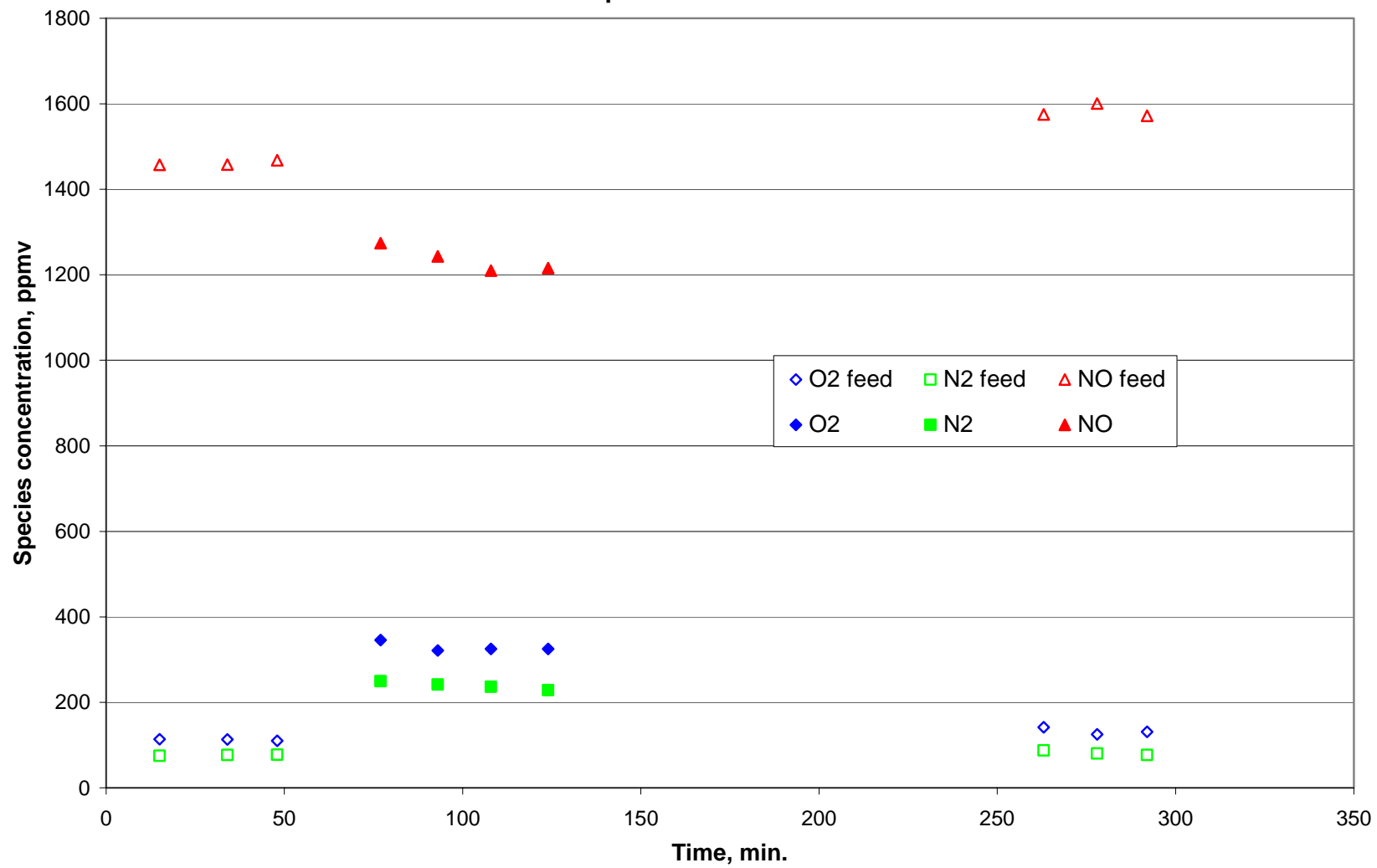


Figure 36. Isothermal Reaction of NO on 15% Pt%SnO<sub>2</sub> at 950K,40sccm, with catalyst pretreated at 900K

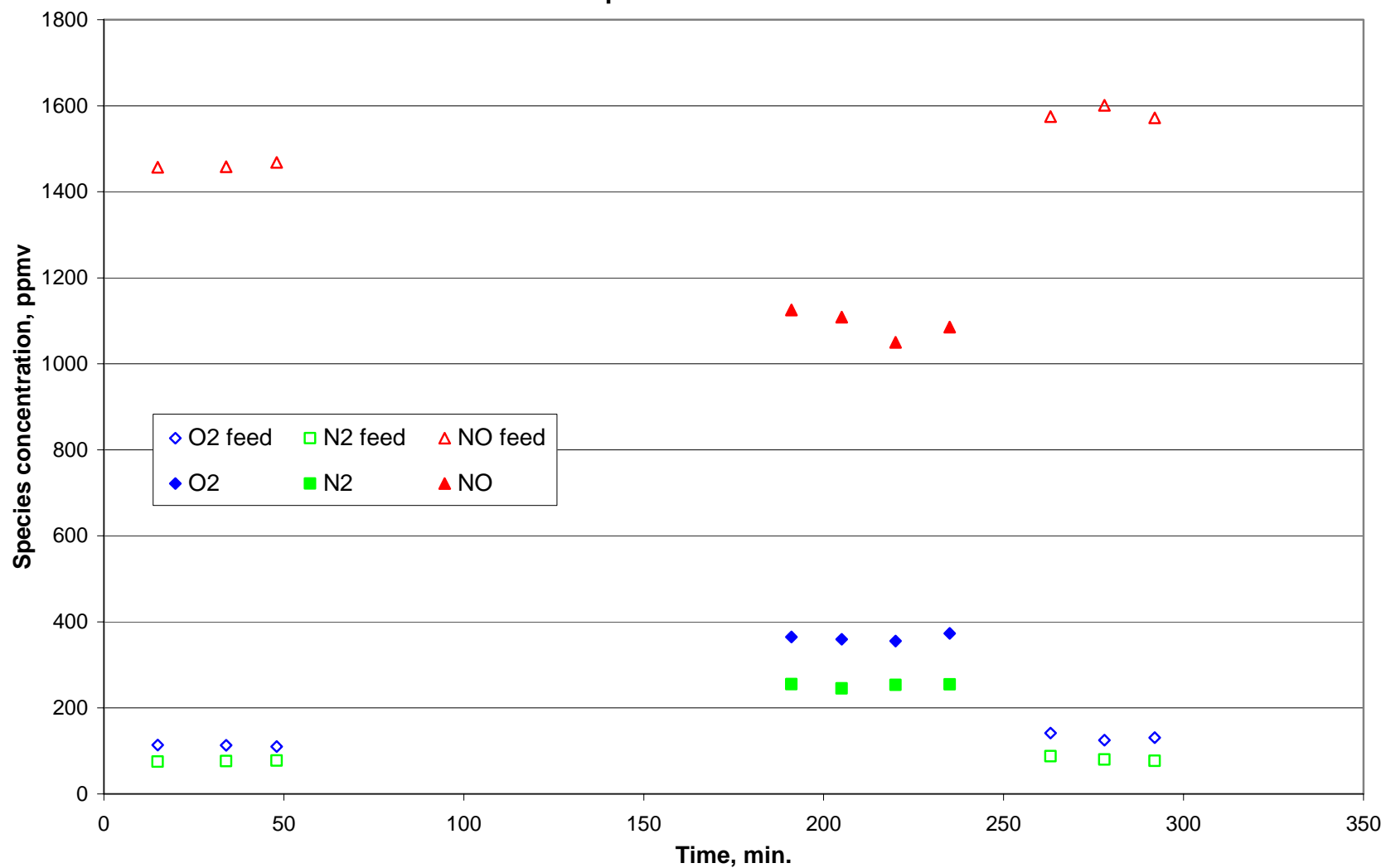


Figure 37. Isothermal Reaction of NO+O<sub>2</sub> on 15% Pt%SnO<sub>2</sub> at 950K,40sccm, with catalyst pretreated at 900K

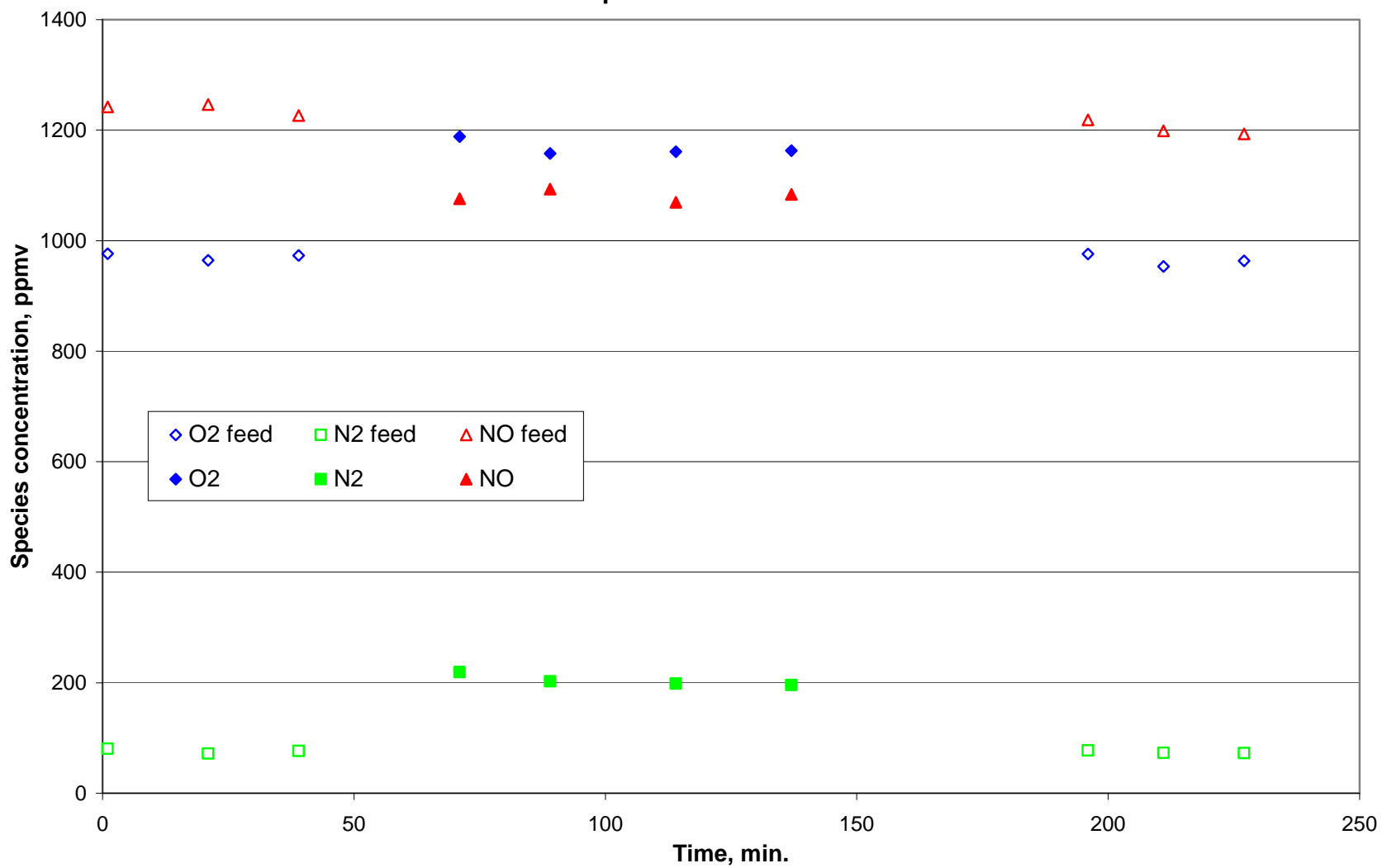


Figure 38. Isothermal Reaction of NO+O<sub>2</sub>+H<sub>2</sub>O on 15% Pt%SnO<sub>2</sub> at 900K,40sccm, with catalyst pretreated at 100C

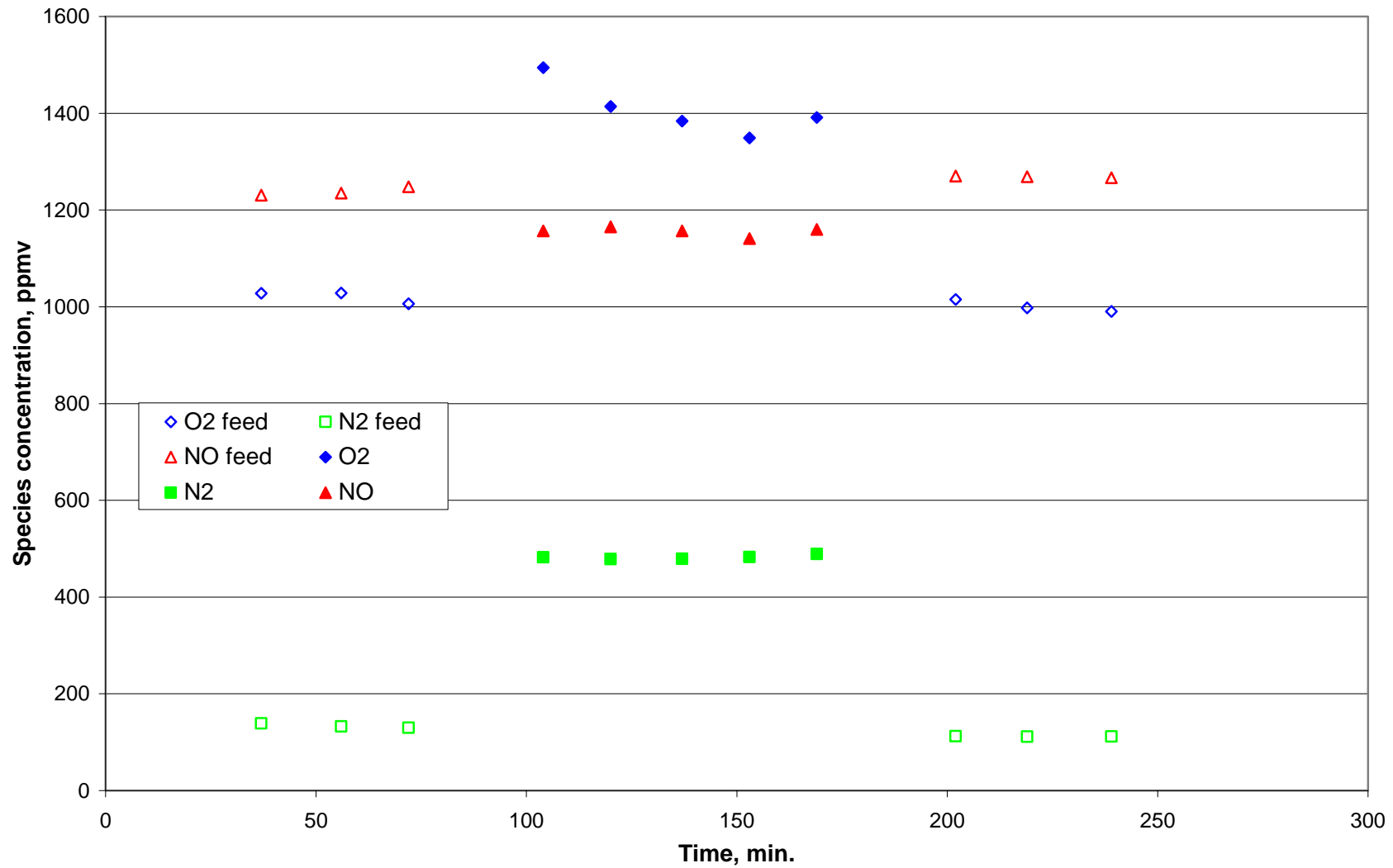


Figure 39. Isothermal Reaction of NO+O2 on 15% Pt%SnO2 at 850K,60sccm, with catalyst pretreated at 900K in He

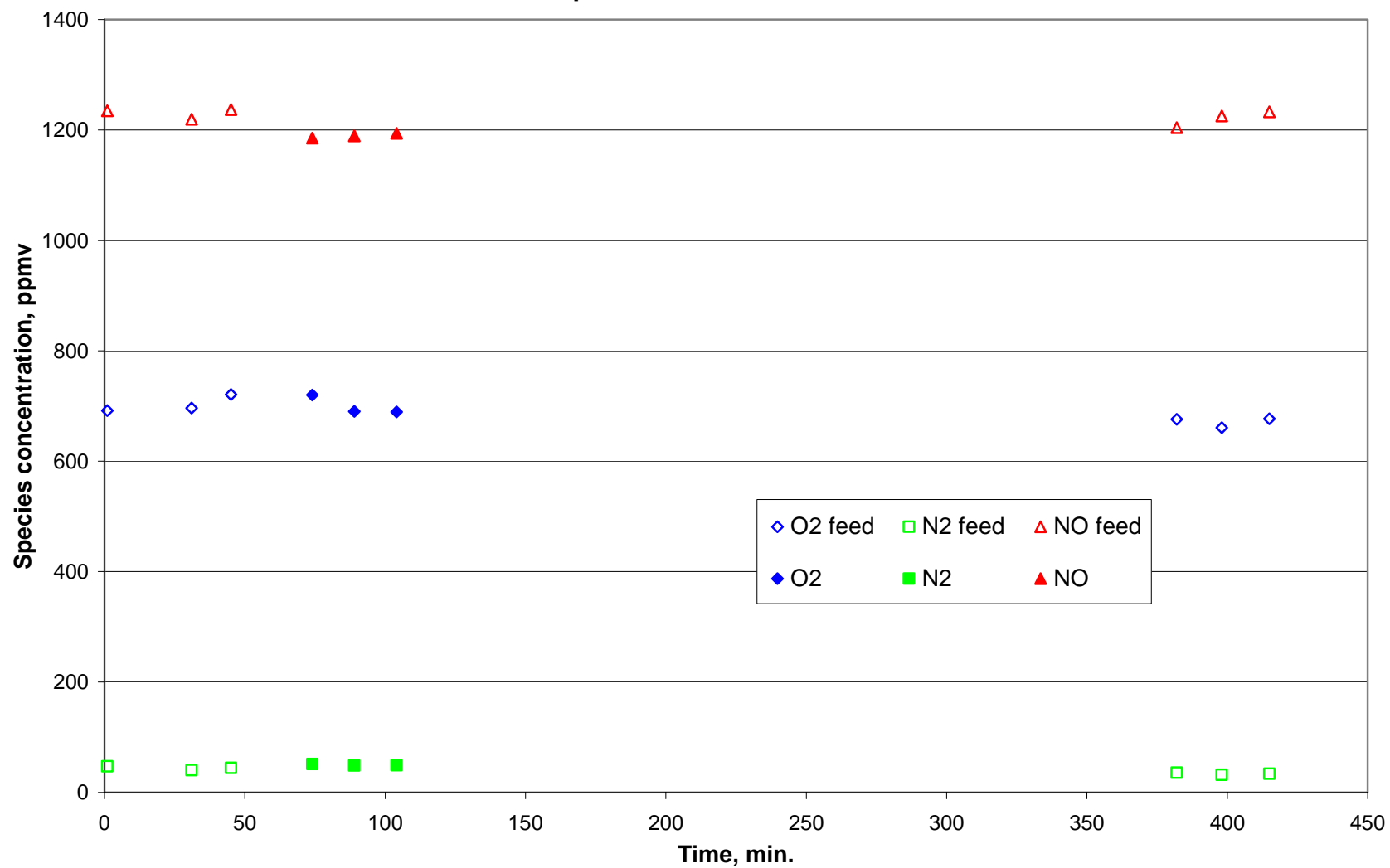


Figure 40. Isothermal Reaction of NO+O<sub>2</sub> on 15% Pt%SnO<sub>2</sub> at 900K,60sccm, with catalyst pretreated at 900K in He

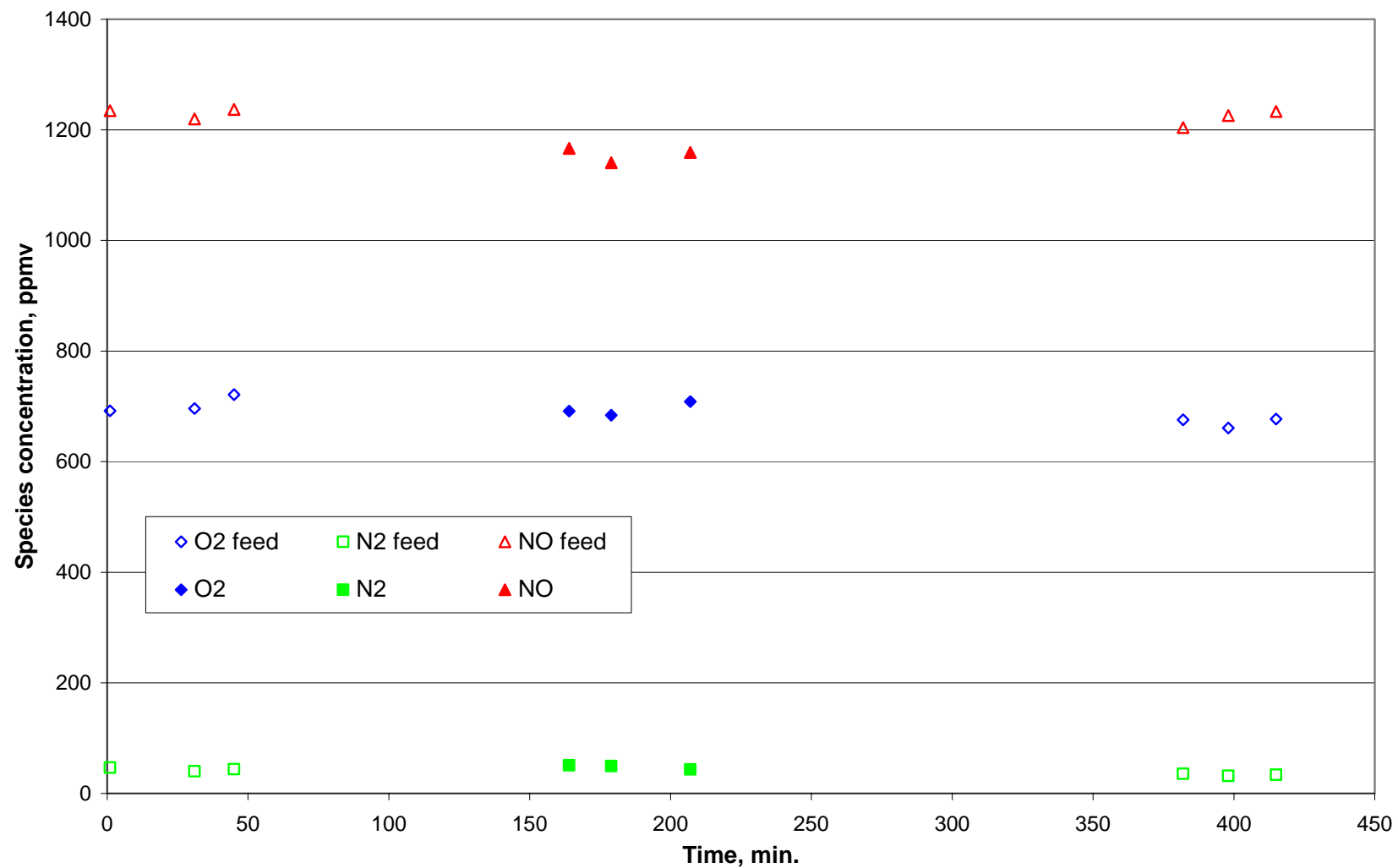


Figure 41. Isothermal Reaction of NO+O2 on 15% Pt%SnO2 at 950K,60sccm, with catalyst pretreated at 900K in He

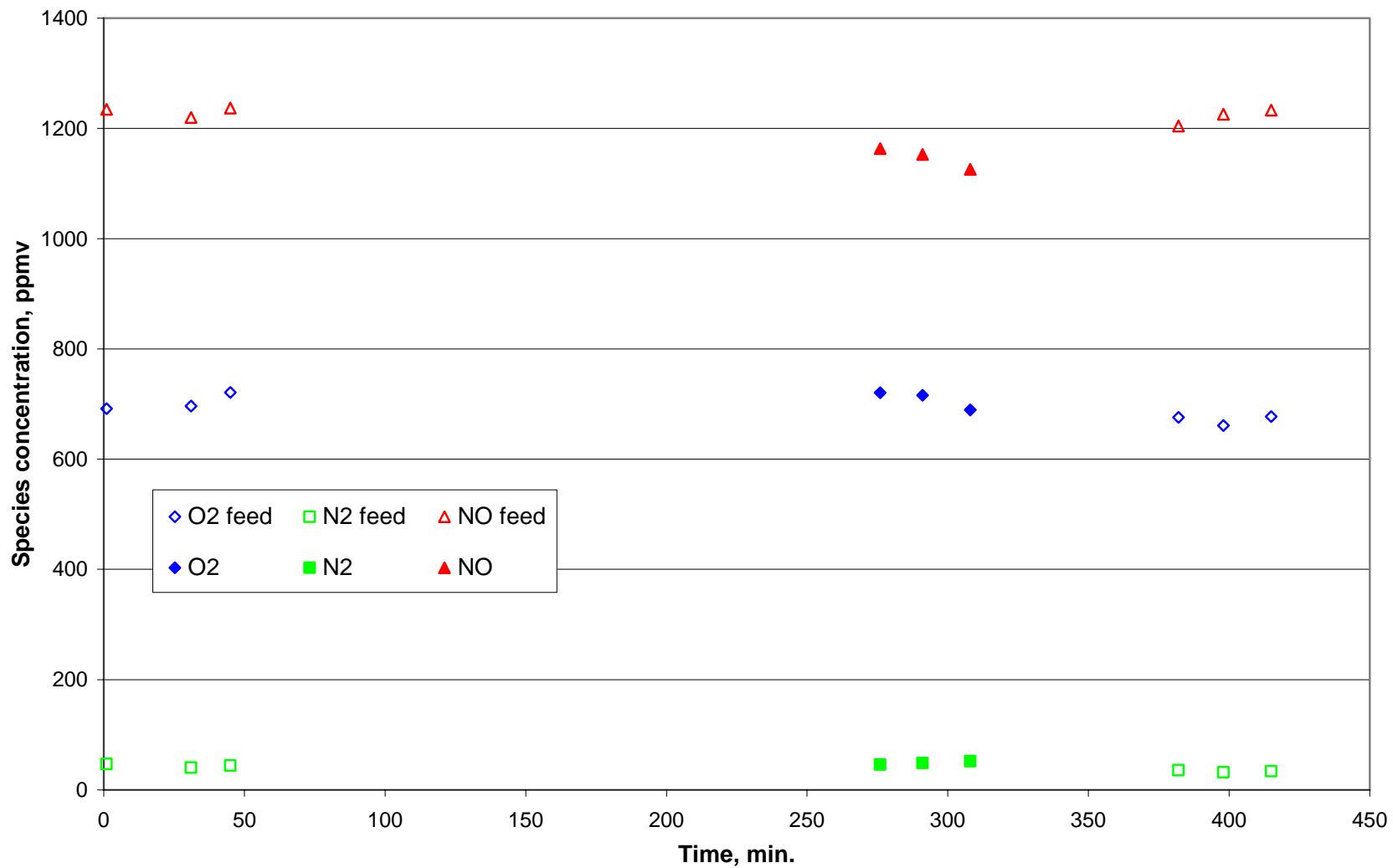


Figure 42. Isothermal Reaction of NO+O2 on 15% Pt%SnO2 at 1000K,60sccm, with catalyst pretreated at 900K in He

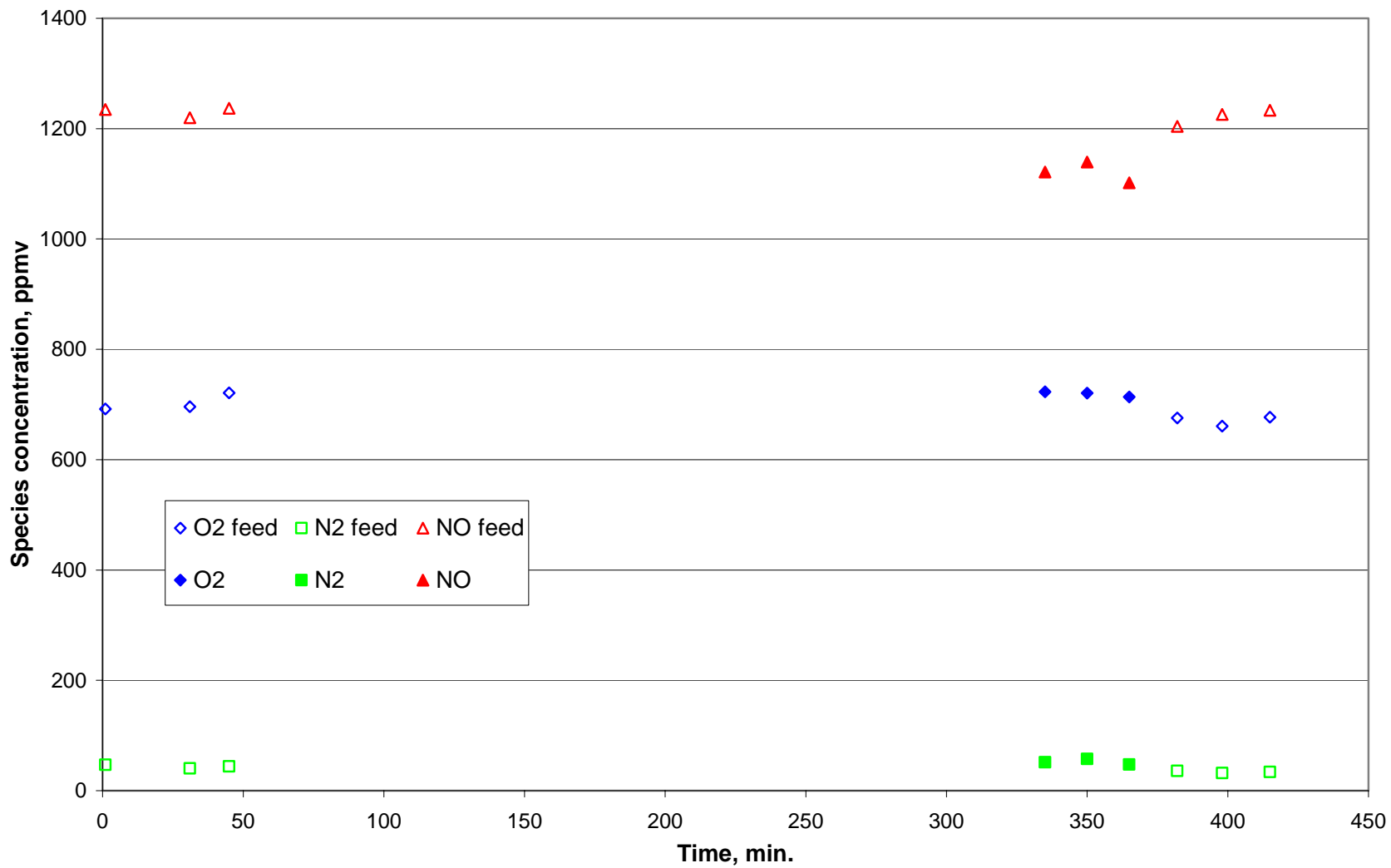
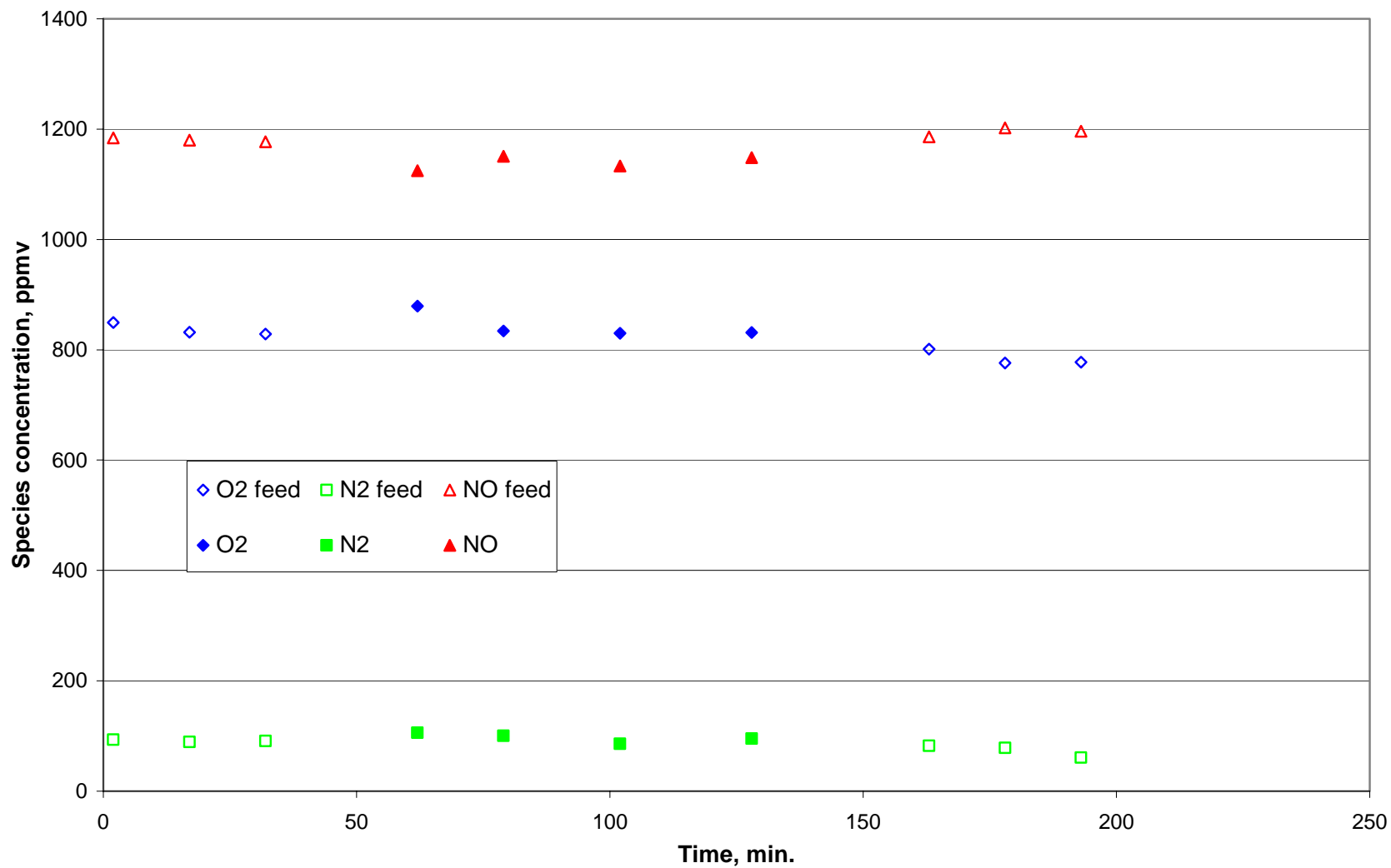
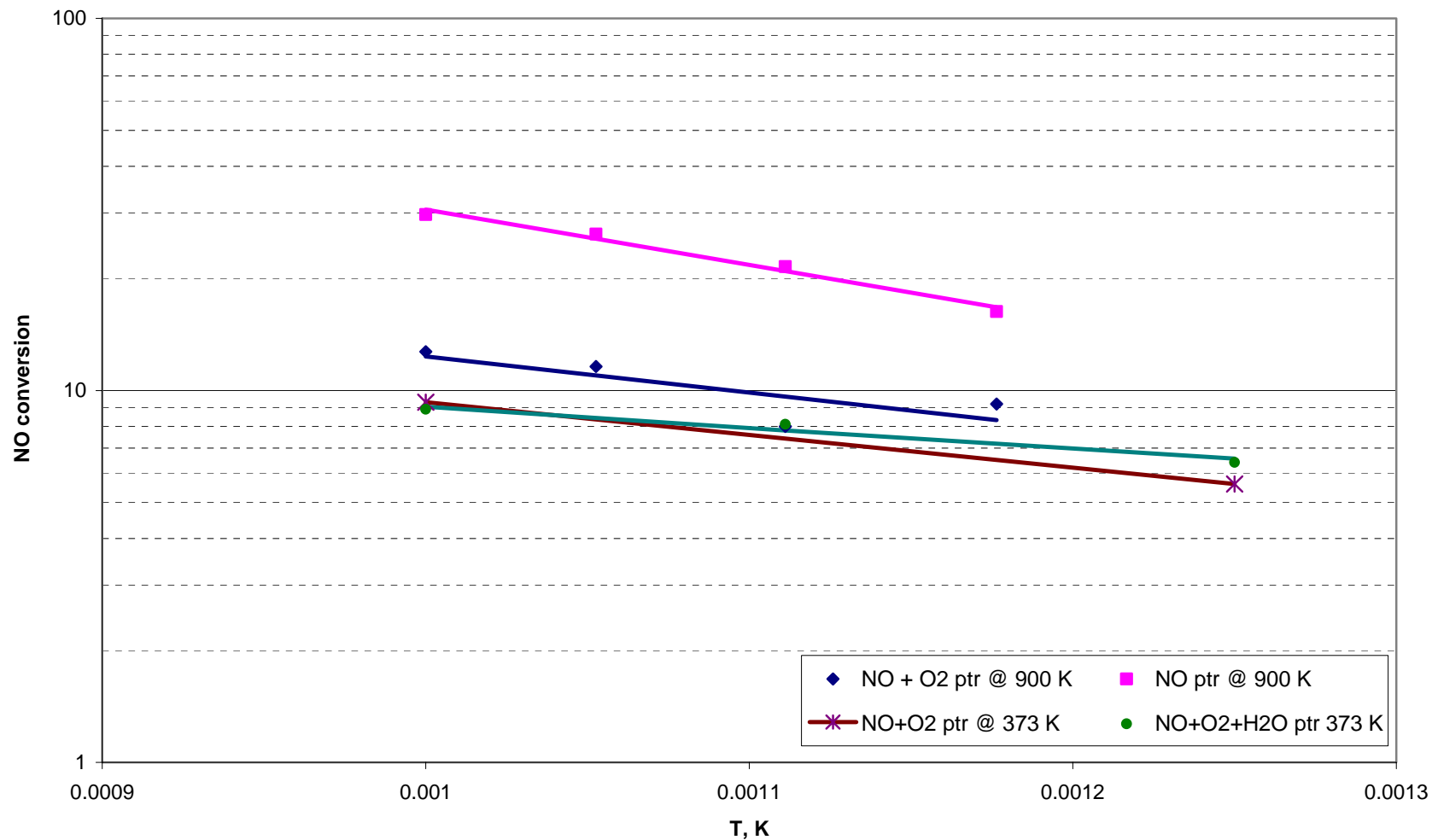


Figure 43. Isothermal Reaction of NO+O<sub>2</sub>+H<sub>2</sub>O on 15% Pt%SnO<sub>2</sub> at 900K,40sccm, with catalyst pretreated at 900K in He



**Figure 44. Effects of Temperature, Oxygen, Water, and Pretreatment Temperature on the NO Conversion. 15 % Pt/SnO<sub>2</sub> Catalyst .**



**Figure 45. Effect of space velocity on NO conversion. 150 mg  
15 % Pt/SnO<sub>2</sub> catalyst pretreated at 900 K**

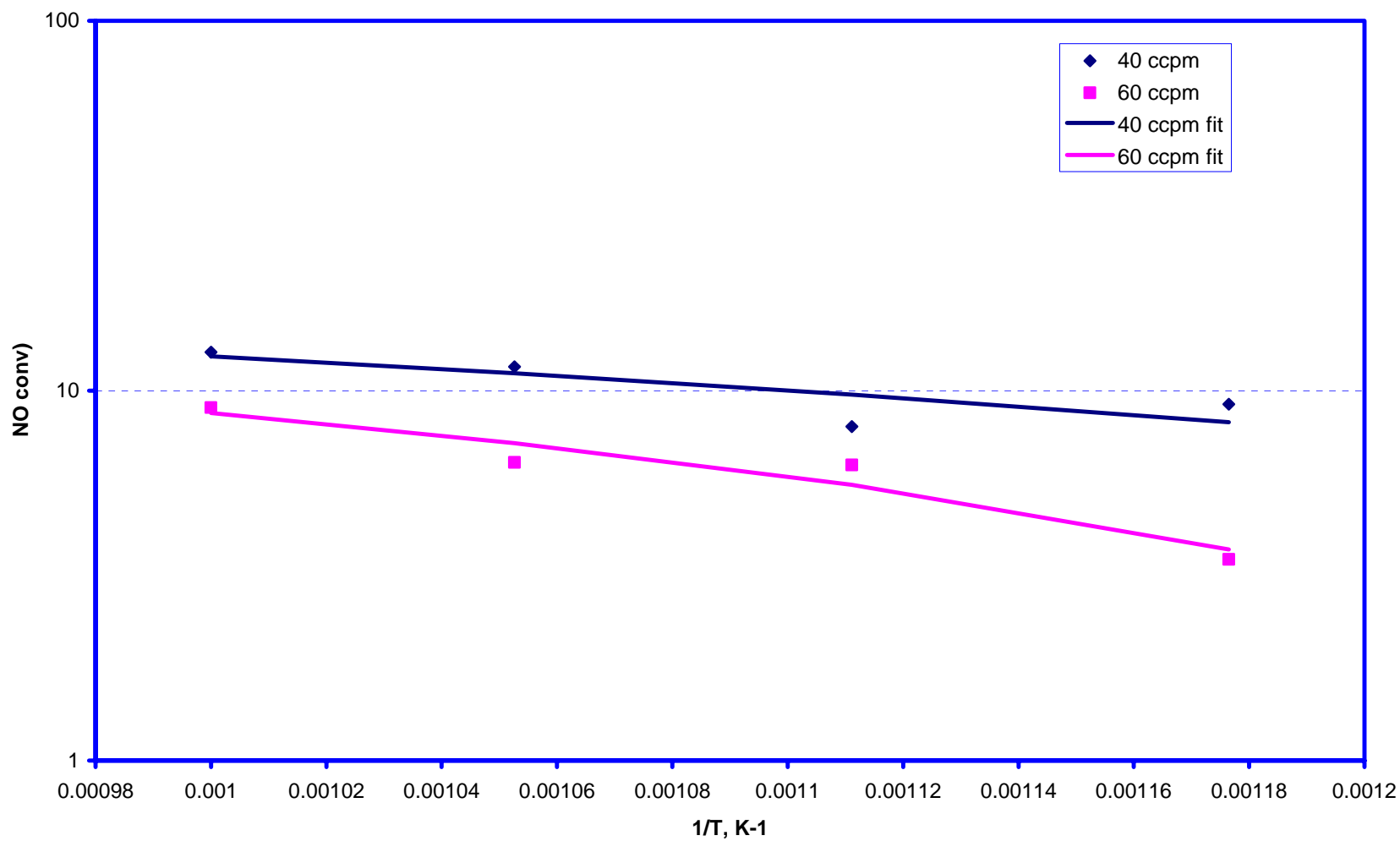


Figure 46. NO dissociation equilibrium at 1 atm. Pure NO.

### NO Dissociation Equilibrium

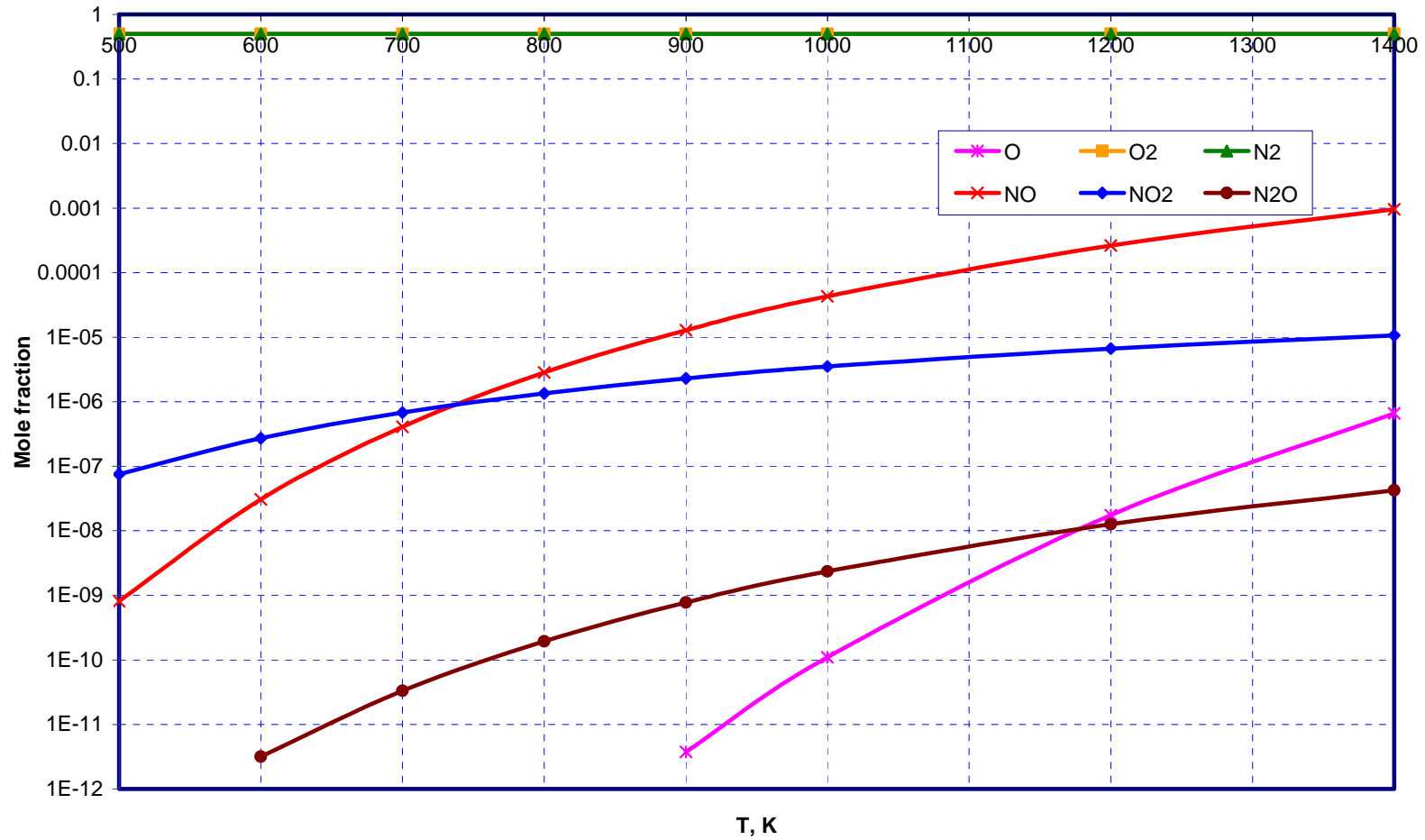


Figure 47. NO dissociation equilibrium for 50 % NO – 50 % O<sub>2</sub> at 1 atm.

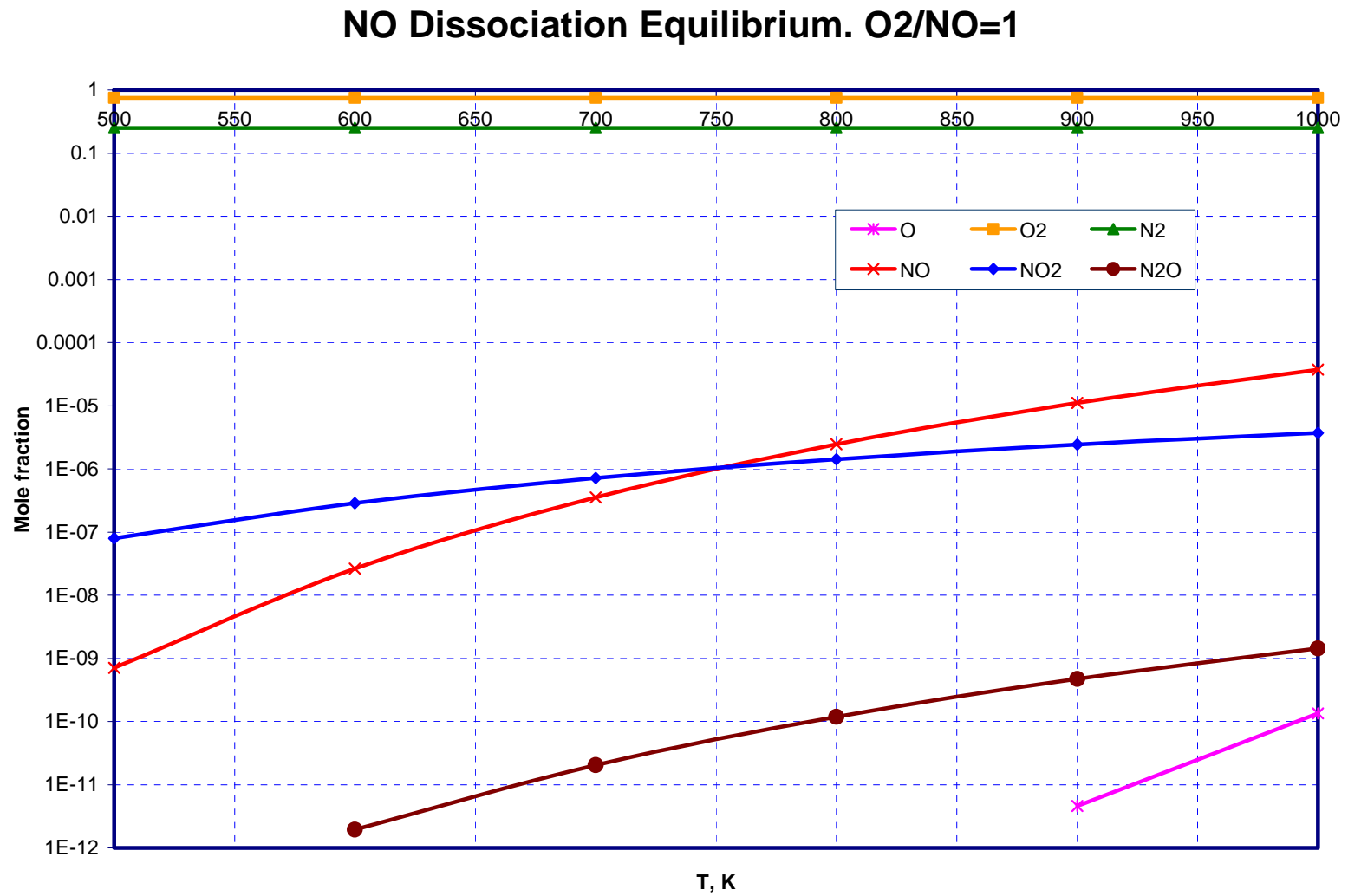


Figure 48. NO dissociation equilibrium at 1 atm. 60 % O<sub>2</sub> – 40 % NO

### NO Dissociation Equilibrium. O<sub>2</sub>/NO=1.5

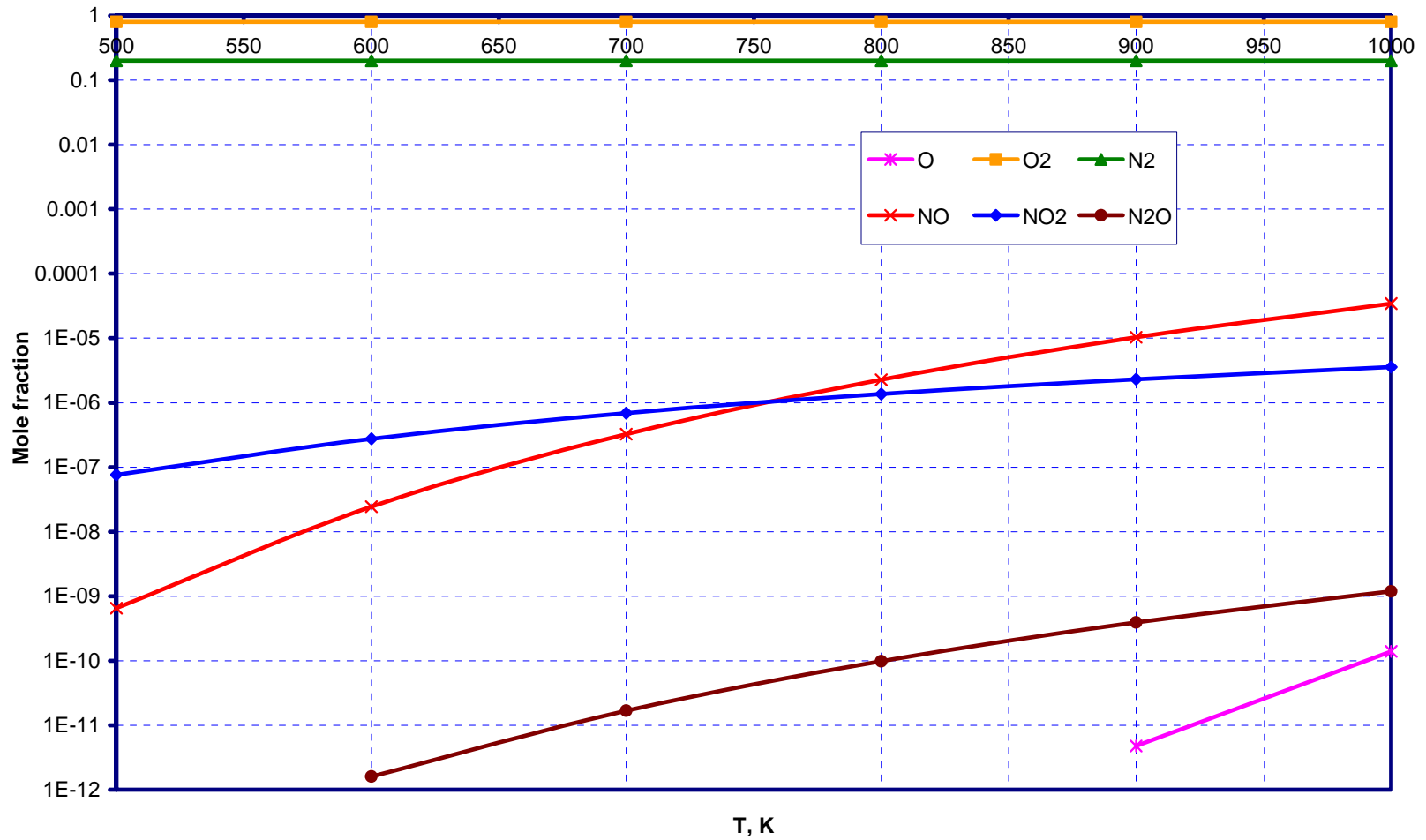


Figure 49. NO dissociation equilibrium at 1 atm. 67 % O<sub>2</sub> – 33 % NO.

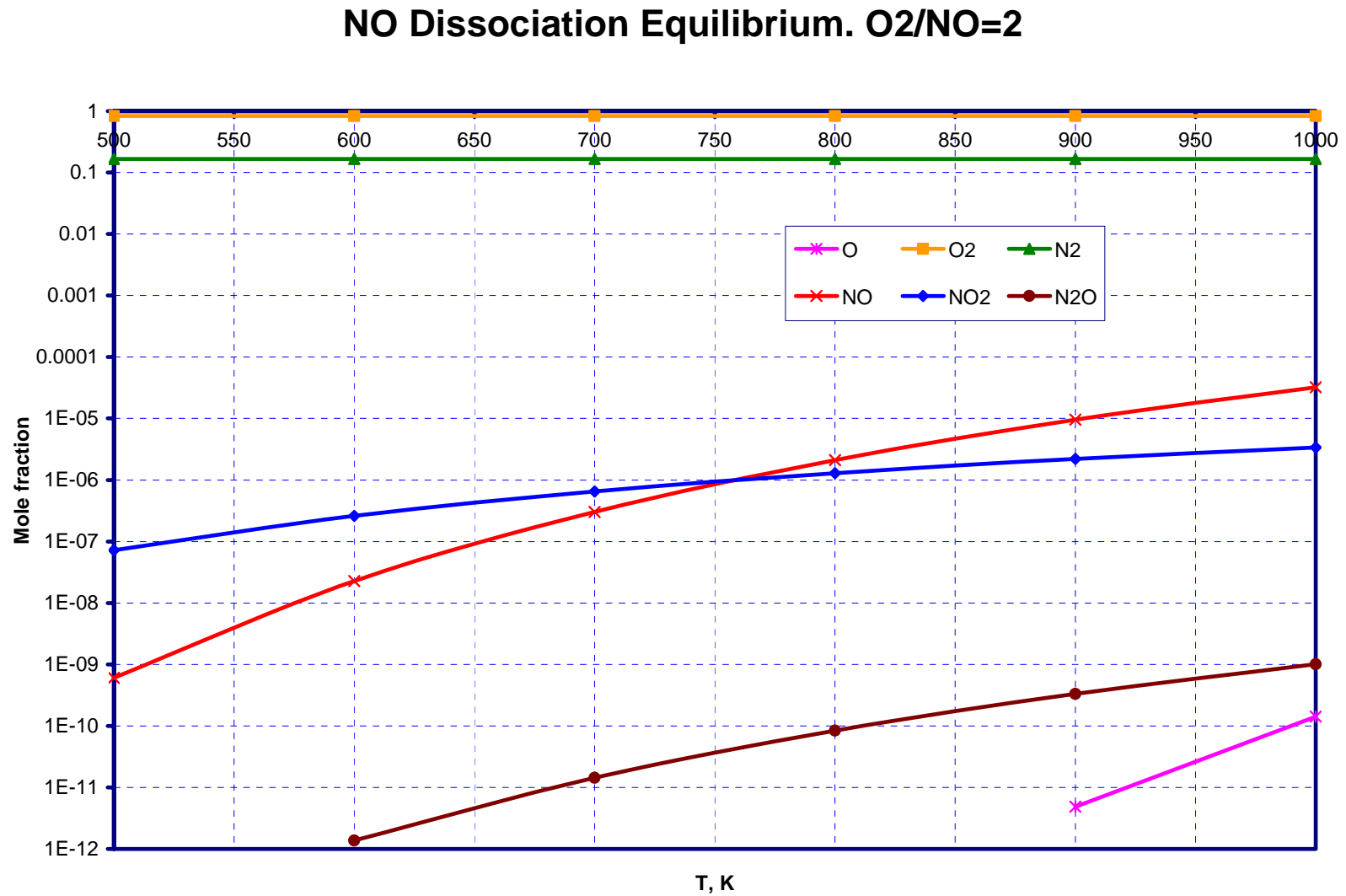


Figure 50. NO dissociation equilibrium at 1 atm. 99 % He – 1 % NO.

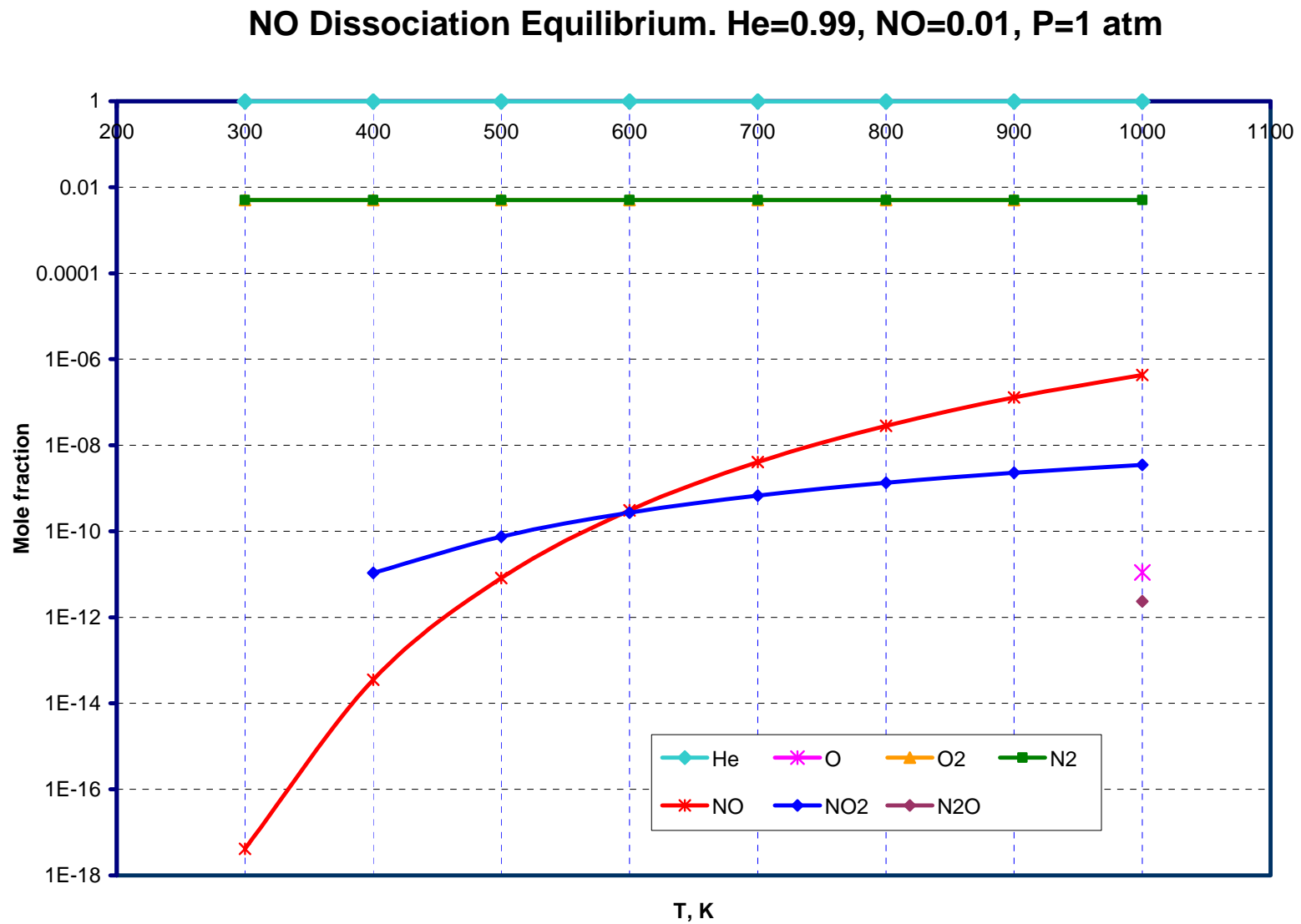


Figure 51. NO dissociation Equilibrium at 1 atm. 98 % He – 1 % NO – 1 % Air

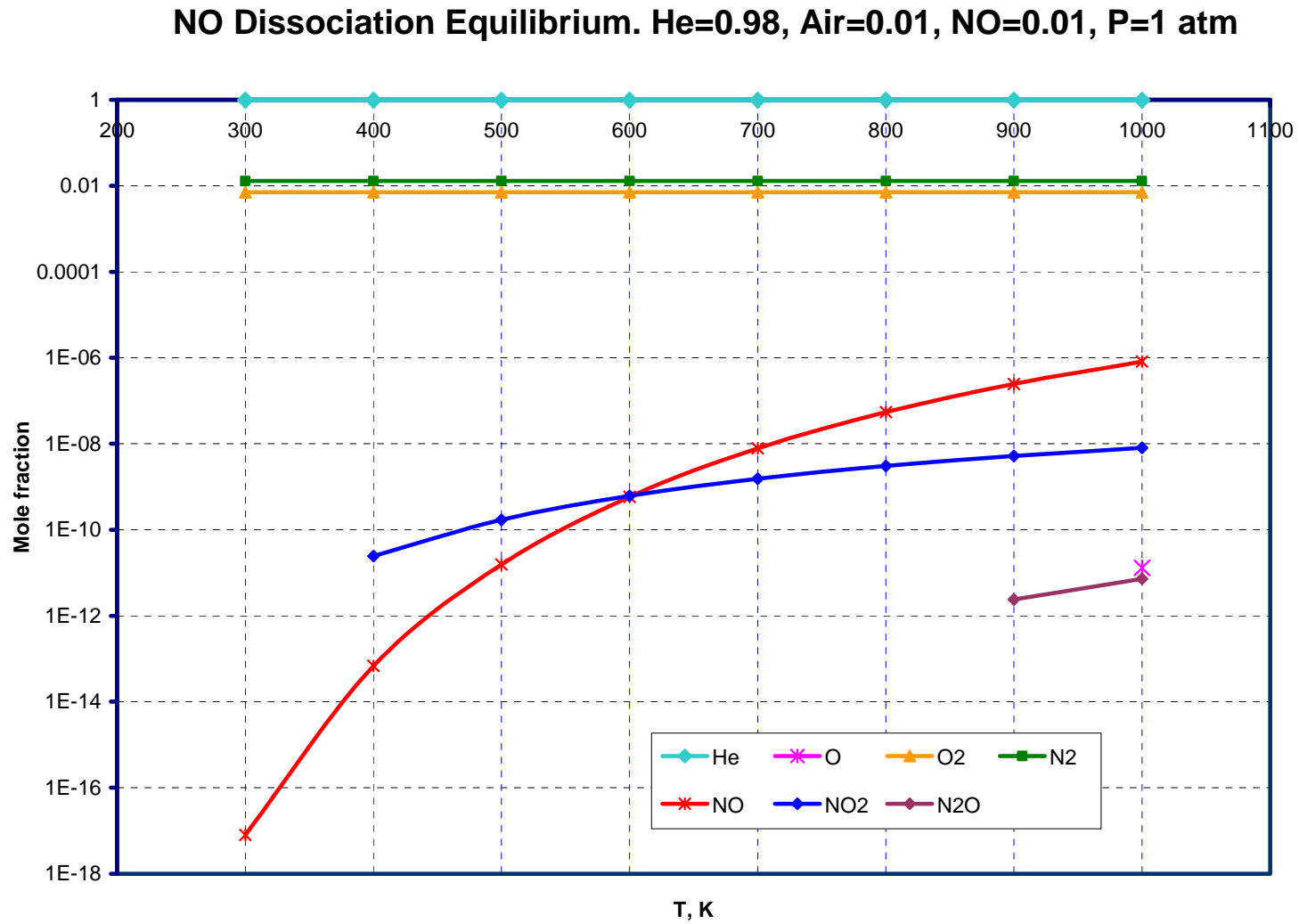


Figure 52. NO dissociation equilibrium at 1 atm. 97 % He – 1 % Air – 1 % O<sub>2</sub> – 1 % NO.

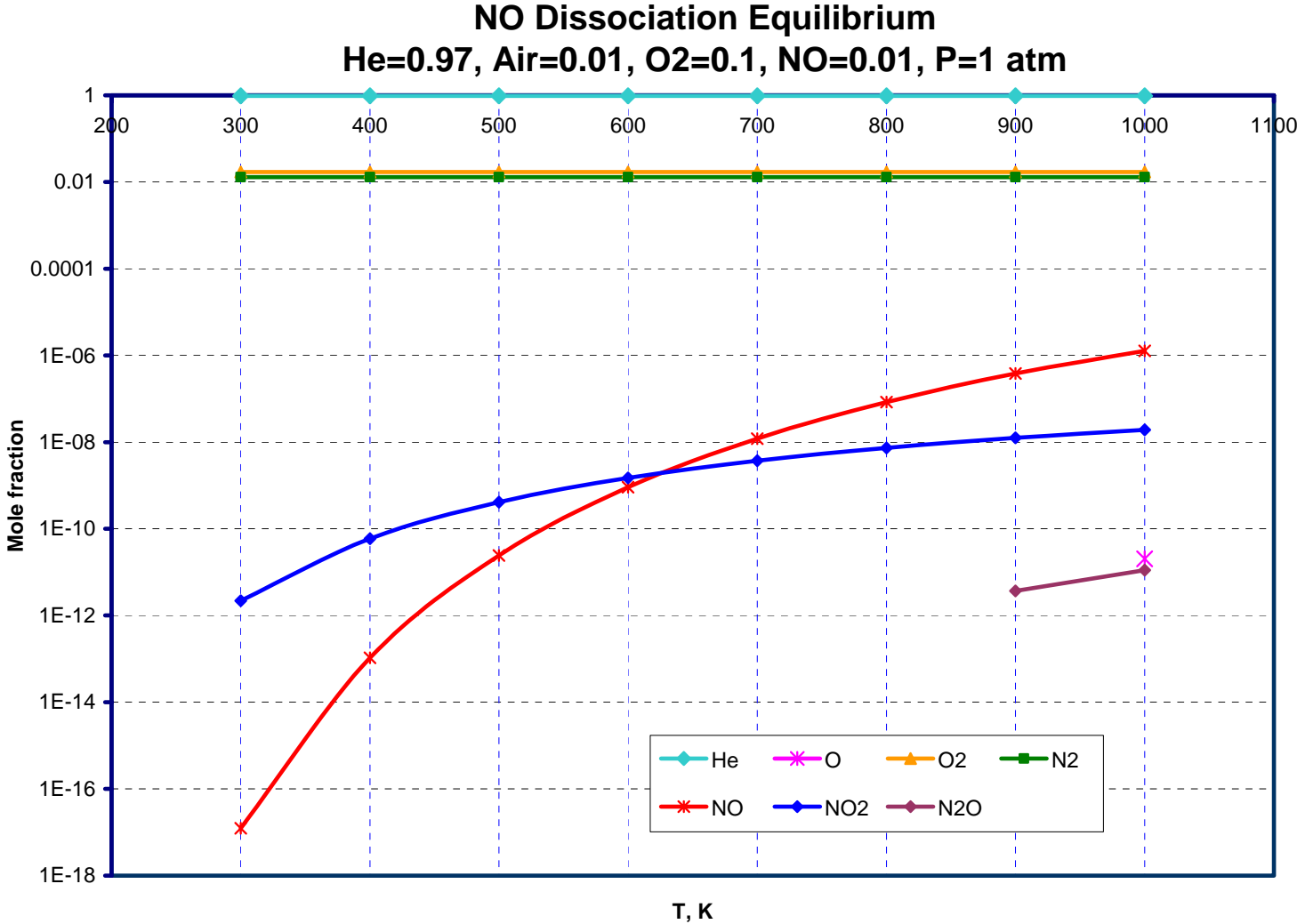


Figure 53. Deactivation of 15%Pt/SnO2 Catalyst During Isothermal Reaction at 900 K. NO feed

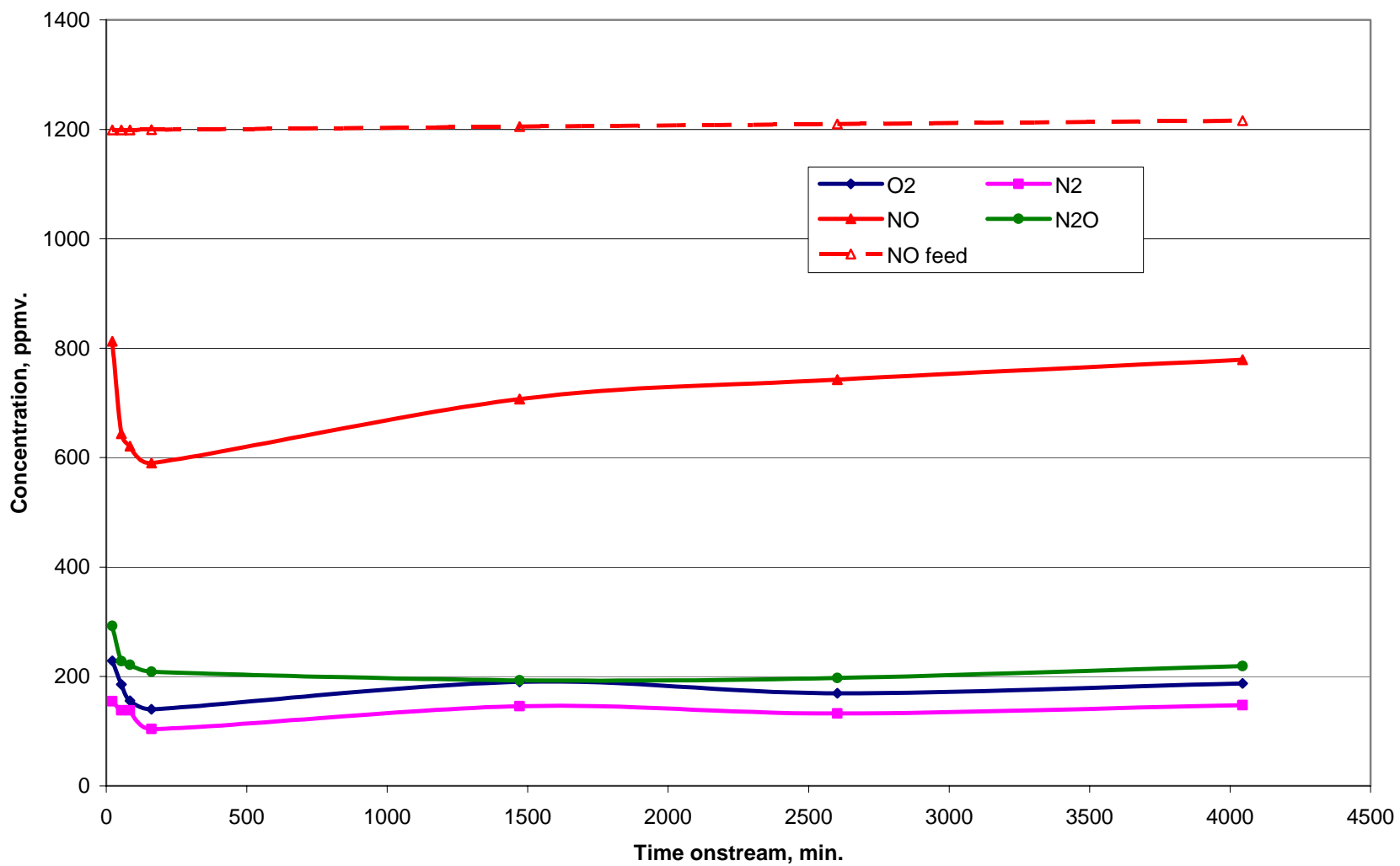


Figure 54. Deactivation of 15%Pt/SnO<sub>2</sub> Catalyst During Isothermal Reaction at 900 K. NO feed

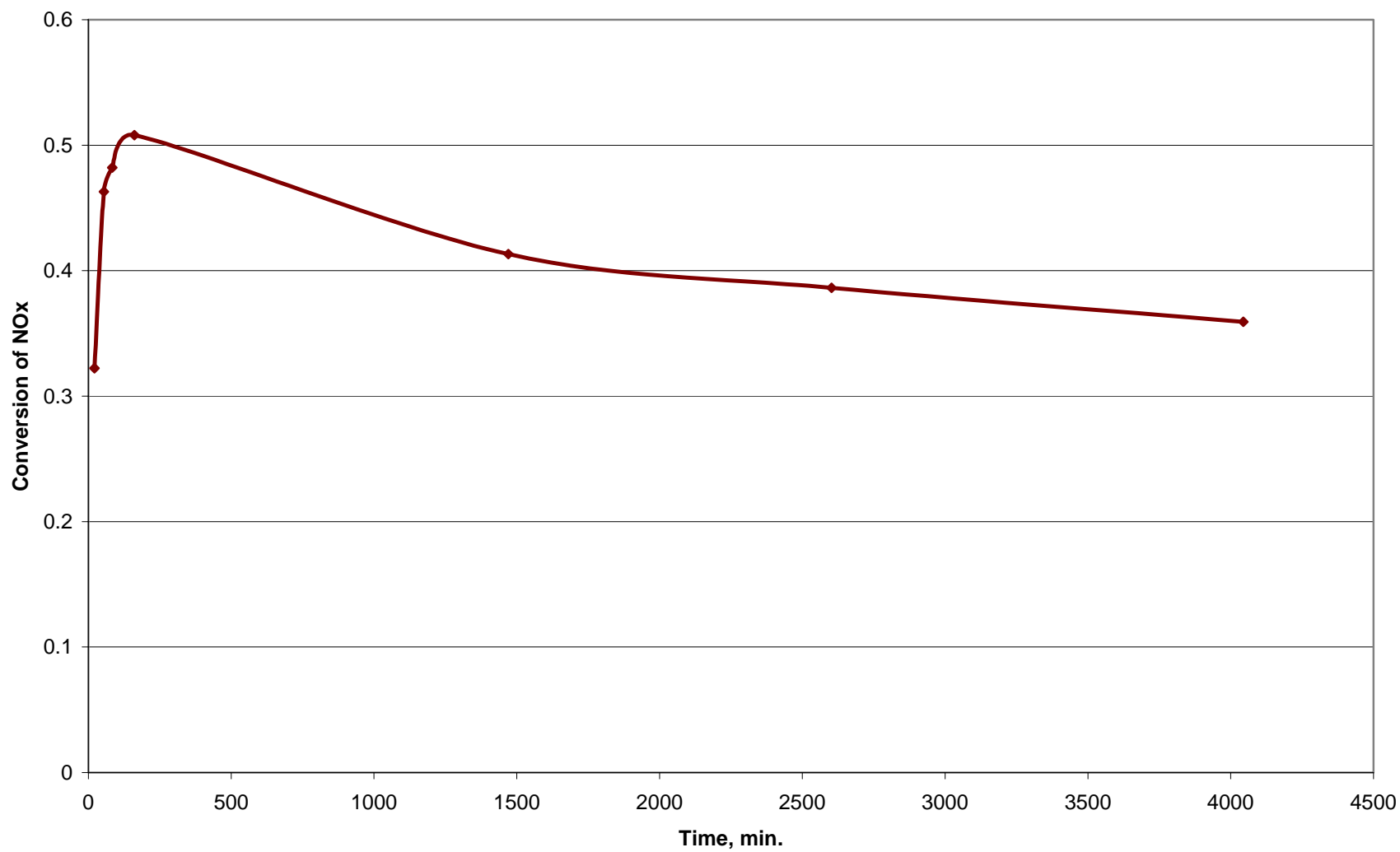
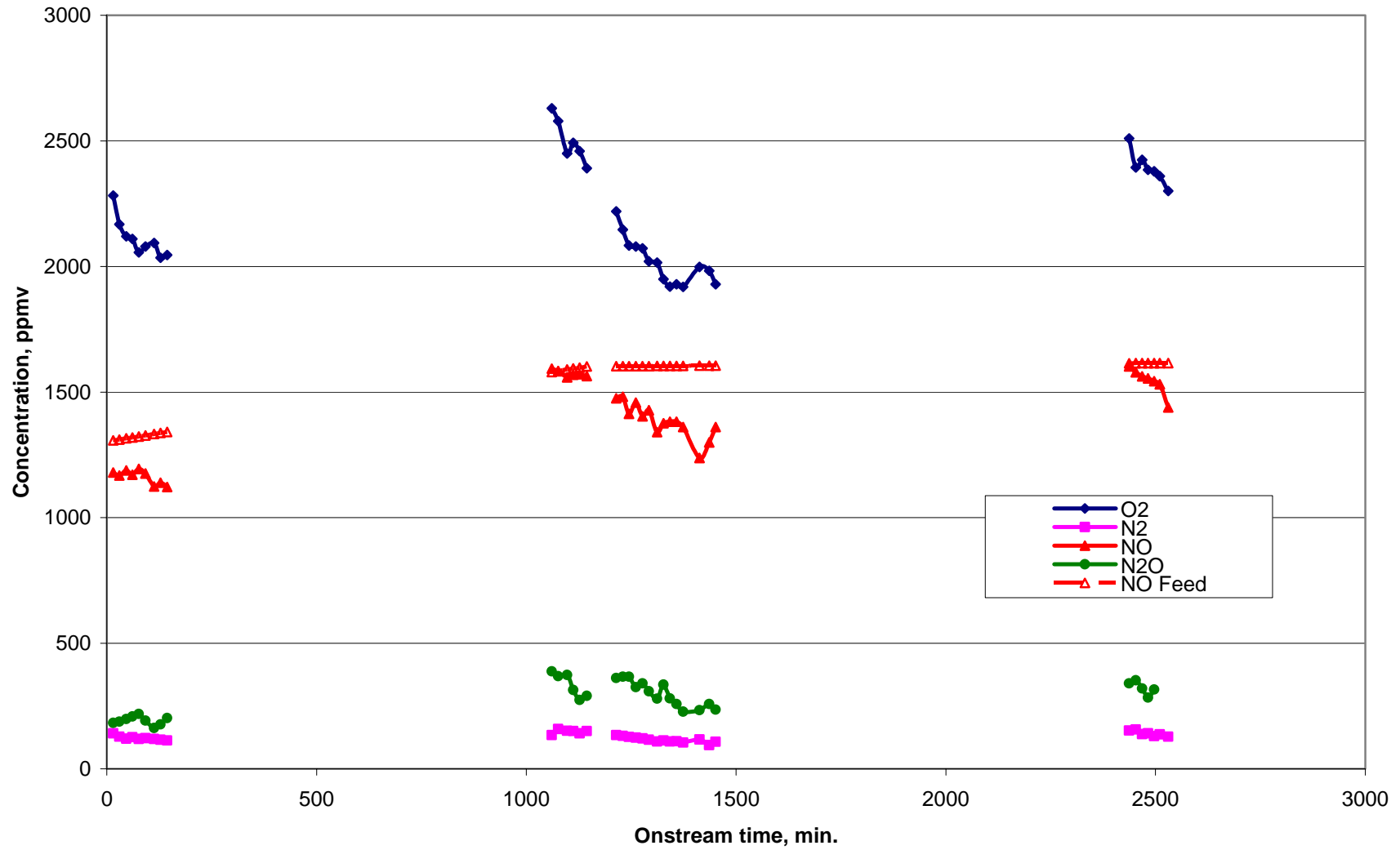


Figure 55. Deactivation of 15%Pt/SnO<sub>2</sub> Catalyst During Isothermal Reaction at 900 K.  
O<sub>2</sub>/NO=1.5



**Figure 56. Deactivation of 15%Pt/SnO<sub>2</sub> Catalyst During Isothermal Reaction at 900 K.  
O<sub>2</sub>/NO=1.5**

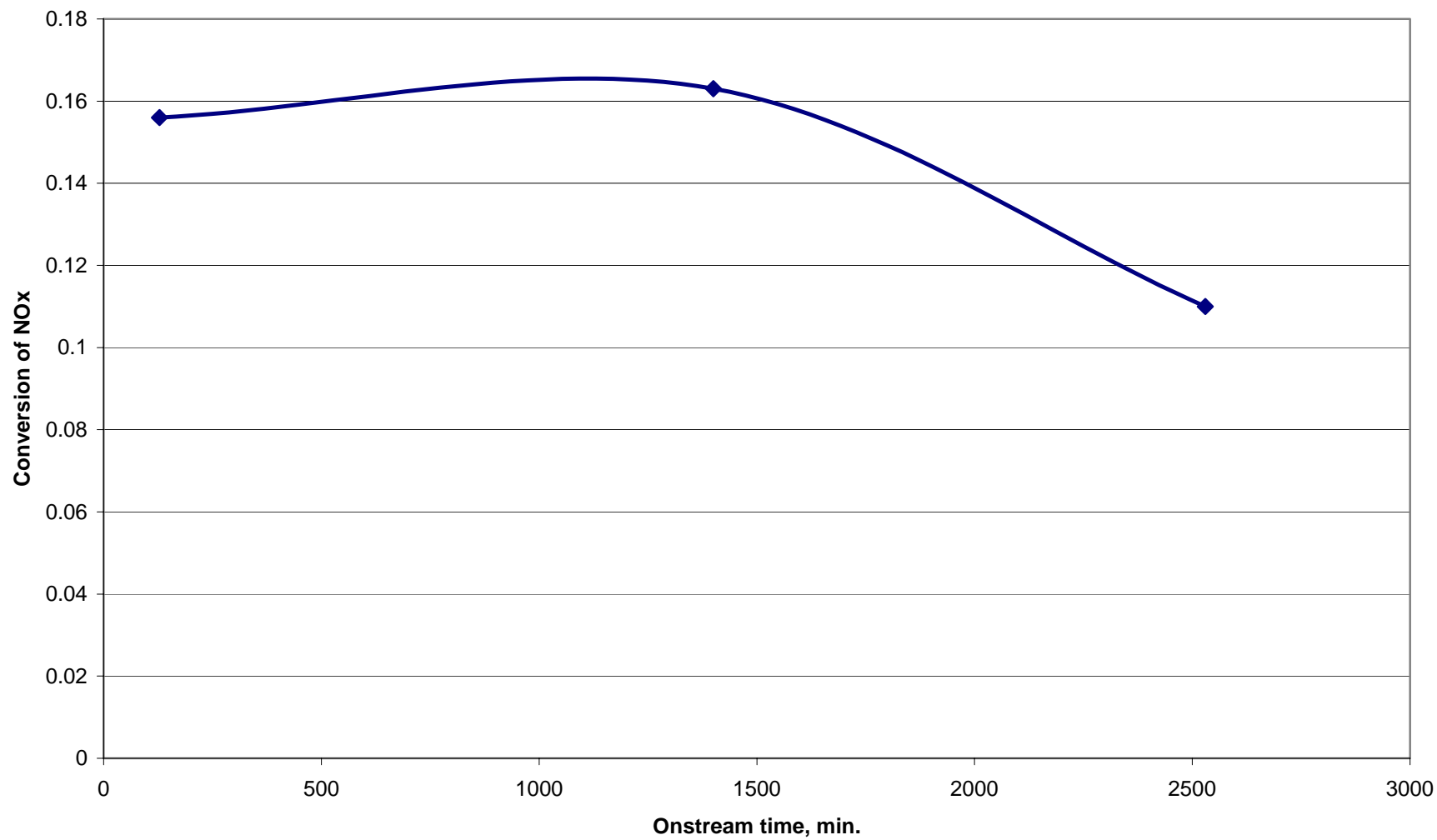


Figure 57. TPRx of NO+O<sub>2</sub> with no catalyst. O<sub>2</sub>/NO=1

